

An improved and extended internally consistent thermodynamic dataset for phases of petrological interest, involving a new equation of state for solids

T. J. B. HOLLAND¹ AND R. POWELL²

¹Department of Earth Sciences, University of Cambridge, Cambridge, CB2 3EQ, UK

²School of Earth Sciences, The University of Melbourne, Victoria 3010, Australia (powell@unimelb.edu.au)

ABSTRACT

The thermodynamic properties of 254 end-members, including 210 mineral end-members, 18 silicate liquid end-members and 26 aqueous fluid species are presented in a revised and updated internally consistent thermodynamic data set. The *PVT* properties of the data set phases are now based on a modified Tait equation of state (EOS) for the solids and the Pitzer & Sterner (1995) equation for gaseous components. Thermal expansion and compressibility are linked within the modified Tait EOS (TEOS) by a thermal pressure formulation using an Einstein temperature to model the temperature dependence of both the thermal expansion and bulk modulus in a consistent way. The new EOS has led to improved fitting of the phase equilibrium experiments. Many new end-members have been added, including several deep mantle phases and, for the first time, sulphur-bearing minerals. Silicate liquid end-members are in good agreement with both phase equilibrium experiments and measured heat of melting. The new dataset considerably enhances the capabilities for thermodynamic calculation on rocks, melts and aqueous fluids under crustal to deep mantle conditions. Implementations are already available in THERMOCALC to take advantage of the new data set and its methodologies, as illustrated by example calculations on sapphirine-bearing equilibria, sulphur-bearing equilibria and calculations to 300 kbar and 2000 °C to extend to lower mantle conditions.

Key words: equation of state; internally consistent dataset; thermodynamic data.

INTRODUCTION

The need for thermodynamic data of sufficient quality to make reliable calculations on rocks continues to grow, particularly to capitalize on new methods of application of phase equilibria that involve increasingly complex solid and fluid solutions, as well as on new advances in software.

The basic philosophy from our earlier summary (Holland & Powell, 1998; hereafter referred to as HP98) is maintained. The thermodynamic data extraction involves using weighted least squares on the different types of data (calorimetric, phase equilibria, natural mineral partitioning) to determine enthalpies of formation of the end-members of the phases. Entropies, volumes, heat capacities, thermal expansions and compressibilities are not derived by regression, but are taken as known in this process. Where they are not known experimentally, they are estimated

Improvements have already been made to the dataset: for the current top-copy, please go to <http://www.esc.cam.ac.uk/people/academic-staff/tim-holland>, or <http://www.metamorph.geo.uni-mainz.de/thermocalc/>.

as outlined in our earlier papers. The new regression involves determination of the enthalpies of 254 end-members, of which 69 are new to the data set, with an overall fit in which σ_{fit} is 1.09 (σ_{fit} being a goodness-of-fit parameter, identical to $\sqrt{\text{MSWD}}$ in geochronology that relates directly to the chi-squared test).

Major methodological changes from HP98 are embodied in this new data set, within the basic philosophy outlined above. They are documented below, along with minor ones that have arisen since HP98, some of which are incorporated in the currently used data set, tc-ds55.txt, from November 2003, but have not been documented properly before.

A list of the chemical compositions of the end-members considered in this study may be found in Table 1. The end-members are listed under the headings orthosilicates and ring silicates (garnet, olivine, etc.), chain silicates (pyroxene and pyroxenoid, amphibole, etc.), sheet silicates (mica, chlorite, etc.), framework silicates, oxides and hydroxides, carbonates, elements, high-pressure phases, gas species, melt species and aqueous species. The new data set itself is given in Table 2. Table 3 lists the calorimetric data used in the dataset generation. Appendix 1 gives the

Group	Abbreviation	End-member	Formula
Garnets & olivines	alm	almandine	$\text{Fe}_3\text{Al}_2\text{Si}_3\text{O}_{12}$
	andr	andradite	$\text{Ca}_3\text{Fe}_2\text{Si}_3\text{O}_{12}$
	gr	grossular	$\text{Ca}_3\text{Al}_2\text{Si}_3\text{O}_{12}$
	knor •	knorringsite	$\text{Mg}_3\text{Cr}_2\text{Si}_3\text{O}_{12}$
	maj •	majorite	$\text{Mg}_4\text{Si}_4\text{O}_{12}$
	py	pyrope	$\text{Mg}_3\text{Al}_2\text{Si}_3\text{O}_{12}$
	spss	spessartine	$\text{Mn}_3\text{Al}_2\text{Si}_3\text{O}_{12}$
	chum	clinohumite	$\text{Mg}_3\text{Si}_4\text{O}_{16}(\text{OH})_2$
	fa	fayalite	Fe_2SiO_4
	fo	forsterite	Mg_2SiO_4
	lrn	larnite	Ca_2SiO_4
	mont	monticellite	CaMgSiO_4
	teph	tephroite	Mn_2SiO_4
Aluminosilicates	and	andalusite	Al_2SiO_5
	ky	kyanite	Al_2SiO_5
	sill	sillimanite	Al_2SiO_5
	amul •	Al-mullite	$\text{Al}_2\text{Si}_{0.5}\text{O}_{4.75}$
	smul •	Si-mullite	Al_2SiO_5
	fctd	Fe-chloritoid	$\text{FeAl}_2\text{SiO}_5(\text{OH})_2$
	mctd	Mg-chloritoid	$\text{MgAl}_2\text{SiO}_5(\text{OH})_2$
	mnctd	Mn-chloritoid	$\text{MnAl}_2\text{SiO}_5(\text{OH})_2$
	fst	Fe-staurolite	$\text{Fe}_4\text{Al}_{18}\text{Si}_{7.5}\text{O}_{44}(\text{OH})_4$
	mst	Mg-staurolite	$\text{Mg}_4\text{Al}_{18}\text{Si}_{7.5}\text{O}_{44}(\text{OH})_4$
	mnst	Mn-staurolite	$\text{Mn}_4\text{Al}_{18}\text{Si}_{7.5}\text{O}_{44}(\text{OH})_4$
	tpz	hydroxy-topaz	$\text{Al}_2\text{SiO}_4(\text{OH})_2$
Other orthosilicates	ak	akermanite	$\text{Ca}_2\text{MgSi}_2\text{O}_7$
	geh	gehlenite	$\text{Ca}_2\text{Al}_2\text{SiO}_7$
	jgd •	julgoldite (FeFe)	$\text{Ca}_4\text{Fe}_6\text{Si}_6\text{O}_{21}(\text{OH})_7$
	merw	merwinite	$\text{Ca}_3\text{MgSi}_2\text{O}_8$
	mpm	pumpellyite (MgAl)	$\text{Ca}_4\text{MgAl}_2\text{Si}_6\text{O}_{21}(\text{OH})_7$
	fpm	pumpellyite (FeAl)	$\text{Ca}_4\text{FeAl}_5\text{Si}_6\text{O}_{21}(\text{OH})_7$
	rnk	rankinite	$\text{Ca}_3\text{Si}_2\text{O}_7$
	sph	sphene	CaTiSiO_5
	spu	spurrite	$\text{Ca}_5\text{Si}_2\text{CO}_{11}$
	ty	tilleyite	$\text{Ca}_5\text{Si}_2\text{C}_2\text{O}_{13}$
	zrc	zircon	ZrSiO_4
Sorosilicates	cz	clinozoisite	$\text{Ca}_2\text{Al}_3\text{Si}_3\text{O}_{12}(\text{OH})$
	ep	epidote(ordered)	$\text{Ca}_2\text{FeAl}_2\text{Si}_3\text{O}_{12}(\text{OH})$
	fep	Fe-epidote	$\text{Ca}_2\text{Fe}_2\text{AlSi}_3\text{O}_{12}(\text{OH})$
	law	lawsonite	$\text{CaAl}_3\text{Si}_3\text{O}_8(\text{OH})_4$
	pmt •	piemontite (ordered)	$\text{Ca}_2\text{MnAl}_3\text{Si}_3\text{O}_{12}(\text{OH})$
	zo	zoisite	$\text{Ca}_2\text{Al}_3\text{Si}_3\text{O}_{12}(\text{OH})$
	vsv	vesuvianite	$\text{Ca}_{19}\text{Mg}_2\text{Al}_1\text{Si}_{18}\text{O}_{69}(\text{OH})_9$
Cyclosilicates	crd	cordierite	$\text{Mg}_2\text{Al}_4\text{Si}_3\text{O}_{18}$
	herd	hydrous-cordierite	$\text{Mg}_2\text{Al}_4\text{Si}_3\text{O}_{17}(\text{OH})_2$
	ferd	Fe-cordierite	$\text{Fe}_2\text{Al}_4\text{Si}_3\text{O}_{18}$
	mnerd	Mn-cordierite	$\text{Mn}_2\text{Al}_4\text{Si}_3\text{O}_{18}$
	osml	osumilite (1)	$\text{KMg}_2\text{Al}_5\text{Si}_{10}\text{O}_{30}$
	osm2	osumilite (2)	$\text{KMg}_3\text{Al}_3\text{Si}_{11}\text{O}_{30}$
	fosm	Fe-osumilite	$\text{KFe}_2\text{Al}_5\text{Si}_{10}\text{O}_{30}$
High- <i>P</i> phases	apv •	Al-perovskite	AlAlO_3
	cpv •	Ca-perovskite	CaSiO_3
	cstn •	CaSi-titanite	CaSi_2O_5
	fak •	Fe-akimotoite	FeSiO_3
	fpv •	Fe-perovskite	FeSiO_3
	frw •	Fe-ringwoodite	Fe_2SiO_4
	fwd •	Fe-wadsleyite	Fe_2SiO_4
	mak •	akimotoite	MgSiO_3
	mpv •	Mg-perovskite	MgSiO_3
	mrw •	Mg-ringwoodite	Mg_2SiO_4
	mwd •	Mg-wadsleyite	Mg_2SiO_4
	pha	phaseA	$\text{Mg}_2\text{Si}_2\text{O}_8(\text{OH})_6$
Pyroxenes & pyroxenoids	acm	acmite	$\text{NaFeSi}_2\text{O}_6$
	caes •	Ca-eskola pyroxene	$\text{Ca}_{0.5}\text{AlSi}_2\text{O}_6$
	cats	Ca-tschermaks pyroxene	$\text{CaAl}_2\text{SiO}_6$
	cen •	clino enstatite	$\text{Mg}_2\text{Si}_2\text{O}_6$
	di	diopside	$\text{CaMgSi}_2\text{O}_6$
	en	enstatite	$\text{Mg}_2\text{Si}_2\text{O}_6$
	fs	ferrosilite	$\text{Fe}_2\text{Si}_2\text{O}_6$
	hed	hedenbergite	$\text{CaFeSi}_2\text{O}_6$
	hen •	Hi-P clinoenstatite	$\text{Mg}_2\text{Si}_2\text{O}_6$
	jd	jadeite	$\text{NaAlSi}_2\text{O}_6$
	kos •	kosmochlor	$\text{NaCrSi}_2\text{O}_6$
	mcts	Mg-tschermaks pyroxene	$\text{MgAl}_2\text{SiO}_6$
	pren •	protoenstatite	$\text{Mg}_2\text{Si}_2\text{O}_6$
	pswo	pseudowollastonite	CaSiO_3
	pxmn	pyroxmangite	MnSiO_3

Table 1. The formulae and abbreviations of the end-members of the phases in the internally consistent data set. A bullet beside an abbreviated name indicates that it is a new end-member in the dataset.

Table 1. (Continued)

Group	Abbreviation	End-member	Formula
Amphibole	rhod	rhodonite	MnSiO ₃
	wal •	walstromite	CaSiO ₃
	wo	wollastonite	CaSiO ₃
	anth	anthophyllite	Mg ₂ Si ₈ O ₂₂ (OH) ₂
	cumm	cummingtonite	Mg ₂ Si ₈ O ₂₂ (OH) ₂
	fact	ferroactinolite	Ca ₂ Fe ₅ Si ₈ O ₂₂ (OH) ₂
	fanth	Fe-anthophyllite	Fe ₂ Si ₈ O ₂₂ (OH) ₂
	fgl	ferroglaucophane	Na ₂ Fe ₃ Al ₂ Si ₈ O ₂₂ (OH) ₂
	gl	glaucophane	Na ₂ Mg ₃ Al ₂ Si ₈ O ₂₂ (OH) ₂
	grun	grunerite	Fe ₂ Si ₈ O ₂₂ (OH) ₂
	parg	pargasite	Na ₂ Ca ₂ Mg ₄ Al ₂ Si ₈ O ₂₂ (OH) ₂
	rieb	riebeckite	Na ₂ Fe ₅ Si ₈ O ₂₂ (OH) ₂
Other chain silicates	tr	tremolite	Ca ₂ Mg ₃ Si ₈ O ₂₂ (OH) ₂
	ts	tschermakite	Ca ₂ Mg ₃ Al ₄ Si ₆ O ₂₂ (OH) ₂
	deer	deerite	Fe ₁₈ Si ₁₂ O ₄₀ (OH) ₁₀
	fcar	ferrocapholite	Fe ₄ Al ₂ Si ₂ O ₆ (OH) ₄
	fspr	Fe-sapphirine (221)	Fe ₄ Al ₂ Si ₂ O ₂₀
	mcar	magnesiocapholite	MgAl ₂ Si ₂ O ₆ (OH) ₄
	spr4	sapphirine (221)	Mg ₄ Al ₂ Si ₂ O ₂₀
Micas	spr5	sapphirine (351)	Mg ₃ Al ₁ Si ₂ O ₂₀
	ann	annite	KFe ₃ AlSi ₄ O ₁₀ (OH) ₂
	cel	celadonite	KMgAlSi ₄ O ₁₀ (OH) ₂
	east	eastonite	KMg ₂ Al ₃ Si ₂ O ₁₀ (OH) ₂
	fecl	ferroceladonite	KFeAlSi ₄ O ₁₀ (OH) ₂
	ma	margarite	CaAl ₃ Si ₂ O ₁₀ (OH) ₂
	mnb	Mn-biotite	KMn ₃ AlSi ₃ O ₁₀ (OH) ₂
	mu	muscovite	KAl ₃ Si ₃ O ₁₀ (OH) ₂
	naph	sodaphlogopite	NaMg ₃ AlSi ₃ O ₁₀ (OH) ₂
	pa	paragonite	NaAl ₃ Si ₃ O ₁₀ (OH) ₂
	pfl	phlogopite	KMg ₃ AlSi ₃ O ₁₀ (OH) ₂
	afchl	Al-free chlorite	Mg ₆ Si ₄ O ₁₀ (OH) ₈
Chlorites	ames	amésite (14A)	Mg ₄ Al ₂ Si ₂ O ₁₀ (OH) ₈
	clin	clinochlore (ordered)	Mg ₅ Al ₂ Si ₃ O ₁₀ (OH) ₈
	daph	daphnite	Fe ₅ Al ₂ Si ₃ O ₁₀ (OH) ₈
	fsud	ferrosudoite	Fe ₂ Al ₄ Si ₃ O ₁₀ (OH) ₈
	mnchl	Mn-chlorite	Mn ₅ Al ₂ Si ₃ O ₁₀ (OH) ₈
	sud	sudoite	Mg ₂ Al ₄ Si ₃ O ₁₀ (OH) ₈
	atg	antigorite	Mg ₄₈ Si ₁₄ O ₈ (OH) ₆₂
	chr	chrysotile	Mg ₃ Si ₂ O ₅ (OH) ₄
	fpre •	ferri-prehnite	Ca ₂ FeAlSi ₃ O ₁₀ (OH) ₂
	fstp •	ferrostilpnomelane	K _{0.5} Fe ₃ Al ₂ Si ₈ O ₁₈ (OH) _{12.5}
Other sheet silicates	fta	ferrotalc	Fe ₃ Si ₂ O ₁₀ (OH) ₂
	glt •	greenalite	Fe ₃ Si ₂ O ₅ (OH) ₄
	kao	kaolinite	Al ₂ Si ₂ O ₅ (OH) ₄
	liz •	lizardite	Mg ₃ Si ₂ O ₅ (OH) ₄
	minm •	Mg-minnesotaite	Mg ₃ Si ₄ O ₁₀ (OH) ₂
	minn •	minnesotaite	Fe ₃ Si ₂ O ₁₀ (OH) ₂
	mstp •	Mg-stilpnomelane	K _{0.5} Mg ₂ Al ₂ Si ₂ O ₁₈ (OH) _{12.5}
	pre	prehnite	Ca ₂ Al ₂ Si ₃ O ₁₀ (OH) ₂
	prl	pyrophyllite	Al ₂ Si ₂ O ₁₀ (OH) ₂
	ta	talc	Mg ₃ Si ₄ O ₁₀ (OH) ₂
	tap •	prl-talc	Al ₂ Si ₂ O ₁₀ (OH) ₂
	tats	tschermak-talc	Mg ₂ Al ₂ Si ₃ O ₁₀ (OH) ₂
Feldspars & feldspathoid	abh	albite (high)	NaAlSi ₃ O ₈
	albite	ab	NaAlSi ₃ O ₈
	an	anorthite	CaAl ₂ Si ₂ O ₈
	anl	analcite	NaAlSi ₂ O ₅ (OH) ₂
	cg •	carnegieite (low)	NaAlSiO ₄
	cgh •	carnegieite (high)	NaAlSiO ₄
	kcm •	K-cymrite	KAlSi ₃ O ₇ (OH) ₂
	cls	kalsilite	KAlSiO ₄
	lc	leucite	KAlSi ₂ O ₆
	mic	microcline	KAlSi ₃ O ₈
	ne	nepheline	NaAlSiO ₄
	san	sanidine	KAlSi ₃ O ₈
Silica minerals	coe	coesite	SiO ₂
	crst	crystobalite (high)	SiO ₂
	q	quartz	SiO ₂
	stv	stishovite	SiO ₂
	trd	tridymite (high)	SiO ₂
Other framework silicates	heu	heulandite	CaAl ₂ Si ₇ O ₁₂ (OH) ₁₂
	hol •	hollandite	KAlSi ₃ O ₈
	lmt	laumontite	CaAl ₂ Si ₄ O ₈ (OH) ₈
	me	meionite	Ca ₄ Al ₆ Si ₆ CO ₂₇
	sdl •	sodalite	Na ₈ Al ₆ Si ₆ O ₂₄ Cl ₂
	stlb	stilbite	CaAl ₂ Si ₇ O ₁₁ (OH) ₁₄
	wa •	Si-wadeite	K ₂ Si ₄ O ₉
	wrk	wairakite	CaAl ₂ Si ₄ O ₁₀ (OH) ₄

Table 1. (Continued)

Group	Abbreviation	End-member	Formula
Oxides	bdy	baddeleyite	ZrO ₂
	bix •	bixbyite	Mn ₂ O ₃
	cor	corundum	Al ₂ O ₃
	cup •	cuprite	Cu ₂ O
	esk •	eskolaite	Cr ₂ O ₃
	fper •	ferropericlase	FeO
	geik	geikielite	MgTiO ₃
	hem	hematite	Fe ₂ O ₃
	herc	hercynite	FeAl ₂ O ₄
	ilm	ilmenite	FeTiO ₃
	lime	lime	CaO
	mang	manganosite	MnO
	mcor •	MgSi-corundum	MgSiO ₃
	mft	magnesioferrite	MgFe ₂ O ₄
	mt	magnetite	Fe ₃ O ₄
	NiO	nickel oxide	NiO
	per	periclaste	MgO
	picr •	picrochromite	MgCr ₂ O ₄
	pnt	pyrophanite	MnTiO ₃
	ru	rutile	TiO ₂
	sp	spinel	MgAl ₂ O ₄
	ten •	tenorite	CuO
	usp	ulvöspinel	Fe ₂ TiO ₄
Hydroxides	br	brucite	Mg(OH) ₂
	dsp	diaspore	AlO(OH)
	gth	goethite	FeO (OH)
Carbonates	ank	ankerite	CaFe(CO ₃) ₂
	arag	aragonite	CaCO ₃
	cc	calcite	CaCO ₃
	dol	dolomite	CaMg(CO ₃) ₂
	mag	magnesite	MgCO ₃
	rhc	rhodochrosite	MnCO ₃
	sid	siderite	FeCO ₃
Halides & sulphides	any •	anhydrite	CaSO ₄
	hlt •	halite	NaCl
	lot •	low troilite	FeS
	pyr •	pyrite	FeS ₂
	syy •	sylvite	KCl
	tro •	troilite	FeS
	trot •	pyrrhotite	FeS
	trov •	pyrrhotite	Fe _{0.875} S
Elements	Cu •	copper	Cu
	diam	diamond	C
	gph	graphite	C
	iron	iron	Fe
	Ni	nickel	Ni
	S •	sulphur	S
Gas species	H ₂ O	water	H ₂ O
	CO ₂	carbon dioxide	CO ₂
	CO	carbon monoxide	CO
	CH ₄	methane	CH ₄
	O ₂	oxygen	O ₂
	H ₂	hydrogen	H ₂
	S ₂ •	sulphur gas	S ₂
	H ₂ S •	Hydrogen sulphide	H ₂ S
Melt species	abL	albite liquid	NaAlSi ₃ O ₈
	anL	anorthite liquid	CaAl ₂ Si ₂ O ₈
	corL •	corundum liquid	Al ₂ O ₃
	diL	diopside liquid	CaMgSi ₂ O ₆
	enL	enstatite liquid	Mg ₂ Si ₂ O ₆
	faL	fayalite liquid	Fe ₂ SiO ₄
	foL	forsterite liquid	Mg ₂ SiO ₄
	h2oL	H ₂ O liquid	H ₂ O
	hltL •	halite liquid)	NaCl
	kspL	K-feldspar liquid	KAlSi ₃ O ₈
	lcL •	leucite liquid	KAlSi ₂ O ₆
	limL •	CaO liquid	CaO
	neL •	nepheline liquid	NaAlSiO ₄
	perL •	MgO liquid	MgO
	qL	quartz liquid	SiO ₂
	silL	sillimanite liquid	Al ₂ SiO ₅
	sylL •	sylvite (liquid)	KCl
	woL •	wollastonite liquid	CaSiO ₃

Table 1. (Continued)

Group	Abbreviation	End-member	Formula
Aqueous species	H ⁺	hydrogen ion	H +
	Cl ⁻	chloride ion	Cl ⁻
	OH ⁻	hydroxyl ion	HO ⁻
	Na ⁺	sodium ion	Na ⁺
	K ⁺	potassium ion	K ⁺
	Ca ⁺⁺	calcium ion	Ca ²⁺
	Mg ⁺⁺	magnesium ion	Mg ²⁺
	Fe ⁺⁺	ferrous ion	Fe ²⁺
	Al ⁺⁺⁺	aluminium ion	Al ³⁺
	CO ₃ ²⁻	carbonate ion	CO ₃ ²⁻
	AlOH ₃	aluminium hydroxide	Al(OH) ₃
	AlOH ₄ ⁻	aluminium hydroxide	AlH ₄ O ₄
	KOH	potassium hydroxide	K(OH)
	HCl	hydrogen chloride	HCl
	KCl	potassium chloride	KCl
	NaCl	sodium chloride	NaCl
	CaCl ₂	calcium chloride	CaCl ₂
	CaCl ⁺	calcium chloride	CaCl ⁺
	MgCl ₂	magnesium chloride	MgCl ₂
	MgCl ⁺	magnesium chloride	MgCl ⁺
	FeCl ₂	ferrous chloride	FeCl ₂
	aqSi	silica (aq)	SiO ₂
	HS ⁻ •	sulphide (aq)	HS ⁻
	HSO ₃ ⁻ •	sulphite (aq)	HSO ₃ ⁻
	SO ₄ ²⁻ •	sulphate (aq)	SO ₄ ²⁻
	HSO ₄ ⁻ •	sulphate2 (aq)	HSO ₄ ⁻

data sources for the thermodynamic properties, and Appendix 2 is a summary table of the experimental studies used in the data set regression. Appendix 3 provides information on minor changes since the publication of HP98. The table of all the experimentally determined mineral equilibrium brackets used in the least squares analysis and the calculated fit to them is presented in Table S1 as well as at <http://www.esc.cam.ac.uk/people/academic-staff/tim-holland> and <http://www.metamorph.geo.uni-mainz.de/thermocalc/>. This is in the form of full computer output from the data extraction program LSQDS. Table S2 contains the activity–composition relations that were used in the generation of the data set.

CHANGES TO METHODOLOGY

The principal differences in methodology from HP98 are outlined before the details of the new data set are presented and discussed.

Equation of state (EOS) for solids

The EOS for solid phases in HP98 involved a thermal expansion expression at 1 bar pressure, with an independent Murnaghan EOS to take the ambient pressure molar volumes to high pressures. To link the expansion and compression terms, a simple linear temperature dependence for the bulk modulus was used. This is now replaced with a more general EOS, and the expansion and compression terms are now linked.

Freund & Ingalls (1989) investigated nine separate EOS to determine which might be most suitable for high pressure work in solids. Their aim was to find a suitable EOS with only two or three adjustable para-

meters which best fit compression data to very high pressures. The modified Tait equation of Huang & Chow (1974) was one of the best of the equations investigated, in terms of fits to the compression data, and it is adopted here. We then augment this EOS for high temperature use by adding a thermal pressure term, as outlined below, thus integrating the expansion and compression contributions to Gibbs energy. Below, this modified Tait EOS, augmented with a thermal pressure term, is referred to as TEOS.

The 298K (ambient) temperature TEOS, expressed as a three-parameter equation in volume at $T = T_0$ (where $T_0 = 298.15\text{K}$) is:

$$\frac{V}{V_0} = 1 - a(1 - (1 + bP)^{-c}) \quad (1)$$

and, in terms of pressure may be rearranged as:

$$P = \frac{1}{b} \left(\left[\frac{(V/V_0) + a - 1}{a} \right]^{-1/c} - 1 \right) \quad (2)$$

The relationship of the parameters to the bulk modulus and its derivatives at zero pressure is (Freund & Ingalls, 1989):

$$\begin{aligned} a &= \frac{1 + \kappa'_0}{1 + \kappa'_0 + \kappa_0 \kappa''_0}, \\ b &= \frac{\kappa'_0}{\kappa_0} - \frac{\kappa''_0}{1 + \kappa'_0}, \\ c &= \frac{1 + \kappa'_0 + \kappa_0 \kappa''_0}{\kappa'^2_0 + \kappa'_0 - \kappa_0 \kappa''_0}, \end{aligned} \quad (3)$$

where κ_0 is the bulk modulus at ambient conditions,

Table 2a. Molar thermodynamic properties (units: kJ, K, kbar) of the end-members whose formulae can be found in Table 1.

Group	End-member	$\Delta_f H$	$\sigma(\Delta_f H)$	S	V	C_P				$\alpha\kappa$				ℓ
						a	b	c	d	α_0	κ_0	κ'_0	κ''_0	
Garnet and olivine	Almandine (alm)	-5260.65	1.31	342.00	11.525	0.6773	0	-3772.7	-5.0440	2.12	1900.0	2.98	-0.0016	
	Andradite (andr)	-5769.08	1.56	316.40	13.204	0.6386	0	-4955.1	-3.9892	2.86	1588.0	5.68	-0.0036	
	grossular (gr)	-6642.95	1.46	255.00	12.535	0.6260	0	-5779.2	-4.0029	2.20	1720.0	5.53	-0.0032	
	Knorrtingite (knor)	-5687.75	3.88	317.00	11.738	0.6130	0.3606	-4178.0	-3.7294	2.37	1743.0	4.05	-0.0023	
	Majorite (maj)	-6050.33	9.62	255.20	11.457	0.7136	-0.0997	-1158.2	-6.6223	1.83	1600.0	4.56	-0.0028	
	Pyrope (py)	-6282.13	1.06	269.50	11.313	0.6335	0	-5196.1	-4.3152	2.37	1743.0	4.05	-0.0023	
	Spessartine (spss)	-5693.65	3.14	335.30	11.792	0.6469	0	-4525.8	-4.4528	2.27	1740.0	6.68	-0.0038	
	Clinohumite (chum)	-9609.82	2.49	443.00	19.785	1.0700	-1.6533	-7899.6	-7.3739	2.91	1194.0	4.79	-0.0040	
	Fayalite (fa)	-1477.74	0.68	151.00	4.631	0.2011	1.7330	-1960.6	-0.9009	2.82	1256.0	4.68	-0.0037	
	Forsterite (fo)	-2172.57	0.57	95.10	4.366	0.2333	0.1494	-603.8	-1.8697	2.85	1285.0	3.84	-0.0030	
	Larnite (lrn)	-2307.04	0.90	127.60	5.160	0.2475	-0.3206	0	-2.0519	2.90	985.0	4.07	-0.0041	1
	Monticellite (mont)	-2251.31	0.52	109.50	5.148	0.2507	-1.0433	-797.2	-1.9961	2.87	1134.0	3.87	-0.0034	
	Tephroite (teph)	-1733.95	1.05	155.90	4.899	0.2196	0	-1292.7	-1.3083	2.86	1256.0	4.68	-0.0037	
Aluminosilicates	Andalusite (and)	-2588.72	0.68	92.70	5.153	0.2773	-0.6588	-1914.1	-2.2656	1.81	1442.0	6.89	-0.0048	
	Kyanite (ky)	-2593.02	0.67	83.50	4.414	0.2794	-0.7124	-2055.6	-2.2894	1.92	1601.0	4.05	-0.0025	
	Sillimanite (sill)	-2585.85	0.68	95.40	4.986	0.2802	-0.6900	-1375.7	-2.3994	1.12	1640.0	5.06	-0.0031	2
	Mullite (amul)	-2485.51	0.91	113.00	5.083	0.2448	0.0968	-2533.3	-1.6416	1.36	1740.0	4.00	-0.0023	
	Mullite (smul)	-2569.28	0.69	101.50	4.987	0.2802	-0.6900	-1375.7	-2.3994	1.36	1740.0	4.00	-0.0023	
	Chloritoid (fcld)	-3208.31	0.80	167.00	6.980	0.4161	-0.3477	-2835.9	-3.3603	2.80	1456.0	4.06	-0.0028	
	Chloritoid (mcld)	-3549.31	0.75	146.00	6.875	0.4174	-0.3771	-2920.6	-3.4178	2.63	1456.0	4.06	-0.0028	
	Chloritoid (mncld)	-3336.20	1.68	166.00	7.175	0.4644	-1.2654	-1147.2	-4.3410	2.60	1456.0	4.06	-0.0028	
	Staurolite (fst)	-23 755.04	6.34	1010.00	44.880	2.8800	-5.6595	-10642.0	-25.3730	1.83	1800.0	4.76	-0.0026	
	Staurolite (mnst)	-24 246.42	8.60	1034.00	45.460	2.8733	-8.9064	-12688.0	-24.7490	2.09	1800.0	4.76	-0.0026	
	Staurolite (mst)	-25 124.32	6.28	910.00	44.260	2.8205	-5.9366	-13774.0	-24.1260	1.81	1684.0	4.05	-0.0024	
	Topaz (tpz)	-2900.76	0.96	100.50	5.339	0.3877	-0.7120	-857.2	-3.7442	1.57	1315.0	4.06	-0.0031	
Other orthosilicates	Akermanite (ak)	-3865.63	0.94	212.50	9.254	0.3854	0.3209	-247.5	-2.8899	2.57	1420.0	4.06	-0.0029	
	Gehlenite (geh)	-3992.26	1.33	198.50	9.024	0.4057	-0.7099	-1188.3	-3.1744	2.23	1080.0	4.08	-0.0038	2
	Julgoldite (jgd)	-11 809.63	8.50	830.00	31.080	1.7954	-3.7986	-4455.7	-14.8880	2.49	1615.0	4.05	-0.0025	
	Merwinite (merw)	-4545.87	1.36	253.10	9.847	0.4175	0.8117	-2923.0	-2.3203	3.19	1200.0	4.07	-0.0034	
	Pumpellyite (fpm)	-14 033.82	2.63	657.00	29.680	1.7372	-2.4582	-5161.1	-14.9630	2.49	1615.0	4.05	-0.0025	
	Pumpellyite (mpm)	-14 386.75	2.41	629.00	29.550	1.7208	-2.4928	-5998.7	-14.6203	2.47	1615.0	4.05	-0.0025	
	Rankinite (rnk)	-3943.92	1.36	210.00	9.651	0.3723	-0.2893	-2462.4	-2.1813	3.28	950.0	4.09	-0.0043	
	Sphene (sph)	-2601.65	0.96	124.00	5.565	0.2279	0.2924	-3539.5	-0.8943	1.58	1017.0	9.85	-0.0097	1
	Spurrite (spu)	-5847.08	2.23	332.00	14.697	0.6141	-0.3508	-2493.1	-4.1680	3.40	950.0	4.09	-0.0043	
	Tilleyite (ty)	-6368.39	2.21	390.00	17.039	0.7417	-0.5345	-1434.6	-5.8785	3.41	950.0	4.09	-0.0043	
	Zircon (zrc)	-2035.05	1.66	83.03	3.926	0.2320	-1.4405	0	-2.2382	1.25	2301.0	4.04	-0.0018	
Sorosilicates	Clinozoisite (cz)	-6895.42	1.31	301.00	13.630	0.6309	1.3693	-6645.8	-3.7311	2.33	1197.0	4.07	-0.0034	
	Epidote (ep)	-6473.90	1.17	315.00	13.920	0.6133	2.2070	-7160.0	-2.9877	2.34	1340.0	4.00	-0.0030	
	Epidote (fep)	-6027.57	1.23	329.00	14.210	0.5847	3.0447	-7674.2	-2.2443	2.31	1513.0	4.00	-0.0026	
	Lawsonite (law)	-4868.61	0.81	229.00	10.132	0.6878	0.1566	375.9	-7.1792	2.65	1229.0	5.45	-0.0044	
	Piemontite (pmt)	-6543.04	2.70	340.00	13.820	0.5698	2.7790	-5442.9	-2.8126	2.38	1197.0	4.07	-0.0034	
	Zoisite (zo)	-6896.21	1.31	298.00	13.575	0.6620	1.0416	-6006.4	-4.2607	3.12	1044.0	4.00	-0.0038	
Cyclosilicates	Vesuvianite (vsv)	-42 345.19	8.95	1890.00	85.200	4.4880	-5.7952	-22269.3	-33.4780	2.75	1255.0	4.80	-0.0038	
	Cordierite (crd)	-9163.48	1.51	404.10	23.322	0.9061	0	-7902.0	-6.2934	0.68	1290.0	4.10	-0.0031	2
	Cordierite (ferd)	-8444.02	1.66	461.00	23.710	0.9240	0	-7039.4	-6.4396	0.67	1290.0	4.10	-0.0031	2
	Cordierite (herd)	-9449.32	1.52	475.60	23.322	0.9802	0	-7035.9	-6.6808	0.67	1290.0	4.10	-0.0031	2
	Cordierite (mncrd)	-8693.64	3.60	473.00	24.027	0.8865	0	-8840.0	-5.5904	0.69	1290.0	4.10	-0.0031	2
	Osumilite (fosc)	-14 238.91	3.99	762.00	38.320	1.6560	-3.4163	-6497.7	-14.1143	0.49	800.0	4.10	-0.0051	
High-pressure phases	Osumilite (osml)	-14 959.21	3.83	701.00	37.893	1.6258	-3.5548	-8063.5	-13.4909	0.47	810.0	4.10	-0.0051	
	Osumilite (osm1)	-14 799.99	4.05	724.00	38.440	1.6106	-3.4457	-8262.1	-13.1288	0.47	810.0	4.10	-0.0051	
	Osumilite (osm2)	-14 799.99	4.05	724.00	38.440	1.6106	-3.4457	-8262.1	-13.1288	0.47	810.0	4.10	-0.0051	
	akimotoite (fak)	-1142.14	10.12	91.50	2.760	0.1003	1.3328	-4364.9	0.4198	2.12	2180.0	4.55	-0.0022	
	Akimotoite (mak)	-1490.85	0.62	59.30	2.635	0.1478	0.2015	-2395.0	-0.8018	2.12	2110.0	4.55	-0.0022	
	CaSi-titanite (cstn)	-2496.17	2.81	99.50	4.818	0.2056	0.6034	-5517.7	-0.3526	1.58	1782.0	4.00	-0.0022	
Pyroxene and pyroxenoid	Perovskite (apv)	-1646.76	1.12	51.80	2.540	0.1395	0.5890	-2460.6	-0.5892	1.80	2030.0	4.00	-0.0020	
	Perovskite (cpv)	-1541.73	1.80	73.50	2.745	0.1593	0	-967.3	-1.0754	1.87	2360.0	3.90	-0.0016	
	Perovskite (fpv)	-1084.64	8.14	91.00	2.548	0.1332	1.0830	-3661.4	-0.3147	1.87	2810.0	4.14	-0.0016	
	Perovskite (mpv)	-1443.02	0.69	62.60	2.445	0.1493	0.2918	-2983.0	-0.7991	1.87	2510.0	4.14	-0.0016	
	PhaseA (pha)	-7132.27	1.90	348.00	15.442	0.9640	-1.1521	-4517.8	-7.7247	3.79	1450.0	4.06	-0.0028	
	Ringwoodlite (frw)	-1471.79	0.76	140.00	4.203	0.1668	4.2610	-1705.4	-0.5414	2.22	1977.0	4.92	-0.0025	
	Ringwoodlite (mrw)	-2127.66	0.78	90.00	3.949	0.2133	0.2690	-1410.4	-1.4959	2.01	1781.0	4.35	-0.0024	
	Wadsleyite (fwd)	-1467.92	0.97	146.00	4.321	0.2011	1.7330	-1960.6	-0.9009	2.73	1690.0	4.35	-0.0026	
	Wadsleyite (mw)	-2138.50	0.76	93.90	4.051	0.2087	0.3942	-1709.5	-1.3028	2.37	1726.0	3.84	-0.0022	
	Acmite (acm)	-2583.50	2.43	170.60	6.459	0.3071	1.6758	-1685.5	-2.1258	2.11	1060.0	4.08	-0.0038	
	Ca-eskola pyroxene (caes)	-3002.01	1.74	127.00	6.050	0.3620	-1.6944	-175.9	-3.5657	2.31	1192.0	5.19	-0.0044	2
	Ca-Tschermak pyroxene (cats)	-3310.14	0.80	135.00	6.356	0.3476	-0.6974	-1781.6	-2.7575	2.08	1192.0	5.19	-0.0044	2
	Clinoenstatite (cen)	-3091.12	0.66	132.00	6.264	0.3060	-0.3793	-3041.7	-1.8521	2.11	1059.0	8.65	-0.0082	
	Clinoenstatite high-P (hen)	-3082.74	0.67	131.70	6.099	0.3562	-0.2990	-596.9	-3.1853	2.26	1500.0	5.50	-0.0036	
	Diopside (di)	-3201.69	0.62	142.90	6.619	0.3145	0							

Table 2a. (Continued)

Group	End-member	$\Delta_f H$	$\sigma(\Delta_f H)$	S	V	C_P				$\alpha\kappa$			ℓ	
						a	b	c	d	α_0	κ_0	κ'_0	κ''_0	
	Enstatite (en)	-3090.23	0.66	132.50	6.262	0.3562	-0.2990	-596.9	-3.1853	2.27	1059.0	8.65	-0.0082	
	Ferrosilite (fs)	-2388.72	0.81	189.90	6.592	0.3987	-0.6579	1290.1	-4.0580	3.26	1010.0	4.08	-0.0040	
	Hedenbergite (hed)	-2841.92	0.94	175.00	6.795	0.3402	0.0812	-1047.8	-2.6467	2.38	1192.0	3.97	-0.0033	
	Jadeite (jd)	-3025.26	1.67	133.50	6.040	0.3194	0.3616	-1173.9	-2.4695	2.10	1281.0	3.81	-0.0030	
	Kosmochlore (kos)	-2746.80	2.46	149.65	6.309	0.3092	0.5419	-664.6	-2.1766	1.94	1308.0	3.00	-0.0023	
	Mg-Tschermak pyroxene (mgts)	-3196.61	0.73	131.00	6.050	0.3714	-0.4082	-398.4	-3.5471	2.17	1028.0	8.55	-0.0083	
	Protoenstatite (pren)	-3084.57	0.67	137.00	6.476	0.3562	-0.2990	-596.9	-3.1853	2.30	1059.0	8.65	-0.0082	
	Pseudowollastonite (pswo)	-1627.94	0.47	87.80	4.008	0.1578	0	-967.3	-1.0754	2.85	1100.0	4.08	-0.0037	
	Pyroxmangite (pxmn)	-1323.14	0.73	99.30	3.472	0.1384	0.4088	-1936.0	-0.5389	2.80	840.0	4.00	-0.0048	
	Rhodonite (rhod)	-1322.35	0.73	100.50	3.494	0.1384	0.4088	-1936.0	-0.5389	2.81	840.0	4.00	-0.0048	
	Walstromite (wal)	-1625.88	0.48	83.50	3.763	0.1593	0	-967.3	-1.0754	2.54	795.0	4.10	-0.0052	
	Wollastonite (wo)	-1633.75	0.47	82.50	3.993	0.1593	0	-967.3	-1.0754	2.54	795.0	4.10	-0.0052	
Amphibole	Anthophyllite (anth)	-12066.85	2.48	537.00	26.540	1.2773	2.5825	-9704.6	-9.0747	2.52	700.0	4.11	-0.0059	
	Anthophyllite (fanth)	-9624.53	8.80	725.00	27.870	1.3831	3.0669	-4224.7	-11.2576	2.74	700.0	4.11	-0.0059	
	Cummingtonite (cumm)	-12064.71	2.48	538.00	26.330	1.2773	2.5825	-9704.6	-9.0747	2.52	700.0	4.11	-0.0059	
	Ferroactinolite (fact)	-10503.82	2.88	710.00	28.420	1.2900	2.9992	-8447.5	-8.9470	2.88	760.0	4.10	-0.0054	
	Glaucophane (fgl)	-10880.25	5.15	624.00	26.590	1.7629	-11.8992	9423.7	-20.2071	1.83	890.0	4.09	-0.0046	
	Glaucophane (gl)	-11960.24	3.55	530.00	25.980	1.7175	-12.1070	705.0	-19.2720	1.49	883.0	4.09	-0.0046	
	Grunerite (grun)	-9607.15	3.02	735.00	27.840	1.3831	3.0669	-4224.7	-11.2576	2.74	648.0	4.12	-0.0064	
	Pargasite (parg)	-12664.49	2.27	635.00	27.190	1.2802	2.2997	-12359.5	-8.0658	2.80	912.0	4.09	-0.0045	
	Riebeckite (rieb)	-10024.77	5.30	695.00	27.490	1.7873	-12.4882	9627.1	-20.2755	1.80	890.0	4.09	-0.0046	
Other chain silicates	Tremolite (tr)	-12304.56	2.17	553.00	27.270	1.2602	0.3830	-11455.0	-8.2376	2.61	762.0	4.10	-0.0054	
	Tschermakite (ts)	-12555.30	1.77	533.00	26.800	1.2448	2.4348	-11965.0	-8.1121	2.66	760.0	4.10	-0.0054	
	Deerite (deer)	-18341.50	6.45	1650.00	55.740	3.1644	-2.7883	-5039.1	-26.7210	2.75	630.0	4.12	-0.0065	
	Carpholite (fcar)	-4411.57	1.01	251.10	10.695	0.6866	-1.2415	186.0	-6.8840	2.21	525.0	4.14	-0.0079	
	Carpholite (mcar)	-4771.22	0.79	221.50	10.590	0.6830	-1.4054	291.0	-6.9764	2.43	525.0	4.14	-0.0079	
Other sheet silicates	Sapphirine (fspr)	-9659.86	5.87	485.00	19.923	1.1329	-0.7348	-10420.2	-7.0366	1.96	2500.0	4.04	-0.0017	
	Sapphirine (spr4)	-11022.40	3.10	425.50	19.900	1.1331	-0.7596	-8816.6	-8.1806	2.05	2500.0	4.04	-0.0016	
	Sapphirine (spr5)	-11135.69	3.83	419.50	19.750	1.1034	0.1015	-10957.0	-7.4092	2.06	2500.0	4.04	-0.0016	
	Mica	annite (ann)	-5144.23	3.19	418.00	15.432	0.8157	-3.4861	19.8	-7.4667	3.80	513.0	7.33	-0.0143
	Celadonite (cel)	-5834.87	2.83	290.00	13.957	0.7412	-1.8748	-2368.8	-6.6169	3.07	700.0	4.11	-0.0059	
Chlorites	Celadonite (fcel)	-5468.47	2.86	330.00	14.070	0.7563	-1.9147	-1586.1	-6.9287	3.18	700.0	4.11	-0.0059	
	Eastonite (east)	-6330.48	3.04	318.00	14.738	0.7855	-3.8031	-2130.3	-6.8937	3.80	530.0	7.33	-0.0143	
	Margarite (ma)	-6242.11	1.40	265.00	12.964	0.7444	-1.6800	-2074.4	-6.7832	2.33	1000.0	4.08	-0.0041	
	Mn-biotite (mnb)	-5477.59	4.85	433.00	15.264	0.8099	-5.9213	-1514.4	-6.9987	3.80	530.0	7.33	-0.0143	
	Muscovite (mu)	-5976.56	2.90	292.00	14.083	0.7564	-1.9840	-2170.0	-6.9792	3.07	490.0	4.15	-0.0085	
	Na-phlogopite (naph)	-6171.92	1.99	318.00	14.450	0.7735	-4.0229	-2597.9	-6.5126	3.28	513.0	7.33	-0.0143	
	Paragonite (pa)	-5942.91	1.81	277.00	13.211	0.8030	-3.1580	217.0	-8.1510	3.70	515.0	6.51	-0.0126	
Other sheet silicates	Phlogopite (phl)	-6214.95	2.90	326.00	14.964	0.7703	-3.6939	-2328.9	-6.5316	3.80	513.0	7.33	-0.0143	
	Al-free chlorite (afchl)	-8728.65	2.27	439.00	21.570	1.1550	-0.0417	-4024.4	-9.9529	2.04	870.0	4.09	-0.0047	
	Amesite (ames)	-9039.80	1.96	413.00	20.710	1.1860	-0.2599	-3627.2	-10.6770	2.00	870.0	4.09	-0.0047	
	Clinochlore (clin)	-8909.23	1.55	437.00	21.140	1.1708	-0.1508	-3825.8	-10.3150	2.04	870.0	4.09	-0.0047	
	Daphnite (daph)	-7116.71	3.20	584.00	21.620	1.1920	-0.5940	-4826.4	-9.7683	2.27	870.0	4.09	-0.0047	
	Mn-chlorite (mchl)	-7702.37	8.36	595.00	22.590	1.1365	-0.5243	-5548.1	-8.9115	2.23	870.0	4.09	-0.0047	
	Sudoite (fsud)	-7900.11	2.08	456.00	20.400	1.4663	-4.7365	-1182.8	-14.3880	2.08	870.0	4.09	-0.0047	
	Sudoite (sud)	-8626.91	1.65	395.00	20.300	1.4361	-4.8749	-2748.5	-13.7640	1.99	870.0	4.09	-0.0047	
	Antigorite (atg)	-71416.61	15.14	3600.00	175.480	9.6210	-9.1183	-35941.6	-83.0342	2.60	496.0	6.31	-0.0127	
	Chrysotile (chr)	-4360.96	0.98	221.30	10.746	0.6247	-2.0770	-172.8	-5.6194	2.20	628.0	4.00	-0.0064	
Feldspar and feldspathoid	Fe-talc (fta)	-4798.43	4.24	352.00	14.225	0.5797	3.9494	-6459.3	-3.0881	1.80	430.0	6.17	-0.0144	
	Greenalite (gt)	-3297.65	1.69	310.00	11.980	0.5764	0.2984	-3757.0	-4.1662	2.28	630.0	4.00	-0.0063	
	Kaolinite (kao)	-4122.10	0.78	203.70	9.934	0.4367	-3.4295	-4055.9	-2.6991	2.51	645.0	4.12	-0.0064	
	Lizardite (liz)	-4369.14	1.08	212.00	10.645	0.6147	-2.0770	-172.8	-5.6194	2.20	710.0	3.20	-0.0045	
	Minnesoataite (minn)	-4819.29	1.49	355.00	14.851	0.5797	3.9494	-6459.3	-3.0881	1.80	430.0	6.17	-0.0144	
	Minnesoataite (mimm)	-5866.01	10.26	263.90	14.291	0.6222	0	-6385.5	-3.9163	1.80	430.0	6.17	-0.0144	
	Prehnite (fpre)	-5766.75	1.35	320.00	14.800	0.7371	-1.6810	-1957.3	-6.3581	1.58	1093.0	4.01	-0.0037	
	Prehnite (pre)	-6202.10	1.11	292.80	14.026	0.7249	-1.3865	-2059.0	-6.3239	1.58	1093.0	4.01	-0.0037	
	Prl-talc (tap)	-5589.24	1.03	245.00	13.450	0.7845	-4.2948	1251.0	-8.4959	4.50	370.0	10.00	-0.0271	
	Pyrophyllite (prl)	-5640.68	1.01	239.00	12.804	0.7845	-4.2948	1251.0	-8.4959	4.50	370.0	10.00	-0.0271	
Feldspar and feldspathoid	Stilpnomelane (fstp)	-12550.45	9.09	930.20	37.239	1.9443	-1.2289	-4840.2	-16.6350	3.68	513.0	7.33	-0.0143	
	Stilpnomelane (mstp)	-14288.03	25.51	847.40	36.577	1.8622	-1.4018	-8983.1	-14.9230	3.71	513.0	7.33	-0.0143	
	Talc (ta)	-5897.17	1.16	259.00	13.665	0.6222	0	-6385.5	-3.9163	1.80	430.0	6.17	-0.0144	
	Tschermak-talc (tats)	-5992.20	0.98	259.00	13.510	0.5495	3.6324	-8606.6	-2.5153	1.80	430.0	6.17	-0.0144	
	Albite (ab)	-3935.49	1.69	207.40	10.067	0.4520	-1.3364	-1275.9	-3.9536	2.36	541.0	5.91	-0.0109	
	Albite-high (abhh)	-3921.49	1.68	224.30	10.105	0.4520	-1.3364	-1275.9	-3.9536	2.40	541.0	5.91	-0.0109	
	Analcite (anl)	-3307.25	1.68	232.00	9.740	0.6435	-1.6067	9302.3	-9.1796	2.76	400.0	4.18	-0.0104	
Feldspar and feldspathoid	Anorthite (an)	-4232.70	0.79	200.50	10.079	0.3705	1.0010	-4339.1	-1.9606	1.41	860.0	4.09	-0.0048	
	Carnegieite-high (cgh)	-2077.99	1.76	135.00	5.670	0.2292	1.1876	0	-1.9707	4.67	465.0	4.16	-0.0089	
	Carnegieite-low (cg)	-2091.70	1.76	118.70	5.603	0.1161	8.6021	-1992.7	0	4.50	465.0	4.16	-0.0089	
	Kalsilite (cls)	-2122.89	2.91	136.00	6.052	0.2420	-0.4482	-895.8	-1.9358	3.16	514.0	2.00	-0.0039	

Table 2a. (Continued)

Group	End-member	Δ_fH	$\sigma(\Delta_fH)$	S	V	C_P				$\alpha\kappa$				ℓ
						a	b	c	d	α_0	κ_0	κ'_0	κ''_0	
Silica minerals	Leucite (lc)	-3029.23	2.82	198.50	8.826	0.3698	-1.6332	684.7	-3.6831	1.85	450.0	5.70	-0.0127	2
	Microcline (mic)	-3975.33	2.80	214.30	10.871	0.4488	-1.0075	-1007.3	-3.9731	1.65	583.0	4.02	-0.0069	
	Nepheline (ne)	-2094.54	1.75	124.40	5.419	0.2727	-1.2398	0	-2.7631	4.63	465.0	4.16	-0.0089	1
	Sanidine (san)	-3966.68	2.80	214.30	10.871	0.4488	-1.0075	-1007.3	-3.9731	1.65	583.0	4.02	-0.0069	2
Other framework silicates	Coesite (coe)	-907.02	0.27	39.60	2.064	0.1078	-0.3279	-190.3	-1.0416	1.23	979.0	4.19	-0.0043	
	Cristobalite (crst)	-904.24	0.27	50.86	2.745	0.0727	0.1304	-4129.0	0	0	160.0	4.35	-0.0272	
	Quartz (q)	-910.70	0.27	41.43	2.269	0.0929	-0.0642	-714.9	-0.7161	0	730.0	6.00	-0.0082	1
	Stishovite (stv)	-876.39	0.49	24.00	1.401	0.0681	0.6010	-1978.2	-0.0821	1.58	3090.0	4.60	-0.0015	
	Tridymite (trd)	-907.08	0.27	44.10	2.800	0.0749	0.3100	-1174.0	-0.2367	0	150.0	4.36	-0.0291	
Oxides	Heulandite (heu)	-10 545.09	1.80	783.00	31.700	1.5048	-3.3224	-2959.3	-13.2972	1.57	274.0	4.00	-0.0146	
	Hollandite (hol)	-37 91.94	5.27	166.20	7.128	0.4176	-0.3617	-4748.1	-2.8199	2.80	1800.0	4.00	-0.0022	
	Laumontite (lmt)	-7262.64	1.12	465.00	20.370	1.0134	-2.1413	-2235.8	-8.8067	1.37	860.0	4.09	-0.0048	
	Meionite (me)	-13 841.95	2.61	752.00	33.985	1.3590	3.6442	-8594.7	-9.5982	1.82	870.0	4.09	-0.0047	
	K-cymrite (kcm)	-4232.63	2.81	281.50	11.438	0.5365	-1.0090	-980.4	-4.7350	3.21	425.0	2.00	-0.0047	
	Sodalite (sdl)	-13405.41	10.54	910.00	42.130	1.5327	4.7747	-2972.8	-12.4270	4.63	465.0	4.16	-0.0089	
	Stilbite (stlb)	-10 896.63	2.23	710.00	32.870	1.5884	-3.2043	-3071.6	-13.9669	1.51	860.0	4.09	-0.0048	
	Wadeite (wa)	-4271.79	6.46	254.00	10.844	0.4991	0	0	-4.3501	2.66	900.0	4.00	-0.0044	
	Wairakite (wrk)	-6662.40	1.11	380.00	19.040	0.8383	-2.1460	-2272.0	-7.2923	1.49	860.0	4.09	-0.0048	
Hydroxides	Baddelyite (bdy)	-1100.34	1.63	50.40	2.115	0.1035	-0.4547	-416.2	-0.7136	2.00	953.0	3.88	-0.0041	
	Bixbyite (bix)	-959.00	1.09	113.70	3.137	0.1451	2.3534	721.6	-1.0084	2.91	2230.0	4.04	-0.0018	
	Corundum (cor)	-1675.33	0.75	50.90	2.558	0.1395	0.5890	-2460.6	-0.5892	1.80	2540.0	4.34	-0.0017	
	Cuprite (cup)	-170.60	0.11	92.40	2.344	0.1103	0	0	-0.6748	3.33	1310.0	5.70	-0.0043	
	Eskolaite (esk)	-1137.35	4.31	83.00	2.909	0.1190	0.9496	-1442.0	-0.0034	1.59	2380.0	4.00	-0.0017	
	Geikielite (geik)	-1568.97	0.89	73.60	3.086	0.1510	0	-1890.4	-0.6522	2.15	1700.0	8.30	-0.0049	
	Hematite (hem)	-825.65	0.68	87.40	3.027	0.1639	0	-2257.2	-0.6576	2.79	2230.0	4.04	-0.0018	1
	Hercynite (herc)	-1953.09	0.85	113.90	4.075	0.2167	0.5886	-2430.2	-1.1783	2.06	1922.0	4.04	-0.0021	2
	Ilmenite (ilm)	-1230.43	0.84	109.50	3.169	0.1389	0.5081	-1288.8	-0.4637	2.40	1700.0	8.30	-0.0049	1
	Lime (lime)	-634.61	0.50	38.10	1.676	0.0524	0.3673	-750.7	-0.0510	3.41	1130.0	3.87	-0.0034	
	Manganosite (mang)	-385.55	0.41	59.70	1.322	0.0598	0.3600	-31.4	-0.2826	3.69	1645.0	4.46	-0.0027	
	Mg-corundum (mcor)	-1474.43	2.87	59.30	2.635	0.1478	0.2015	-2395.0	-0.8018	2.12	2110.0	4.55	-0.0022	
	Magnesioferrite (mft)	-1442.29	2.71	121.00	4.457	0.2705	-0.7055	-999.2	-2.0224	3.63	1857.0	4.05	-0.0022	1
	Magnetite (mt)	-1114.51	0.95	146.90	4.452	0.2625	-0.7205	-1926.2	-1.6557	3.71	1857.0	4.05	-0.0022	1
	Ni-oxide (NiO)	-239.47	0.36	38.00	1.097	0.0477	0.7824	-392.5	0	3.30	2000.0	3.94	-0.0020	1
Carbonates	Periclase (per)	-601.55	0.27	26.50	1.125	0.0605	0.0362	-535.8	-0.2992	3.11	1616.0	3.95	-0.0024	
	Periclase (pfer)	-271.97	2.05	60.60	1.206	0.0444	0.8280	-1214.2	0.1852	7.43	1520.0	4.90	-0.0032	
	Picrochromite (picr)	-1762.60	3.28	118.30	4.356	0.1961	0.5398	-3126.0	-0.6169	1.80	1922.0	4.04	-0.0021	2
	Pyrophanite (pnt)	-1361.99	2.16	105.50	3.288	0.1435	0.3373	-1940.7	-0.4076	2.40	1700.0	8.30	-0.0049	
	Rutile (ru)	-944.37	0.78	50.50	1.882	0.0904	0.2900	0	-0.6238	2.24	2220.0	4.24	-0.0019	
	Spinel (sp)	-2301.26	0.84	82.00	3.978	0.2229	0.6127	-1686.0	-1.5510	1.93	1922.0	4.04	-0.0021	2
	Tenorite (ten)	-156.10	2.18	42.60	1.222	0.0310	1.3740	-1258.0	0.3693	3.57	2000.0	3.94	-0.0020	
Sulphides and halides	Ulvospinel (usp)	-1491.10	1.01	180.00	4.682	-0.1026	14.2520	-9144.5	5.2707	3.86	1857.0	4.05	-0.0022	
	Brucite (br)	-925.65	0.30	63.20	2.463	0.1584	-0.4076	-1052.3	-1.1713	6.20	415.0	6.45	-0.0155	
	Diaspore (dsp)	-999.86	0.38	34.50	1.786	0.1451	0.8709	584.4	-1.7411	3.57	2280.0	4.04	-0.0018	
	Goethite (gth)	-561.79	0.35	60.30	2.082	0.1393	0.0147	-212.7	-1.0778	4.35	2500.0	4.03	-0.0016	
	Ankerite (ank)	-1970.62	0.77	188.46	6.606	0.3410	-0.1161	0	-3.0548	3.46	914.0	3.88	-0.0043	2
	Aragonite (arag)	-1207.82	0.46	89.80	3.415	0.1923	-0.3052	1149.7	-2.1183	6.14	614.0	5.87	-0.0096	1
Elements	Calcite (co)	-1207.88	0.46	92.50	3.689	0.1409	0.5029	-950.7	-0.8584	2.52	733.0	4.06	-0.0055	1
	Dolomite (dol)	-2325.76	0.58	156.10	6.429	0.3589	-0.4905	0	-3.4562	3.28	943.0	3.74	-0.0040	2
	Magnesite (mag)	-1110.93	0.32	65.50	2.803	0.1864	-0.3772	0	-1.8862	3.38	1028.0	5.41	-0.0053	
	Rhodochrosite (rhc)	-892.28	0.41	98.00	3.107	0.1695	0	0	-1.5343	2.44	953.0	3.88	-0.0041	
	Siderite (sid)	-762.22	0.57	93.30	2.943	0.1684	0	0	-1.4836	4.39	1200.0	4.07	-0.0034	
	Anhydrite (any)	-1434.40	3.50	106.90	4.594	0.1287	4.8545	-1223.0	-0.5605	4.18	543.8	4.19	-0.0077	
	Halite (hl)	-411.30	0.22	72.10	2.702	0.0452	1.7970	0	0	11.47	238.0	5.00	-0.0210	
	Pyrite (pyr)	-171.64	1.28	52.90	2.394	0.0373	2.6715	-1817.0	0.6493	3.10	1395.0	4.09	-0.0029	
	Pyrrhotite (trot)	-99.03	1.34	65.50	1.819	0.0502	1.1052	-940.0	0	5.68	658.0	4.17	-0.0063	1
	Pyrrhotite (trov)	-96.02	1.17	57.50	1.738	0.0511	0.8307	-669.7	0	5.94	658.0	4.17	-0.0063	1
Gas species	Troilite (tot)	-102.16	0.48	60.00	1.818	0.0502	1.1052	-940.0	0	4.93	658.0	4.17	-0.0063	1
	Troilite (tro)	-97.76	0.48	70.80	1.819	0.0502	1.1052	-940.0	0	5.73	658.0	4.17	-0.0063	1
	Sylvite (sylv)	-436.50	0.22	82.60	3.752	0.0462	1.7970	0	0	11.09	170.0	5.00	-0.0294	
	Copper (Cu)	0	0.00	33.14	0.711	0.0124	0.9220	-379.9	0.2335	3.58	1625.0	4.24	-0.0026	
	Diamond (diam)	2.00	0.06	2.38	0.342	0.0243	0.6272	-377.4	-0.2734	0.49	4465.0	1.61	-0.0004	
	Graphite (gph)	0.00	0.00	5.74	0.530	0.0510	-0.4429	488.6	-0.8055	1.67	312.0	3.90	-0.0125	
	Iron (iron)	0.00	0.00	27.09	0.709	0.0462	0.5159	723.1	-0.5562	3.56	1640.0	5.16	-0.0031	1
	Nickel (Ni)	0.00	0.00	29.87	0.659	0.0498	0	585.9	-0.5339	4.28	1905.0	4.25	-0.0022	1
	Sulphur (S)	0.00	0.00	32.05	1.551	0.0566	-0.4557	638.0	-0.6818	6.40	145.0	7.00	-0.0063	
	Methane (CH_4)	-74.81	0.37	186.26	0	0.1501	0.2063	3427.7	-2.6504	0	0	0	0	
	Carbon monoxide (CO)	-110.53	0.19	197.67	0	0.0457	-0.0097	662.7	-0.4147	0	0	0	0	
	Carbon dioxide (CO_2)	-393.51	0.08	213.70	0	0.0878	-0.2644	706.4	-0.9989	0	0	0	0	
	Hydrogen (H_2)	0.00	0.00	130.70	0	0.0233	0.4627	0	0.0763	0	0	0	0	
	Hydrogen sulphide (H_2S)	-20.30	0.44	205.77	0	0.0474	1.0240	615.9	-0.3978	0	0	0	0	

Table 2a. (Continued)

Group	End-member	$\Delta_f H$	$\sigma(\Delta_f H)$	S	V	C_p				$\alpha\kappa$			ℓ	
						a	b	c	d	α_0	κ_0	κ'_0	κ''_0	
	Oxygen (O ₂)	-0.00	0.00	205.20	0	0.0483	-0.0691	499.2	-0.4207	0	0	0	0	
	Sulphur gas (S ₂)	128.54	0.32	231.00	0	0.0371	0.2398	-161.0	-0.0650	0	0	0	0	
	Water (H ₂ O)	-241.81	0.02	188.80	0	0.0401	0.8656	487.5	-0.2512	0	0	0	0	
Melt species	Albite liq (abL)	-3926.05	1.69	149.90	10.858	0.3580	0	0	0	3.37	176.0	14.35	-0.0815	4
	Anorthite liq (anL)	-4277.91	0.84	29.00	10.014	0.4300	0	0	0	5.14	210.0	6.38	-0.0304	4
	Corundum liq (corL)	-1632.02	1.02	14.90	3.369	0.1576	0	0	0	7.03	150.0	6.00	0	4
	Diopside liq (diL)	-3193.70	0.70	42.10	7.288	0.3340	0	0	0	8.51	249.0	8.04	-0.0323	4
	Enstatite liq (enL)	-3096.58	0.80	-4.00	6.984	0.3536	0	0	0	6.81	218.0	7.20	-0.0330	4
	Fayalite liq (faL)	-1463.04	0.71	96.00	4.677	0.2437	0	0	0	10.71	290.0	10.42	-0.0359	4
	Forsterite liq (foL)	-2237.32	0.60	-62.00	4.312	0.2694	0	0	0	9.20	362.0	10.06	-0.0278	4
	Water liq (h ₂ oL)	-295.01	0.03	45.50	1.460	0.0800	0	0	0	46.33	46.2	1.50	-0.0325	4
	Halite liq (hltL)	-392.99	0.23	80.10	2.938	0.0720	-0.3223	0	0	29.50	64.0	4.61	-0.0720	4
	K-feldspar liq (kspL)	-3980.06	2.80	132.20	11.431	0.3680	0	0	0	4.93	174.0	6.84	-0.0393	4
	Leucite liq (leL)	-3068.37	2.82	102.00	8.590	0.2870	0	0	0	6.70	175.0	7.00	-0.0394	4
	Lime liq (limL)	-692.37	0.52	-47.50	1.303	0.0990	0	0	0	17.50	362.0	10.06	-0.0278	4
	Nepheline liq (neL)	-2116.71	1.76	52.90	5.200	0.2165	0	0	0	13.70	250.0	7.37	-0.0295	4
	Periclaste liq (perL)	-654.14	0.36	-64.30	0.839	0.0990	0	0	0	22.60	362.0	10.06	-0.0278	4
	Quartz liq (qL)	-921.03	0.27	16.30	2.730	0.0825	0	0	0	0	220.0	9.46	-0.0430	4
	Sillimanite liq (silL)	-2594.05	1.79	10.00	6.051	0.2530	0	0	0	4.08	220.0	6.36	-0.0289	4
	Sylvite liq (syvL)	-417.41	0.23	94.50	3.822	0.0669	0	0	0	30.10	56.0	4.65	-0.0830	4
	Wollastonite liq (woL)	-1642.20	0.51	22.50	3.965	0.1674	0	0	0	6.69	305.0	9.38	-0.0308	4
Aqueous species	H ⁺	0	0.00	0	0	0	0	0	0	0	0	0	0	3
	Cl ⁻	-167.08	0.11	56.73	1.779	0	0	0	0	0	0	0	0	3
	OH ⁻	-230.02	0.11	-10.71	-0.418	0	0	0	0	0	0	0	0	3
	Na ⁺	-240.30	0.11	58.40	-0.111	0	19.1300	0	0	0	0	0	0	3
	K ⁺	-252.17	0.11	101.04	0.906	0	7.2700	0	0	0	0	0	0	3
	Ca ⁺⁺	-543.30	1.09	-56.50	-1.806	0	-6.9000	0	0	0	0	0	0	3
	Mg ⁺⁺	-465.96	1.09	-138.10	-2.155	0	-4.6200	0	0	0	0	0	0	3
	Fe ⁺⁺	-90.42	3.28	-107.11	-2.220	0	0	0	0	0	0	0	0	3
	Al ⁺⁺⁺	-527.23	1.64	-316.30	-4.440	0	0	0	0	0	0	0	0	3
	CO ₃ ⁻⁻	-675.23	0.11	-50.00	-0.502	0	0	0	0	0	0	0	0	3
	AlOH ₃	-1251.85	1.09	53.60	0	0	0	0	0	0	0	0	0	3
	AlOH ₄ ⁻	-1495.78	1.09	126.90	0	0	0	0	0	0	0	0	0	3
	KOH	-473.62	1.31	109.62	-0.800	0	9.4500	0	0	0	0	0	0	3
	HCl	-162.13	0.87	56.73	1.779	0	9.0300	0	0	0	0	0	0	3
	KCl	-400.03	1.42	184.81	4.409	0	5.4300	0	0	0	0	0	0	3
	NaCl	-399.88	1.20	126.09	2.226	0	19.1300	0	0	0	0	0	0	3
	CaCl ₂	-877.06	1.31	46.00	3.260	0	13.6900	0	0	0	0	0	0	3
	CaCl ⁺	-701.28	1.75	27.36	0.574	0	-6.9000	0	0	0	0	0	0	3
	MgCl ₂	-796.08	2.29	-22.43	2.920	0	23.9900	0	0	0	0	0	0	3
	MgCl ⁺	-632.48	0.87	-81.37	0.126	0	-4.6200	0	0	0	0	0	0	3
	FeCl ₂	-375.34	3.28	109.88	2.700	0	45.0300	0	0	0	0	0	0	3
	aqSi	-887.81	0.68	46.35	1.832	0	17.7500	0	0	0	0	0	0	3
	HS ⁻	-16.04	5.46	68.00	2.065	0	0	0	0	0	0	0	0	3
	HSO ₃ ⁻	-623.82	5.46	139.00	3.330	0	0	0	0	0	0	0	0	3
	SO ₄ ²⁻	-906.12	5.46	18.80	1.388	0	0	0	0	0	0	0	0	3
	HSO ₄ ⁻	-885.70	5.46	125.04	3.520	0	0	0	0	0	0	0	0	3

$\Delta_f H$ is the regressed enthalpy of formation from the elements; $\sigma(\Delta_f H)$ is 1 SD on the enthalpy of formation; S is the entropy; V the volume (all properties at 1 bar and 298 K); a , b , c and d are the coefficients in the heat capacity polynomial $C_p = a + bT + cT^{-2} + dT^{-1/2}$; α and κ are thermal expansion and bulk modulus; α_0 is the thermal expansion parameter; κ_0 , κ'_0 and κ''_0 are the bulk modulus (at 298 K, 1 bar) and its first and second pressure derivatives; ℓ is a flag, 1 signifying a phase transition described via Landau theory and 2 signifying a phase transition described via Bragg-Williams theory, 3 signifies an aqueous species and 4 signifies a melt end-member.

and κ'_0 and κ''_0 are the first and second derivatives of κ_0 with pressure also at ambient conditions. Conversely,

$$\begin{aligned}\kappa_0 &= \frac{1}{abc}, \\ \kappa'_0 &= \frac{c+1}{ac} - 1, \\ \kappa''_0 &= \frac{b}{a}(1-a)(c+1).\end{aligned}\quad (4)$$

By substituting equation (3) into equation (1) or (2) and setting $\kappa''_0 = 0$, TEOS reduces to the simpler two-parameter Murnaghan equation, with

$$a = 1, \quad b = \frac{\kappa'_0}{\kappa_0} \quad \text{and} \quad c = \frac{1}{\kappa'_0}$$

and

$$\frac{V}{V_0} = (1+bP)^{-c},$$

as used in HP98, with, as a default there, $\kappa'_0 = 4$ (or $c = \frac{1}{4}$).

A major advantage of the three-parameter TEOS over Murnaghan is that the inclusion of the second

Table 2b. Landau theory parameters used for end-members in the data set.

	T_c	S_{\max}	V_{\max}
lrn	1710	10.03	0.0500
sph	485	0.40	0.0050
q	847	4.95	0.1188
ne	467	10.00	0.0800
hem	955	15.60	0
NiO	520	5.70	0
ilm	1900	12.00	0.0200
mt	848	35.00	0
mft	665	17.00	0
cc	1240	10.00	0.0400
arag	1240	9.00	0.0450
trot	598	12.00	0.0410
tro	598	12.00	0.0410
lot	420	10.00	0
trov	595	10.00	0.0160
iron	1042	8.30	0
Ni	631	3.00	0

T_c is the critical temperature at 1 bar, S_{\max} and V_{\max} are the entropy of disordering at T_c . See Holland & Powell (1998) for further details.

Table 2c. Symmetric formalism (SF; a generalized Bragg-Williams theory) parameters used for end-members in the data set.

	ΔH	ΔV	W	W_V	n	Fac
sill	4.75	0.0100	4.75	0.0100	1	0.25
geh	7.51	0.0900	7.50	0.0900	1	0.80
crd	36.71	0.1000	36.70	0.1000	2	1.50
herd	36.71	0.1000	36.70	0.1000	2	1.50
ferd	36.71	0.1000	36.70	0.1000	2	1.50
mncrd	36.71	0.1000	36.70	0.1000	2	1.50
cats	3.80	0.0100	3.80	0.0100	1	0.25
ab	14.00	0.0420	13.00	0.0420	3	0.90
san	8.65	0.0240	8.50	0.0240	3	0.80
an	42.01	0.1000	42.00	0.1000	1	2.00
lc	11.61	0.4000	11.60	0.4000	2	0.70
sp	8.00	0	1.20	0	2	0.50
herc	18.30	0	13.60	0	2	1.00
picr	8.00	0	1.20	0	2	0.50
dol	11.91	0.0160	11.90	0.0160	1	1.00
ank	11.91	0.0160	11.90	0.0160	1	1.00

ΔH and ΔV are the total enthalpy and volume of disordering, W and W_V are the interaction energy terms used in $W = W_H + PW_V$, n is the number of Si disordering with each Al, and fac is a scaling factor on the energy of disordering. See Holland & Powell (1996a,b) for further details.

derivative of bulk modulus gives more flexibility, and allows extrapolation to very high pressures in a sensible fashion when the size and sign of κ''_0 is known. Although Freund & Ingalls (1989) state that experiments do not allow this term to be determined to better than 100% error, their applications suggest that all the successful EOS do seem to point to a fairly uniform but small negative value of κ''_0 for the range of elements and compressible compounds investigated. Jackson & Niesler (1982) suggested that $\kappa''_0 \approx -\phi/\kappa_0$, where ϕ is a small number between 0 and 10, and this was confirmed for periclase by Jacobs & Oonk (2000). More importantly, a negative value for κ''_0 is shown to be a requirement in the analysis of Stacey (2005), and should therefore be implemented in such an EOS. Here, to maintain this

Table 2d. Values for $d\kappa_0/dT$, the temperature dependence of the bulk modulus for melt end-members in the data set.

	$d\kappa_0/dT$
SyvL	-0.02000
hlL	-0.01500
perL	-0.04100
limL	-0.04100
corL	-0.03500
qL	-0.03500
h2oL	-0.00001
foL	-0.04400
faL	-0.05500
woL	-0.02000
enL	-0.02400
diL	-0.03730
silL	-0.02900
anL	-0.05500
kspL	-0.00900
abL	-0.02600
neL	-0.02600
lcL	0

See Holland & Powell (1998) for further details.

Table 2e. $C_{P,\text{aq}}$, the augmented b term in the heat capacity for aqueous species in the modified density model of Anderson *et al.*, (1991), $C_p^* = C_p^\circ + bT$.

	$C_{P,\text{aq}}$
Na ⁺	0.0306
K ⁺	0.0072
AlOH ₃	0.1015
AlOH ₄ ⁻	0.0965
HCl	0.0540
CaCl ₂	0.0343
CaCl ⁺	0.0400
MgCl ₂	0.0186
MgCl ⁺	0.1126
FeCl ₂	0.0124
aqSi	0.0283
SO ₄ ²⁻	0.2680
HSO ₄ ⁻	0.0220

See Holland & Powell (1998) for further details.

requirement for a small negative κ''_0 , we adopt the heuristic $\kappa''_0 = -\kappa'_0/\kappa_0$, with ϕ chosen to scale with κ'_0 (see below). With this, the isothermal TEOS can be written in two-parameter form as:

$$\frac{V}{V_0} = -\kappa'_0 + (1 + \kappa'_0) \left(1 + \frac{\kappa'_0(2 + \kappa'_0)}{\kappa_0(1 + \kappa'_0)} P \right)^{-1/(2 + \kappa'_0)},$$

or as

$$\frac{V}{V_0} = 1 - \sqrt{\frac{1+c}{c}} (1 - (1 + bP)^{-c}). \quad (5)$$

The relationship between TEOS and the commonly used third-order Birch-Murnaghan, can be seen in series expansion. The latter can be written as:

$$P = 3f(1 + 2f)^{5/2} \left(\kappa_0 + \frac{3}{2} \kappa_0(\kappa'_0 - 4)f \right)$$

with the Eulerian strain $f = 1/2(y^{2/3} - 1)$, and $y = V_0/V$. Now, Murnaghan in terms of y is:

Table 3a. Regressed values for enthalpy of formation (kJ/mol) from the elements and their uncertainties compared with the compilation of Robie & Hemingway (1995). The $\Delta_f H$ and corresponding standard deviation (σ) are from the original data tabulation, for ambient conditions. The e^* are residuals, the difference between fitted values and tabulated values, normalised to σ . The fitted values and their standard deviations are given in Table 2. hat is the diagonal element of the hat matrix.

	$\Delta_f H$	σ	e^*	hat
fo	-2173.00	2.00	-0.22	0.07
fa	-1478.20	1.40	-0.34	0.20
teph	-1731.50	3.00	0.82	0.10
lrn	-2306.70	3.00	0.11	0.08
py	-6285.00	4.00	-0.72	0.06
alm	-5264.70	5.00	-0.81	0.06
gr	-6643.00	3.00	-0.02	0.20
andr	-5771.00	5.90	-0.32	0.06
and	-2589.90	2.00	-0.59	0.10
ky	-2593.80	2.00	-0.39	0.10
sill	-2586.10	2.00	-0.13	0.10
ak	-3865.40	3.00	0.08	0.08
crd	-9161.50	5.90	0.34	0.06
sph	-2602.90	3.00	-0.41	0.09
zrc	-2034.20	3.10	0.27	0.24
en	-3091.20	3.00	-0.32	0.04
cen	-3091.10	3.00	0.01	0.04
fs	-2390.40	6.00	-0.28	0.02
di	-3201.50	2.00	0.10	0.08
jd	-3029.30	3.60	-1.12	0.18
cats	-3306.30	5.00	0.77	0.02
rhod	-1321.60	2.00	0.38	0.11
pxmn	-1322.30	2.00	0.42	0.11
wo	-1634.80	1.40	-0.75	0.09
pswo	-1627.60	1.40	0.25	0.09
prl	-5640.00	1.50	0.46	0.38
ta	-5897.20	2.00	-0.02	0.28
kao	-4120.10	4.00	0.50	0.03
chr	-4360.00	3.00	0.32	0.09
ab	-3935.00	2.60	0.19	0.35
abh	-3921.00	5.00	0.10	0.10
mic	-3974.60	3.90	0.19	0.43
san	-3965.60	4.10	0.26	0.39
an	-4234.00	3.00	-0.43	0.06
q	-910.70	0.50	-0.01	0.25
trd	-907.00	4.00	0.02	0.00
coe	-905.60	2.10	0.67	0.01
ne	-2092.10	3.90	0.63	0.17
cg	-2089.30	4.00	0.60	0.16
anl	-3310.10	5.00	-0.57	0.09
lime	-635.10	0.90	-0.54	0.26
ru	-944.00	0.80	0.46	0.79
per	-601.60	0.30	-0.18	0.70
fper	-260.00	5.00	-0.03	0.42
mang	-385.20	0.50	0.71	0.57
cor	-1675.70	1.30	-0.28	0.28
hem	-826.20	1.30	-0.43	0.23
bix	-959.00	1.00	0	1.00
NiO	-239.30	0.40	0.44	0.69
pnt	-1360.10	4.00	0.47	0.24
ilm	-1232.00	2.50	-0.63	0.09
bdy	-1100.60	1.70	-0.15	0.77
ten	-156.10	2.00	0	1.00
cup	-170.60	0.10	0	1.00
sp	-2299.10	2.00	1.08	0.15
mt	-1115.73	2.10	-0.58	0.17
mft	-1441.50	3.00	0.26	0.68
usp	-1493.80	3.00	-0.90	0.09
pirc	-1762.60	3.00	0	1.00
br	-924.50	2.00	0.58	0.02
dsp	-1000.60	5.00	-0.15	0.00
gth	-562.60	2.10	-0.39	0.02
cc	-1207.40	1.30	0.37	0.11
arag	-1207.40	1.40	0.30	0.09
mag	-1113.30	4.00	-0.59	0.01
sid	-760.60	3.00	0.54	0.03
rhc	-892.90	0.50	-1.24	0.58
dol	-2324.50	1.50	0.84	0.13
syv	-436.50	0.20	0	1.00
hlt	-411.30	0.20	0	1.00
pyr	-171.50	1.70	0.08	0.48
lot	-101.00	3.00	0.39	0.02
trov	-97.50	5.00	-0.30	0.05
any	-1434.40	3.20	0	1.00
diam	1.90	0.10	-1.01	0.26
S ₂	128.60	0.30	0.19	0.98
H ₂ S	-20.60	0.70	-0.42	0.33

	Reaction	T °C	H (cal)	σ	H (298)	e^*	hat
mwd	mwd = fo	702	30.0	3.0	32.3	-0.6	0.02
mrw	mrw = fo	702	39.1	2.6	43.6	-0.5	0.04
mrw	mrw = mwd	702	9.1	2.6	11.2	0.1	0.01
fwd	fwd = fa	702	9.6	1.3	9.6	-0.2	0.23
frw	frw = fwd	702	-5.8	2.7	-4.1	-0.1	0.07
mak	mak = mpv	697	-51.1	6.6	-51.0	-0.5	0.00
mak	2mak = en	697	118.2	8.6	121.8	1.5	0.01
mrw	mrw = mpv + per	697	-96.8	5.8	-92.8	-1.7	0.01
mag	mag = per + CO ₂	25	-116.8	1.0	-116.8	-0.9	0.03
cc	cc = lime + CO ₂	25	-178.3	1.2	-178.3	1.2	0.04
dol	dol = per + lime + 2CO ₂	25	-304.3	1.9	-304.3	-0.9	0.03
sill	sill = cor + q	697	-2.4	1.2	-0.5	-0.6	0.00
and	and = cor + q	697	-5.0	1.2	-3.6	-0.7	0.00
ky	ky = cor + q	697	-8.3	1.2	-7.1	-0.1	0.00
sp	sp = per + cor	697	-22.5	1.2	-25.7	-1.1	0.03
py	py = 3per + cor + 3q	697	-74.1	5.5	-69.8	0.1	0.01
py	2py = 3en + 2cor	700	55.5	8.6	61.0	0.5	0.00
fo	fo = 2per + q	750	-59.5	1.9	-58.0	0.4	0.04
en	en = 2per + 2q	697	-67.9	3.5	-66.8	-0.3	0.01
mont	mont = lime + per + q	750	-104.8	1.7	-103.4	0.6	0.03
ak	ak = 2lime + per + 2q	750	-178.2	1.6	-172.5	0.6	0.11
crd	crd = 2per + 2cor + 5q	697	-68.9	3.0	-58.6	-0.8	0.02
spr4	spr4 = 4per + 4cor + 2q	697	-85.7	4.0	-87.7	1.4	0.04
di	di = lime + per + 2q	697	-146.4	1.7	-143.6	0.3	0.04
wo	wo = lime + q	697	-89.9	1.5	-87.8	0.4	0.03
pswo	pswo = lime + q	697	-83.3	1.3	-80.3	1.8	0.04
an	an = wo + cor + q	727	-13.5	1.5	-10.7	1.5	0.03
rhod	rhod = mang + q	713	-26.4	1.3	-24.4	1.3	0.22
rhod	rhod = ppxm	713	0.2	2.0	0.2	-0.3	0.00
zrc	zrc = q + bdy	25	-24.0	3.0	-24.0	0.0	0.01
ky	ky = sill	701	-6.2	1.2	-6.8	0.3	0.00
and	and = sill	701	-2.8	1.0	-3.3	-0.4	0.01
herd	herd = crd + H ₂ O	25	-42.5	3.0	-42.5	0.5	0.00
clin	2clin = ames + afchl	25	-50.0	1.0	-50.0	0	1.00
ep	2ep = fep + cz	25	-25.0	10.0	-25.0	0.0	0.00
ab	ab = abh	25	-14.0	0.1	-14.0	-0.0	0.98
mic	mic = san	25	-8.6	0.1	-8.6	-0.0	1.00
cg	cg = cgh	693	-8.1	1.0	-13.7	0.0	0.00
stv	stv = coe	25	29.9	1.2	29.9	-0.6	0.10
CO ₂	CO ₂ = gph + O ₂	25	-393.5	0.1	-393.5	0.1	0.98
H ₂ O	2H ₂ O = 2H ₂ + O ₂	25	-483.6	0.0	-483.6	-0.0	1.00
H ₂ S	H ₂ S = 2H ₂ + S	25	-20.6	0.6	-20.6	-0.5	0.45
CH ₄	CH ₄ = gph + 2H ₂	25	-74.8	0.3	-74.8	0	1.00
CO	2CO = 2gph + O ₂	25	-221.1	0.3	-221.1	0	1.00
aqSi	aqSi = q	25	22.9	0.6	22.9	0	1.00
corL	corL = cor	2050	107.5	5.4	42.8	-0.1	0.04
diL	diL = di	1397	137.7	7.0	8.1	0.0	0.00
faL	faL = fa	1217	90.0	3.0	14.0	-0.2	0.00
foL	foL = fo	1890	114.0	15.0	-61.0	0.3	0.00
anL	anL = an	1557	134.0	3.0	-38.2	2.3	0.01
abL	abL = abh	1120	64.5	3.0	-6.9	-0.8	0.00
kspL	kspL = san	1200	63.0	5.0	-14.4	-0.2	0.00
qL	qL = crst	1726	8.9	2.0	-17.0	-0.1	0.00
enL	enL = en	1561	155.6	12.0	-9.8	-0.3	0.00
woL	woL = pswo	1544	57.3	2.9	-14.5	-0.1	0.00
neL	neL = ne	1447	46.3	2.0	-22.2	-0.0	0.00
lcL	lcL = lc	1686	40.0	10.0	-38.4	0.1	0.00
cgh	cgh = neL	1526	-21.7	3.0	39.7	0.3	0.00
perL	perL = per	2825	77.0	10.0	-53.7	-0.1	0.00
limL	limL = lime	2572	52.0	10.0	-57.9	-0.0	0.00
lot	lot = iron + S	25	-102.6	3.0	-102.6	-0.1	0.02
pyr	pyr = iron + 2S	25	-171.6	1.7	-171.6	-0.0	0.48

Table 3b. Oxide and reaction calorimetry. Enthalpies (kJ), with uncertainty (σ), are given at T and 298K. e^* is the normalised enthalpy residual, and hat is the diagonal element of the hat matrix.

$$P = \frac{\kappa_0}{\kappa'_0} (y^{\kappa'_0} - 1). \quad (6)$$

Accepting that this EOS works well at small compression, TEOS, equation (2), and third-order Birch–Murnaghan, equation (6), can be expanded in terms of

$y^{\kappa'_0}$ around 1 (i.e. no compression). For TEOS to the third power in $y^{\kappa'_0} - 1$ this gives

$$P = \frac{\kappa_0}{\kappa'_0} (y^{\kappa'_0} - 1) \left(1 + \frac{1}{6} \kappa''_0 \frac{\kappa_0}{\kappa'^2_0} (y^{\kappa'_0} - 1)^2 + \dots \right), \quad (7)$$

and for third-order Birch–Murnaghan

$$P = \frac{\kappa_0}{\kappa'_0} (y^{\kappa'_0} - 1) \\ \left(1 + \frac{1}{6} \left\{ \left(7 - \kappa'_0 - \frac{143}{9\kappa'_0} \right) \frac{\kappa'_0}{\kappa_0} \right\} \frac{\kappa_0}{\kappa'^2} (y^{\kappa'_0} - 1)^2 + \dots \right), \quad (8)$$

with this written such that the term in curly brackets corresponds to

$$(\kappa''_0)_{\text{bm}3} = \left(\frac{\partial^2 \kappa}{\partial P^2} \right)_{T, P_0, T_0} = \left(7 - \kappa'_0 - \frac{143}{9\kappa'_0} \right) \frac{\kappa'_0}{\kappa_0}. \quad (9)$$

This brings out that in third-order Birch–Murnaghan, κ''_0 is specified by κ_0 and κ'_0 , in contrast to TEOS where κ''_0 is a free parameter to be determined from data (or, e.g. via the heuristic above). Note that the term in brackets in equation (9) is close to -1 for $\kappa'_0 \approx 4$, in relation to the heuristic adopted above to approximate κ''_0 . Note also that fourth-order Birch–Murnaghan reduces to third order if the adjustable parameter $(\kappa''_0)_{\text{bm}4}$ is substituted with the above expression for $(\kappa''_0)_{\text{bm}3}$. Analogously fourth-order Birch–Murnaghan reduces to third-order Birch–Murnaghan, approximately, if the above heuristic, $\kappa''_0 = -(\kappa'_0/\kappa_0)$ is adopted. Similar to third-order Birch–Murnaghan, in the so-called universal EOS of Vinet (e.g. Stacey, 2005), κ''_0 is specified by κ_0 and κ'_0

$$(\kappa''_0)_{\text{vinet}} = \left(\frac{\partial^2 \kappa}{\partial P^2} \right)_{T, P_0, T_0} = \left(-\frac{1}{2} - \frac{\kappa'_0}{4} + \frac{19}{36\kappa'_0} \right) \frac{\kappa'_0}{\kappa_0} \quad (10)$$

and an exactly equivalent expression to equation (8) can be written for it.

The EOS adopted here, equation (1), or with the κ''_0 heuristic, equation (5), is derived only for ambient temperature. We may extend it to high temperature by adding a thermal pressure term P_{th} to equation (2), and using the relationship (Anderson, 1997):

$$P_{\text{th}} = \int_{T_0}^T \alpha \kappa dT \Big|_V. \quad (11)$$

For the very few phases that there are sufficient data, Anderson (1997) showed that there is no simple relationship to use for $\alpha \kappa$ as a function of T , with $\alpha \kappa$ for some phases becoming constant to high- T , while others increase or decrease slightly. Rearranging the Grüneisen relation gives $\alpha \kappa = (\gamma/V) C_v$, and noting that γ/V is nearly independent of temperature, the form of $\alpha \kappa$ should have the shape of a heat capacity function, rising to an approximately constant value. That this is approximately so may be seen for the phases tabulated in Anderson & Isaak (1995) and illustrated here for their forsterite data in Fig. 1a. Here we adopt the simplest regularization that $\alpha \kappa$ becomes constant to high- T , taking an Einstein function to represent how $\alpha \kappa$ decreases to zero as temperature decreases to 0 K:

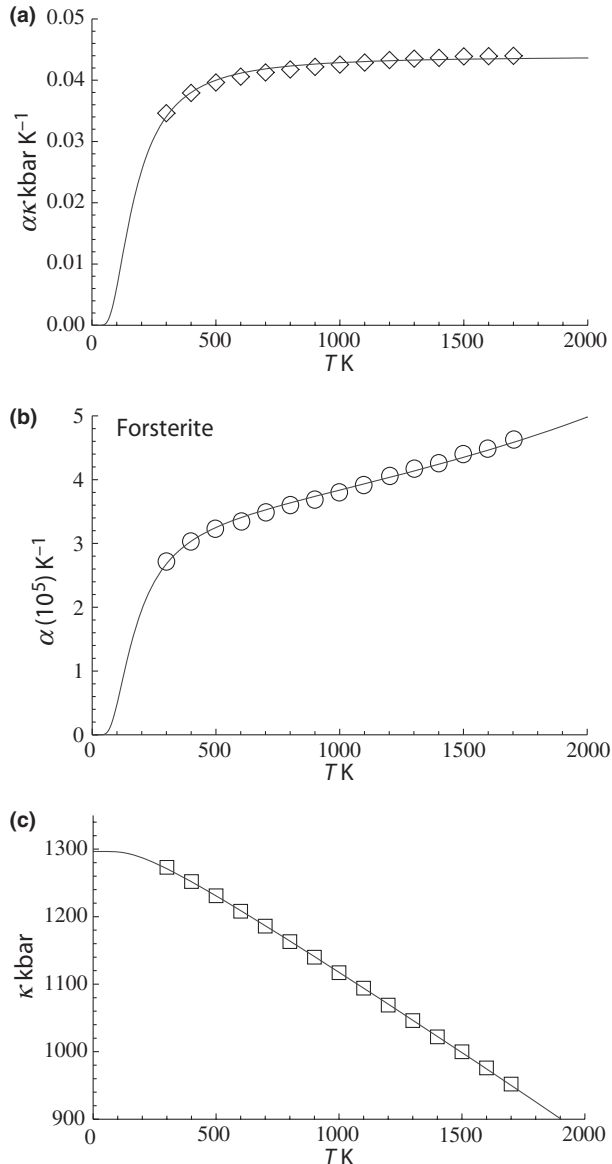


Fig. 1. For forsterite, (a) $\alpha \kappa$, (b) α and (c) κ , are shown as a function of temperature, at 1 bar. The shape of the temperature dependence is a consequence of the involvement of the Einstein function in the thermal pressure term. The symbols are data from Anderson & Isaak (1995) and the curves are Tait equation of state fits to their data. The Anderson and Isaak data are used here because they present separate values for α and κ , but for the thermodynamic data set itself we have preferred to use the experimental molar volumes listed in Appendix 1.

$$\xi = \frac{u^2 e^u}{(e^u - 1)^2}$$

with $u = \theta/T$, and θ the Einstein temperature. For equation (11), $\alpha \kappa$ is written as $\alpha \kappa = n \xi$, where n is a normalization constant, equal to $\alpha \kappa$ at infinite temperature, so $n = \alpha_0 \kappa_0 (1/\xi_0)$, and $\alpha \kappa = \alpha_0 \kappa_0 (\xi/\xi_0)$, with α_0 , κ_0 and ξ_0 being the values of α , κ and ξ at ambient temperature. Then, using equation (11)

$$\begin{aligned} P_{\text{th}} &= \int_{T_0}^T \alpha_0 \kappa_0 \frac{\xi}{\xi_0} dT = \alpha_0 \kappa_0 \frac{1}{\xi_0} \int_{T_0}^T \alpha_0 \kappa_0 \xi dT \\ &= \alpha_0 \kappa_0 \frac{\theta}{\xi_0} \left(\frac{1}{e^u - 1} - \frac{1}{e^{u_0} - 1} \right). \end{aligned}$$

Writing $P = P|_{T_0} + P_{\text{th}}$, this may be rearranged in volume explicit form as:

$$\frac{V}{V_0} = 1 - a(1 - (1 + b(P - P_{\text{th}}))^{-c}). \quad (12)$$

Integrating V with respect to P gives the G contribution

$$\begin{aligned} G|_{P,T} - G|_{P_0,T} &= PV_0 \left(1 - a + \frac{a((1 - bP_{\text{th}})^{1-c} - (1 + b(P - P_{\text{th}}))^{1-c})}{b(c-1)P} \right) \end{aligned} \quad (13)$$

This EOS contains an implicit thermal expansion at ambient pressure conditions. At $P=0$, the thermal expansion α is:

$$\begin{aligned} \alpha &= \frac{1}{V} \left(\frac{\partial V}{\partial T} \right)_P \Big|_{P_0} \\ &= \alpha_0 \frac{\xi}{\xi_0} \left(\frac{1}{(1 - bP_{\text{th}})(a + (1 - a)(1 - b(P - P_{\text{th}}))^c)} \right). \end{aligned}$$

The compressibility is also a function of temperature and pressure, given by

$$\begin{aligned} \kappa &= -V \left(\frac{\partial P}{\partial V} \right)_T \\ &= \kappa_0 (1 + b(P - P_{\text{th}}))(a + (1 - a)(1 + b(P - P_{\text{th}}))^c). \end{aligned}$$

The form of TEOS for thermal expansion is shown in Fig. 1b, with the characteristic shape provided by the Einstein function, and in Fig. 1c the implicit negative temperature dependence of the bulk modulus. These curves are fits of TEOS to the experimental data for forsterite tabulated in Anderson & Isaak (1995). Use of the expressions above necessitates a value for the Einstein temperature θ for each end-member. Only very rarely are accurate thermal expansion data made at temperatures below ambient, thus making direct determination of θ by data fitting effectively impossible. We have found that the value of θ needs only to be known approximately, and affects mainly the low temperature thermal expansion and volume behaviour. An approximate value for θ is derived for each end-member from the measured entropy (or via Holland, 1989). Thus for end-member i the value of θ_i is given by the empirical relationship, $\theta_i = 10636/(S_i/n_i + 6.44)$, where S_i is the molar entropy (in $\text{J K}^{-1} \text{mol}^{-1}$) of i and n_i is the number of atoms in i .

TEOS relates the volume at any $P-T$ to the standard state volume with only three adjustable parameters (κ_0 , κ'_0 and α_0). The data set includes a term for κ''_0 to anticipate for the rare occasion where a value other than $\kappa''_0 = -(\kappa'_0/\kappa_0)$ might be warranted. Fitting TEOS to volume data for phases where volumes have been measured to very high pressures and temperatures (grossular garnet, stishovite and periclase) and for phases where simultaneous high temperature and high pressure measurements have been made (magnesite, dolomite, aragonite, brucite, grossular, andradite, jadeite and muscovite) shows that it behaves very well (see Fig. 3), in fitting all the data, whether at ambient pressures and high temperatures, ambient temperature and high pressures or at combined high pressures and temperatures.

As an example, the data for stishovite to 2300 kbar are shown in Fig. 2a where the lower pressure data (up to 500 kbar) of Andrault *et al.* (2003) have been fitted with TEOS and, on extrapolation, appear to fit nicely the very high pressure data of Luo *et al.* (2002). The extrapolatory power of TEOS is seen to be excellent. Also shown in Fig. 2b is the volume thermal expansion data and the good form of the fit to the data. The way

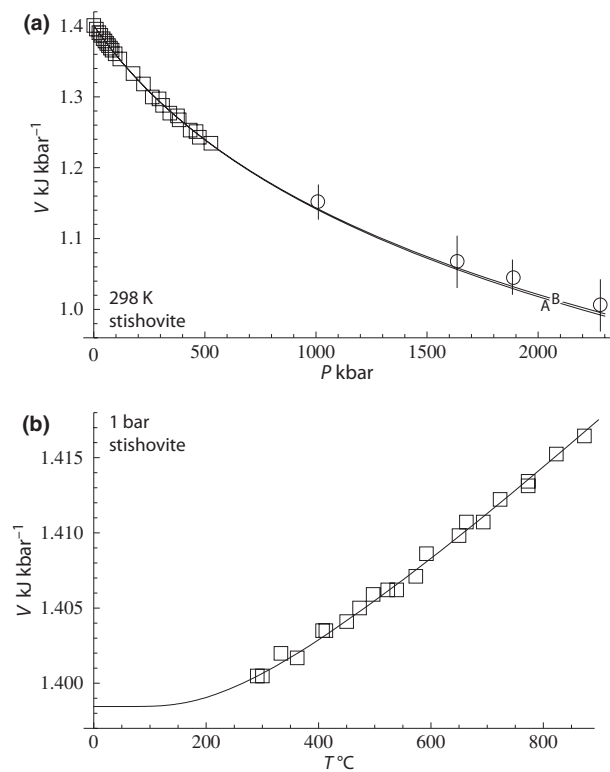


Fig. 2. Stishovite volume data. (a) Precise data of Andrault *et al.* (2003) up to 500 kbar (squares) and the very high pressure data of Luo *et al.* (2002) to 2500 kbar (circles with error bars). Error bars for the lower pressure data are smaller than the symbols. Calculated curves: A – fit to low pressure data of Andrault *et al.* only; B – fit to all data with experimental uncertainties. (b) Volume expansion data of Ito *et al.* (1974) and the calculated fit.

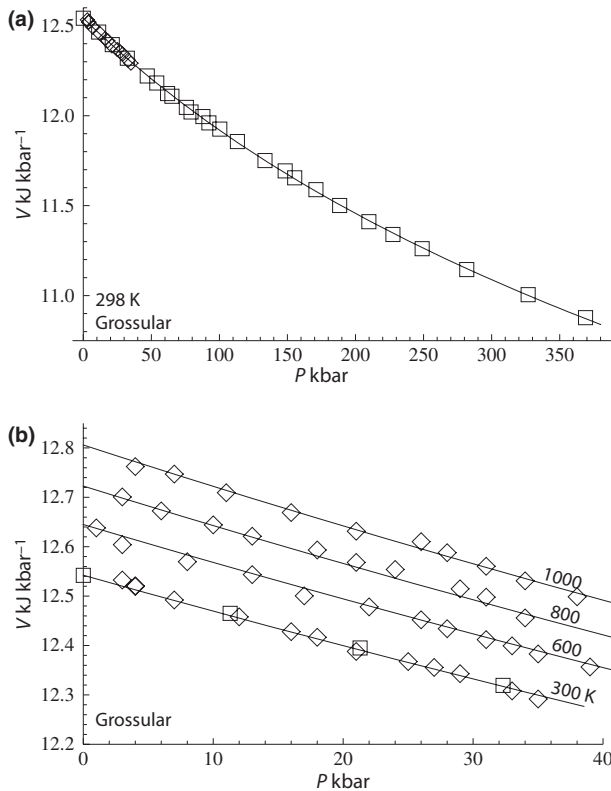


Fig. 3. Experimental data of Pavese *et al.* (2001a,b) and the fitted curves from Tait equation of state. (a) The 298 K data to 360 kbar; (b) the high pressure–high temperature data to 1000 K and 40 kbar.

volume levels off at low temperature is a reflection of the way thermal expansion drops off to zero (Fig. 1) at low temperatures. Figure 3 illustrates the fit of the high pressure volume data for grossular from Pavese *et al.* (2001a,b), first as a function of pressure to over 350 kbar, and second as a function of both pressure and temperature to 1000 K and 40 kbar. TEOS appears to have a form that is well suited to represent such data.

Although using TEOS in place of Murnaghan makes little difference to the derived thermodynamic data, two related factors have led to significant improvement in the overall data fitting. First, not restricting the value of κ' to 4.0 has allowed better extrapolations to very high pressure, and second (and more significantly) the incorporation of the implicit thermal expansion and the consequent temperature dependence of bulk modulus κ through the thermal pressure has made the volume behaviour at high pressures and temperatures more reliable.

Equation of state for fluid phases

Pure fluid species

The EOS for fluids used in HP98 was the CORK equation (Holland & Powell, 1991) which was derived

for the purposes of extrapolation to high pressures. The equations of Pitzer & Sterner (1995) have now been substituted in place of CORK for both H_2O and CO_2 for the following two reasons: (i) the CORK expressions did not fit the volumes for H_2O in the region of the critical point closely (fig. 2 of Holland & Powell, 1991), and (ii) the CORK expressions involved a piecewise continuous transition in compressibility at 2 kbar which made for difficulties in root-finding algorithms for free energy. The differences between CORK and Pitzer & Sterner (1995) volumes and free energies are minor for H_2O , and virtually indistinguishable for CO_2 . Change to the Pitzer & Sterner equations necessitated minor compensating adjustments in entropy for a number of hydrous phases. The CORK equation is, however, retained for calculating volumes and fugacities of CO , CH_4 , H_2 , S_2 and H_2S because of its ease in application of the corresponding-states principle. The constants for the CORK expressions for COH gases are taken from Holland & Powell (1991, table 2). For S_2 and H_2S the critical constants are taken from Reid *et al.* (1977) and used with equation (9) in Holland & Powell (1991).

Mixing in fluids

Mixtures of gases, such as H_2O and CO_2 , as well as other species in the COHS system are now handled via a Van Laar model as described in Holland & Powell (2003), in which the volumes of the end-members control the asymmetry parameters directly, which allows a controlled extrapolation to very high pressures. Because the mixing properties are very similar to those generated by the modified Redlich–Kwong EOS, the latter were used to derive Van Laar parameters for all other COHS gas end-members. The COH a_{ij} values are from Holland & Powell (2003), and the remaining ones from Evans *et al.* (2010). This change has led to an overall reduction in the misfit between mixed silicate-carbonate experiments and thermodynamic data.

The earlier HP98 paper also involved aqueous solution thermodynamic properties, based on a modification of the Anderson density model (Anderson *et al.* (1991) which is retained here. A problem never addressed satisfactorily for aqueous fluids at geological conditions is that of the transition from the dilute region, where Debye–Hückel type (infinite dilution standard state) models are typically used, to the high ionic strength electrolytes such as saturated salt solutions where Raoult's Law type standard states are used. Progress towards resolving this has been made by Evans & Powell (2005), who devised a model which slides smoothly between the two types of behaviour, allowing a single activity–composition expression to be used for mixed aqueous electrolytes and dissolved COHS gas species. An example where such calculations have been used is given below and further examples may be found in Evans *et al.* (2010).

Use of univariant and divariant experimentally determined equilibria involving solid solutions

A new feature of this data set is the use of univariant equilibria in solving for enthalpies and mixing properties of solid solutions simultaneously. As an example, the univariant reaction sapphirine + quartz = orthopyroxene + sillimanite in the MAS system has been determined experimentally by Newton (1972), Hensen, (1972) and Chatterjee & Schreyer (1972). Along the length of this reaction, from 1050 °C to 1475 °C, the compositions of pyroxene and sapphirine change. By fitting simultaneously to a set of independent reactions between the end-members, the enthalpies of all end-members (spr_4 , spr_5 , en, mgt_s, sill, q) may be optimized together. Consideration of the variation of mixing properties, via the interaction energies ($W_{\text{en-mgt}_s}$ and $W_{\text{spr}_4-\text{spr}_5}$) also allowed these values to be refined.

As well as univariant reactions, many divariant equilibria were also fitted in the same manner, allowing easy refinement of mixing energies for a number of solid solutions involved across different reactions. This was particularly helpful in refining the properties of the chlorites in MASH (clin, ames, afchl) through the experiments of Baker & Holland (1996), Jenkins (1981) and Jenkins & Chernosky (1986). It has also been used in a number of Fe–Mg and other exchange equilibria between silicates and between silicates and carbonates.

Order-disorder and Landau models

Treatment of order-disorder in HP98 was done with a Landau tricritical model to account for the sharp lambda peaks in the heat capacity exhibited at the phase transition temperatures in such end-members. This was convenient in making a simple representation of the order-disorder characteristics in stoichiometric phases, but is not satisfactory when dealing with solid solutions involving disordering behaviour because the Landau expansion does not correctly incorporate the configurational entropy associated with cation ordering. We now represent many order disorder transitions with a macroscopic Bragg–Williams type of model, the SF or symmetric formalism of Holland & Powell (1996a,b)). End-members now characterized by the SF model include sillimanite, gehlenite, cordierite, albite, K-feldspar, anorthite, spinel, hercynite, dolomite, ankerite. Using the SF model allows solid solutions involving these end-members to be constructed with standard configurational entropies and thus activity–composition expressions, making them much easier to be used in multicomponent solid-solution phase equilibrium calculations.

Melt species

Following on from the initial modelling of simple granitic systems (Holland & Powell, 2001) and its extension

into partial melting of pelitic compositions (White *et al.*, 2001), the data for melt components has improved considerably over those initially presented in HP98. The principal differences lie in enforcing the heat of melting as a constraint, where known, in addition to fitting the experimental $P-T$ curves and changes introduced through the relaxation of $\kappa' = 4$ constraint. Many melt end-members now have their properties consistent with experiments which go to high pressures (e.g. qL to 60 kbar, faL to 70 kbar, foL to 153 kbar). In addition, several new melt end-members have been introduced since HP98 [perL (MgO), limL (CaO), corL (Al_2O_3), woll (CaSiO_3), neL (NaAlSiO_4), lcL (KAlSi_2O_6), KCl and NaCl liquids].

The new thermal expansion expressions used in TEOS are not suitable for melt end-members, as they are based on a vibrational model. The experimental data currently available do not warrant anything more elaborate than constant thermal expansion at the temperatures investigated (Lange, 1997), and so the constant thermal expansion and linear temperature dependence of bulk modulus as in HP98 is retained for melt end-members.

NEW END-MEMBERS IN THE DATA SET

The following is a brief outline of additions to the data set in a mineral group or system context; all the new end-members are indicated in Table 1. Changes in activity–composition relations that are implicit in data set generation for these and other end-members are included below in the next subsection.

For the first time, sulphides and sulphur-bearing minerals and fluid species have been incorporated into the data set. The details are published in Evans *et al.* (2010) and encompass the solid phases pyrite (FeS_2), troilite (FeS), pyrrhotites (solid solution between hypothetical end-member trot, FeS and vacancy-bearing trov, $\text{Fe}_{0.875}\text{S}$), anhydrite (CaSO_4), elemental sulphur S, gaseous S_2 and H_2S as well as aqueous species HS^- , HSO_3^- , SO_4^{2-} and HSO_4^- . Troilite is described as a low temperature form (lot) from 298 K up to 420 K and a high temperature form (tro) above 420 K. These solids are complicated, involving two lambda transitions in troilites (one at 420 K, one at 598 K) and a lambda transition in trov at 595 K. Examples of phase diagram calculations, including pseudosections involving mixed silicates, carbonates and sulphides may be found in Evans *et al.* (2010).

Several new pyroxene end-members are now included. Clinoenstatite (cen, $\text{Mg}_2\text{Si}_2\text{O}_6$) and proto-enstatite (pren) are new end-members whose enthalpy of formation and entropy are derived from experiments of Atlas (1952), Chen & Presnall (1975) and Boyd & England (1965). A calcium-eskola pyroxene end-member (caes, $\text{Ca}_{0.5}\square_{0.5}\text{AlSi}_2\text{O}_6$) is introduced to account for vacancy substitutions seen in calcic pyroxene at high pressures, and is calibrated on the experimental results of Gasparik (1984). The activity

model used assumes that some short-range ordering between Si–Al on tetrahedral and Mg–Al on octahedral sites can be accommodated by reducing the tetrahedral entropy of mixing to a quarter of the configurational contribution. This then gives the activities of caes and cats in a binary pyroxene as $a_{\text{caes}} = 2X_{\text{Ca},\text{M}2}^{0.5} X_{\square,\text{M}2}^{0.5} X_{\text{Si},\text{T}}^{0.5} \gamma_{\text{caes}}$ and $a_{\text{cats}} = 1.414213 X_{\text{Ca},\text{M}2} X_{\text{Si},\text{T}}^{0.25} X_{\text{Al},\text{T}}^{0.25} \gamma_{\text{cats}}$ with activity coefficients from a regular solution with $W_{\text{caes},\text{cats}} = -15 \text{ kJ}$.

Chromium-bearing end-members are now included: the oxide eskolaite (esk, Cr_2O_3), the pyroxene kosmochlor (kos, $\text{NaCrSi}_2\text{O}_6$), the garnet knorrtingite (knor, $\text{Mg}_3\text{Cr}_2\text{Si}_3\text{O}_{12}$) and the spinel picrochromite (picr, MgCr_2O_4). We have fitted the experiments on the exchange reaction $2\text{jd} + \text{picr} = 2\text{kos} + \text{sp}$, assuming that jd–kos is ideal and that the sp–picr solid solution is non-ideal with a symmetrical interaction energy $W_{\text{picr},\text{sp}} = 25 \text{ kJ}$ (Carroll Webb & Wood, 1986). We have not added a large entropy increment to knorrtingite (as done by Klemme, 2004, and Klemme *et al.*, 2000, who assumed that the low- T anomaly seen in the heat capacity of uvarovite applies to knorrtingite), and thus we have been able to fit the slope and positions of both the reactions $2\text{knor} = 3\text{en} + 2\text{esk}$ (Turkin *et al.*, 1983) and $\text{knor} + \text{fo} = \text{picr} + 2\text{en}$ (Klemme, 2004). The P – T slope of the experimental brackets of Irifune *et al.* (1982) for $2\text{knor} = 3\text{en} + 2\text{esk}$ are incompatible with the other studies and with the thermodynamic data.

Carnegieite and high-carnegieite (cg, cgh, NaAlSiO_4) are fitted to the experiments of Bowen & Greig (1925), Greig & Barth (1938) and Cohen & Klement (1967). These data depend on those for nepheline, and are in turn used to determine those for nepheline liquid and sodalite.

Stilpnomelane with end-members ferrostilpnomelane (fstp, $\text{K}_{0.5}(\text{Fe}_5\text{Al})[\text{Si}_8\text{Al}]\text{O}_{22}(\text{OH})_{4.5}\cdot4\text{H}_2\text{O}$) and magnesiostilpnomelane (mstp, $\text{K}_{0.5}(\text{Mg}_5\text{Al})[\text{Si}_8\text{Al}]\text{O}_{22}(\text{OH})_{4.5}\cdot4\text{H}_2\text{O}$) is now included. The formula for stilpnomelane is not fully known, but the chosen formula units are based on Eggleton (1972) simplified and normalized to 8 Si pfu. The activities are given by assuming that octahedral Al resides on one site, with Fe and Mg mixing on five sites, so that $a_{\text{fstp}} = X_{\text{Fe}}^5 \gamma_{\text{fstp}}$ and $a_{\text{mstp}} = (1 - X_{\text{Fe}})^5 \gamma_{\text{mstp}}$ with activity coefficients from a regular solution with $W_{\text{fstp},\text{mstp}} = 20 \text{ kJ}$. The data for the end-members are derived from the reaction $28\text{fstp} = 14\text{ann} + 5\text{grun} + 21\text{alm} + 79\text{q} + 156\text{H}_2\text{O}$ and the partitioning of Fe and Mg between stilpnomelane and chlorite (Miyano & Klein, 1989).

Minnesotait [minn, $\text{Fe}_3\text{Si}_4\text{O}_{10}(\text{OH})_2$] and its Mg equivalent [minm, $\text{Mg}_3\text{Si}_4\text{O}_{10}(\text{OH})_2$] are derived from the experiments of Engi (1983) for the reaction $2\text{minn} = 3\text{fa} + 5\text{q} + 2\text{H}_2\text{O}$ along with data for partitioning of Fe and Mg between carbonate and minnesotait of Klein (1974). The activities are given by assuming that Fe and Mg mix on three sites, so that $a_{\text{minn}} = X_{\text{Fe}}^3 \gamma_{\text{minn}}$ and $a_{\text{minm}} = (1 - X_{\text{Fe}})^3 \gamma_{\text{minm}}$ with activity coefficients from a regular solution with $W_{\text{minn},\text{minm}} = 12 \text{ kJ}$.

Greenalite [glt, $\text{Fe}_3\text{Si}_2\text{O}_5(\text{OH})_4$] was derived using reactions $\text{glt} + 2\text{q} = \text{minn} + \text{H}_2\text{O}$ and $2\text{glt} + 5\text{min} = 3\text{grun} + 6\text{H}_2\text{O}$ using the constraints discussed by Rasmussen *et al.* (1998).

Considering pumpellyite, in addition to the original MgAl pumpellyite in HP98 data are presented for a solid solution between three end-members, the MgAl end-member [mpm, $\text{Ca}_4\text{MgAlAl}_4\text{Si}_6\text{O}_{21}(\text{OH})_7$], the FeAl end-member [fpm, $\text{Ca}_4\text{FeAlAl}_4\text{Si}_6\text{O}_{21}(\text{OH})_7$] and the FeFe^{3+} end-member julgoldite [jgd, $\text{Ca}_4\text{FeFe}_3^{3+}\text{Si}_6\text{O}_{21}(\text{OH})_7$] are included. As in HP98, the mpm end-member is derived from the experiments of Schiffman & Liou (1980), while data for the iron analogue are taken from the Fe–Mg partition between pumpellyite and chlorite of Evans (1990). The jgd end-member is derived from the Fe^{3+} –Al partitioning data between epidote and pumpellyite given by Cho *et al.* (1986). Ordering of Mg and Fe onto a single M2a site is assumed for these pumpellyites and activities are given by

$$a_{\text{mpm}} = X_{\text{Mg},\text{M}2\text{a}} X_{\text{Al},\text{M}2\text{b}} X_{\text{Al},\text{M}1}^4,$$

$$a_{\text{fpm}} = X_{\text{Fe},\text{M}2\text{a}} X_{\text{Al},\text{M}2\text{b}} X_{\text{Al},\text{M}1}^4$$

and

$$a_{\text{jgd}} = X_{\text{Fe},\text{M}2\text{a}} X_{\text{Fe}^{3+},\text{M}2\text{b}} X_{\text{Fe}^{3+},\text{M}1}^4.$$

Talc now includes a pyrophyllitic end-member [tap, $\text{Al}_2\text{Si}_4\text{O}_{10}(\text{OH})_2$] fitted to the experimental compositions reported by Newton (1972). All experiments involving aluminous talc (e.g. Chernosky, 1978; Massonne *et al.*, 1981; Massonne, 1989; Massonne & Schreyer, 1989; Hoschek, 1995) have been fitted with a model involving both the tschermak substitution and the pyrophyllite-like substitution.

Prehnite now includes a ferric end-member [fpre, $\text{Ca}_2\text{AlFeSi}_3\text{O}_{10}(\text{OH})_2$]. Ferric iron is assumed to substitute for Al on one octahedral site only, and the activity relations simplify to $a_{\text{fpre}} = X_{\text{Fe}} \gamma_{\text{fpre}}$ and $a_{\text{pre}} = (1 - X_{\text{Fe}}) \gamma_{\text{pre}}$ with activity coefficients from a regular solution with $W_{\text{pre},\text{fpre}} = 1 \text{ kJ}$. The data for fpre are derived from the Fe^{3+} –Al partitioning data between epidote and prehnite given by Cho *et al.* (1986).

The halide minerals halite (hlt, NaCl) and sylvite (syv, KCl) and their molten equivalents (hltL and syvL) are included in the data set. The enthalpies of formation of halite and sylvite are taken from Robie & Hemingway (1995), and the molten end-members from fitting to the melting curves to 20 kbar pressure from Clark (1966). The experimental data of Aranovich & Newton (1997, 1998) involving concentrated brines (KCl and NaCl) in equilibrium with brucite and periclase may now be reproduced by direct calculation with the new data set.

Sapphirine has been a difficult phase to quantify thermodynamically, largely because available experiments have not been able to involve characterization of the composition of the sapphirine. A new model for sapphirine is adopted here, based on the revision of

Kelsey *et al.* (2004), which involves the 2:2:1 end-members spr4 ($\text{Mg}_4\text{Al}_8\text{Si}_2\text{O}_{20}$) and fspr ($\text{Fe}_4\text{Al}_8\text{Si}_2\text{O}_{20}$) and the 3:5:1 end-member spr5 ($\text{Mg}_3\text{Al}_{10}\text{SiO}_{20}$). The activity relations, as discussed below, are found by optimization of the fit to the experimental data on sapphirine equilibria (Boyd & England, 1959; Hensen, 1972; Newton, 1972; Seifert, 1974; Doroshev & Malinovskiy, 1974; Malinovsky & Doroshev, 1975; Ackermann *et al.*, 1975; Arima & Onuma, 1977; Perkins *et al.*, 1981; Podlesskii, 1996; Fockenberg, 2008). In the fitting process, the compositions of sapphirine are predicted; they fall in the range $x_{\text{spr}5} = 0.36\text{--}0.45$ for most of the high pressure experiments, but do rise to $x_{\text{spr}5} = 0.60$ when coexisting with mullite. The fit to all these experiments is now quite good. Although a similar quality fit to the H_2O -absent subset of the data in MAS was made by Podlesskii *et al.* (2008), their data set was only constrained within this subset of MAS rather than by all the other phases and equilibria used in this study.

Mullite is a complex solid solution involving an end-member of sillimanite composition (Al_2SiO_5) into which the substitution $\text{Si} + 1/2\text{O} = \text{Al} + 1/2\square$ occurs. This could in principle extend from Al_2SiO_5 ($x = 0$) to a Si-free end-member $\text{Al}_2\text{AlO}_{4.5}$ ($x = 1$), where x is the amount of the substitution above, but in practice rarely extends beyond $x = 0.5$ (Cameron, 1977). We have elected to use this intermediate composition (amul, $\text{Al}_2\text{Si}_{0.5}\text{Al}_{0.5}\text{O}_{4.75}$) as the aluminous end-member in mullite in part because natural compositions rarely become more aluminous than this and in part because of the strong ordering of Al + Si and O + \square . These two different ordering patterns (Al + Si and O + \square) lead to two different symmetries, P_cnnm and P_cbnm and an overall structure with an incommensurate modulation (Angel *et al.*, 1991). Rather than attempt a detailed, and probably incorrect, activity model for this solid solution we take a pragmatic approach that assumes that the high degrees of Al/Si and \square/O ordering can be approximated by a simple two-site mixture of the end-members, such that $a_{\text{amul}} = x_{\text{amul}}^2 \gamma_{\text{amul}}$ and $a_{\text{smul}} = (1 - x_{\text{amul}})^2 \gamma_{\text{smul}}$. Mullite enthalpies (for smul and amul) and the interaction energy ($W_{\text{smul,amul}}$) are derived from the experiments on the reactions muscovite + quartz = mullite + sanidine + H_2O (Segnit & Kennedy, 1961), pyrophyllite = mullite + quartz + H_2O (Carr & Fyfe, 1960), cordierite + corundum = sapphirine + mullite (Seifert, 1974) and the melting equilibria cristobalite + mullite + liquid and mullite + corundum + liquid (Klug *et al.*, 1987). The calculated compositions of mullite are close to that of sillimanite at low temperatures and reproduce the aluminous compositions observed by Klug *et al.* (1987) at the melting temperatures. Calculations involving this mullite are included below.

Lizardite, one of the serpentine group minerals (with antigorite and chrysotile) is now included in the data set. Its properties are assumed to be like those of chrysotile, but with slightly smaller values for volume

and entropy (Evans, 2004; Hilairet *et al.*, 2006). We have accordingly also lowered the heat capacity and compressibility of lizardite. The enthalpy for lizardite, following the arguments of Evans (2004), is derived from accepting that lizardite transforms (metastably) to chrysotile between 413 and 431 °C at 2 kbar (Chernosky, 1975). The calculated stability of lizardite extends only up to 170 °C at 2 kbar where it breaks down to antigorite + brucite. More work needs to be done to determine unambiguously the stability of lizardite relative to chrysotile. The new measured compressibilities for lizardite and chrysotile (Hilairet *et al.*, 2006) and for antigorite (Bose & Navrotsky, 1998) are used, allowing good fits to antigorite in very high pressure experiments (Wunder & Schreyer, 1997; Bose & Navrotsky, 1998; Pawley, 1998).

The new modified TEOS for solids allows reliable extrapolation of mineral volumes to very high pressures, and so we are starting to accumulate a set of thermodynamic data for phases at deep mantle pressures and temperatures. We present preliminary data on the end-members ferropericlase (fper, FeO), Mg-wadsleyite (mdw, Mg_2SiO_4), Fe-wadsleyite (fdw, Fe_2SiO_4), Mg-ringwoodite (mrw, Mg_2SiO_4), Fe-ringwoodite (frw, Fe_2SiO_4), Mg-perovskite (mpv, MgSiO_3), Fe-perovskite (fpv, FeSiO_3), Al-perovskite (apv, AlAlO_3), Ca-perovskite (cpv, CaSiO_3), Mg-akimotoite (mak, MgSiO_3), Fe-akimotoite (fak, FeSiO_3), majorite garnet (maj, $\text{Mg}_4\text{Si}_4\text{O}_{12}$), high-pressure clinoenstatite (hen, $\text{Mg}_2\text{Si}_2\text{O}_6$), Ca-Si-titanite (cstn, CaSi_2O_5), walstromite (wal, CaSiO_3), MgSi-corundum (mcor, MgSiO_3), K-cymrite (kcm, $\text{KAlSi}_3\text{O}_8\cdot\text{H}_2\text{O}$), wadeite (wa, $\text{K}_2\text{Si}_2\text{O}_9$) and hollanlite (hol, KAlSi_3O_8). Experimental details for the equilibria used to extract the data may be found in Appendix 2. These data are tied into, and are consistent with the thermodynamic data for end-members at lower P - T (crustal) conditions.

Mixing model changes

Since HP98 we have changed slightly some solid solution models used in the data set generation. Only the ones which directly affect the fitted enthalpies are discussed here.

For MgAl orthopyroxene, the entropy of mixing is taken over octahedral and tetrahedral sites rather than the earlier octahedral site only model as in Wood & Banno (1973). This is done to facilitate multi-component extensions to the model involving other substitutions. We take only a one-fourth of the full tetrahedral site entropy as an approximation for Al–Si and Mg–Al ordering, writing the activities of en and mgts as $a_{\text{en}} = X_{\text{Mg},\text{M1}} X_{\text{Si},\text{T}}^{1/2} \gamma_{\text{en}}$ and $a_{\text{mgts}} = \sqrt{2} X_{\text{Mg},\text{M1}} X_{\text{Si},\text{T}}^{1/4} X_{\text{Al},\text{T}}^{1/4} \gamma_{\text{mgts}}$, with the activity coefficients taken from a macroscopic regular model (symmetric formalism; Powell & Holland, 1993a,b) with $W_{\text{en,mgts}} = 13.0 - 0.15P$ kJ derived from the measurements of Al

solubility in aluminous pyroxenes coexisting with other phases in the data set, principally garnet and spinel.

For tremolite–tschermakite amphibole, we now take the tetrahedral contribution to be only one-fourth that of the full configurational entropy, as in the pyroxenes above, as was done in Diener *et al.* (2007) to make a comprehensive amphibole mixing model from natural and experimental data. Allowing a small cummingtonite component, the activities are written as

$$\begin{aligned} a_{\text{tr}} &= X_{\text{Ca},\text{M4}}^2 X_{\text{Mg},\text{M2}}^2 X_{\text{Si},\text{T1}} \gamma_{\text{tr}}, \\ a_{\text{ts}} &= 2X_{\text{Ca},\text{M4}}^2 X_{\text{Al},\text{M2}}^2 X_{\text{Si},\text{T}}^{1/2} X_{\text{Al},\text{T}}^{1/2} \gamma_{\text{mgt}s} \text{ and} \\ a_{\text{cumm}} &= X_{\text{Mg},\text{M4}}^2 X_{\text{Mg},\text{M2}}^2 X_{\text{Si},\text{T1}} \gamma_{\text{mgt}s} \end{aligned}$$

with the activity coefficients taken from a regular model with $W_{\text{tr,ts}} = 20 \text{ kJ}$, $W_{\text{tr,cumm}} = 45 \text{ kJ}$ and $W_{\text{ts,cumm}} = 70 \text{ kJ}$ derived from the experiments of Jenkins (1994), Hoschek (1995) and the results of Diener *et al.* (2007).

Chlorite has been slightly simplified since HP98, keeping the basic model the same, but relaxing the degree of ordering required slightly. This has come about in part due to using the X-ray calibration of chlorite compositions from Jenkins & Chernosky (1986), Roots (1994) and Shirozu & Momoi (1972) rather than the data of Baker & Holland (1996) which yielded slightly lower volumes than the other studies. This has affected the adopted molar volumes of the clin, ames and afchl end-members. The molar volume of daph has been changed from the old value (213.4 J bar^{-1}) taken from Helgeson *et al.* (1978) and Holdaway & Lee (1977) to 216.2 J bar^{-1} from Parra *et al.* (2005) as, even though their measurements are quite scattered, they are in better agreement with the measured data of James *et al.* (1976), Vidal *et al.* (2001) and with simple exchange models involving chlorite and biotite, olivine, orthopyroxene and chloritoid. In addition the entropy of clinochlore and daphnite have been taken from Bertoldi *et al.* (2007) with an extra 11.5 J K^{-1} added for tetrahedral site configurational entropy. The entropies of afchl and ames were adjusted slightly in fitting to the phase equilibrium experimental results. The heat capacities were taken from Bertoldi *et al.* (2007), the thermal expansion from Nelson & Guggenheim (1993) and compressibility from Pawley *et al.* (2002). The mixing energies are very similar to those of the earlier data set $W_{\text{afchl,clin}} = 17 \text{ kJ}$, $W_{\text{afchl,ames}} = 20 \text{ kJ}$ and $W_{\text{clin,ames}} = 17 \text{ kJ}$ with an enthalpy of -50.0 kJ for the internal equilibrium afchl + ames = 2 clin.

Epidote has also been slightly modified since HP98. The heat capacities of zoisite and clinozoisite have been refitted to high temperatures using a simple vibrational model. The values for both polymorphs are now very similar, with clinozoisite being very slightly lower than zoisite. The heat capacity of epidote is similarly extrapolated to high temperatures, fitting the

experimental data of Kiseleva *et al.* (1974) and the entropy of epidote is taken from Kiseleva & Ogorodova (1987). The entropy of cz and fep end-members are adjusted slightly to fit phase equilibrium data for the reaction epidote = anorthite + garnet + hematite + quartz + H_2O from Holdaway (1972) and Liou (1973). The activity model is the same as in HP98, but the mixing energies are changed (simplified) to $W_{\text{cz,fep}} = 3 \text{ kJ}$, $W_{\text{cz,ep}} = 1 \text{ kJ}$ and $W_{\text{ep,fep}} = 1 \text{ kJ}$. These small values are based on a value for $W_{\text{Al,Fe}^{3+}} = 2 \text{ kJ}$ for Al–Fe³⁺ mixing in grossular–andradite garnet derived from fitting the experiments of Holdaway (1972) for coexisting garnet + anorthite + wollastonite + quartz. The enthalpy of the internal equilibrium fep + cz = 2ep is -25.0 kJ to account for the degree of order in natural epidote (Dollase, 1973; Bird & Helgeson, 1980).

Talc now incorporates a pyrophyllite as well as a tschermak substitution. The mixing properties are assumed to be given by an ideal solution of the three end-members, ta, tats and tap (see above). The activities are given by

$$\begin{aligned} a_{\text{ta}} &= X_{\text{Mg},\text{M1}} X_{\text{Mg},\text{M23}}^2 X_{\text{Si},\text{T2}}^2, \\ a_{\text{tap}} &= X_{\square,\text{M1}} X_{\text{Al},\text{M23}}^2 X_{\text{Si},\text{T2}}^2 \text{ and} \\ a_{\text{tats}} &= 16X_{\text{Mg},\text{M1}} X_{\text{Mg},\text{M23}} X_{\text{Al},\text{M23}} X_{\text{Al},\text{T2}} X_{\text{Si},\text{T2}} \end{aligned}$$

Sapphirine, following the treatment in Kelsey *et al.* (2004) involves two end-members spr4 and spr5 (see above) related by a tschermak substitution. The activities for the binary are given by $a_{\text{spr4}} = X_{\text{Mg},\text{M3}}^2 X_{\text{Si},\text{T3}} \gamma_{\text{spr4}}$ and $a_{\text{spr5}} = X_{\text{Al},\text{M3}}^2 X_{\text{Al},\text{T3}} \gamma_{\text{spr5}}$, with gammas found from a regular model with $W_{\text{spr4,spr5}} = 10.0 - 0.2P \text{ kJ}$.

Pyrrhotite is treated as a non-ideal solid solution of trov and trot (see above), with activities given by $a_{\text{trov}} = 1.4576 X_{\text{Fe},\text{M2}}^{7/8} X_{\square,\text{M2}}^{1/8} \gamma_{\text{trov}}$ and $a_{\text{trot}} = X_{\text{Fe},\text{M2}} \gamma_{\text{trot}}$. The activity coefficients may be found from a regular model with $W_{\text{trov,trot}} = -3.19 \text{ kJ}$. More details may be found in Evans *et al.* (2010).

There are many additional changes to the data set, mainly relating to changes to thermodynamic parameters taken as assumed in data set generation (entropy, volume, heat capacity, etc.), and in the use of newer experimental data on phase stability that can be included in data set generation. Some changes are very minor and may be found by comparison with the tables in HP98, whereas others are more significant and are listed briefly in Appendix 3. One change that may be of greatest import to metamorphic petrologists is highlighted here, and concerns the aluminium silicate phases kyanite, andalusite and sillimanite. The choice of the Holdaway (1971) experiments, as opposed to those of Richardson *et al.* (1969) for the and = sill reaction is no longer arbitrarily imposed as a constraint. Instead, we prefer to return to the situation in our earlier data sets (Holland & Powell, 1985;

1998) in which no and = sill experimental brackets were used, and a triple point is allowed to emerge from the multitude of other equilibria involved in the data set. The calculated triple point from data in this study lies at 4.3 kbar, 534 °C, in between that of Holdaway (1971) and Richardson *et al.* (1969). The fact that the relaxation of the and = sill constraint yields a triple point almost identical to that advocated by Pattison *et al.* (2002) on the basis of field, petrographic and phase equilibria arguments, suggested to us that the combined reaction data used in the regression provide a reasonable justification of this decision.

EXAMPLES OF CALCULATED PHASE EQUILIBRIA

The following examples are of calculated phase equilibria highlighting new features of the internally consistent data set. All calculations were undertaken with THERMOCALC (Powell & Holland, 1988, 1998), and the activity–composition relations adopted are given in Table S2.

Sapphirine

Calculations in the literature on sapphirine phase equilibria using the Holland and Powell data set have used a special upgrade of the HP98 data set (tc-ds55s), for example, Kelsey *et al.* (2004), Baldwin *et al.* (2007) and Taylor-Jones & Powell (2010). The origin of the

upgrade was that the fitting of the available experimental data in the fifth update of Holland & Powell (1998) in November 2003, tc-ds55 – the extant standard data set – was considered to be partially degraded by inclusion of the sapphirine experimental data. Now, as discussed above, a successful incorporation of the sapphirine end-members into the data set has been undertaken.

Sapphirine equilibria are important geologically as they have been used widely in higher temperature rocks in which sapphirine-bearing mineral assemblages occur to estimate P – T conditions of metamorphism. Phase equilibria in the simple systems $\text{MgO} \text{--} \text{Al}_2\text{O}_3 \text{--} \text{SiO}_2$ (MAS) and $\text{MgO} \text{--} \text{Al}_2\text{O}_3 \text{--} \text{SiO}_2 \text{--} \text{H}_2\text{O}$ (MASH) are experimentally determined, so they in turn constrain the corresponding thermodynamic data of the mineral end-members. Figure 4 shows the calculated phase equilibria in the system $\text{MgO} \text{--} \text{Al}_2\text{O}_3 \text{--} \text{SiO}_2$, with the ultimate stability of sapphirine, and sapphirine + quartz indicated. The main invariant points (a–d) are at a slightly lower pressure (< 0.4 kbar) and higher temperature (< 30 °C) than those calculated with tc-ds55s. Note that mullite-bearing equilibria, at the highest temperature on Fig. 4, can now be calculated.

Not specifically shown in Fig. 4 are the corresponding MASH equilibria as these can be easily envisaged in Fig. 4. Addition of H_2O to MAS affects only equilibria involving cordierite, at least until melt is stabilized. Thus, on addition of H_2O , the MAS invariant points become MASH univariant lines

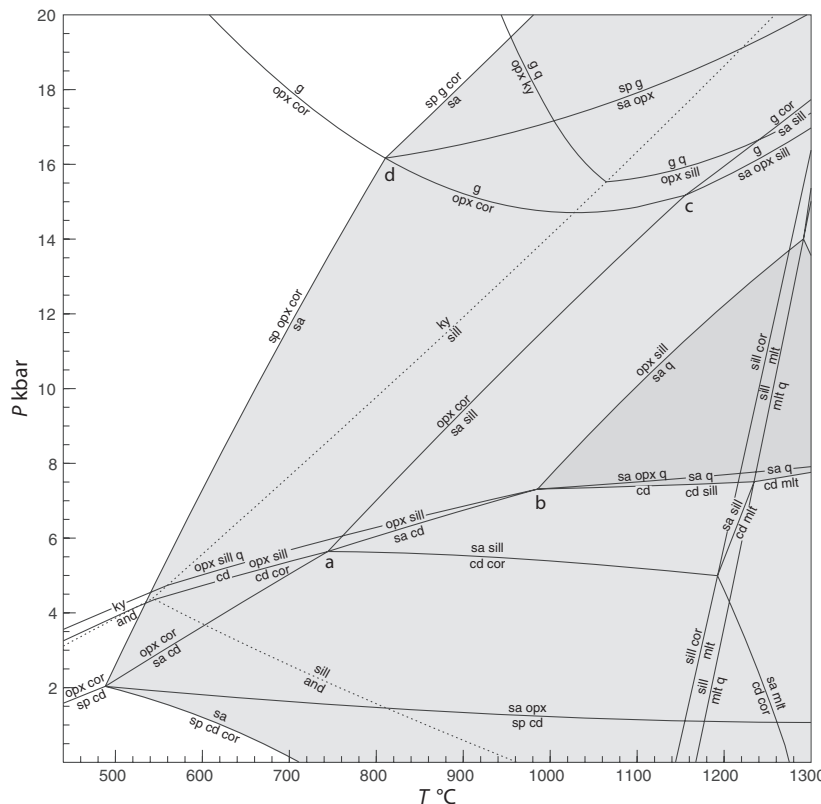


Fig. 4. P – T projection for sapphirine equilibria in the $\text{MgO} \text{--} \text{Al}_2\text{O}_3 \text{--} \text{SiO}_2$ system, showing the maximum stability fields for sa (light shading) and sa + q (darker shading). Phases: g, garnet; sa, sapphirine; cor, corundum; sp, spinel; opx, orthopyroxene; ky, kyanite; and, andalusite; sill, sillimanite; cd, cordierite; mlt, mullite; q, quartz. a, b, c, d are invariant points from which $\text{FeO} \text{--} \text{MgO} \text{--} \text{Al}_2\text{O}_3 \text{--} \text{SiO}_2$ univariants emerge (see Fig. 5). For a – x relationships used, see Table S2.

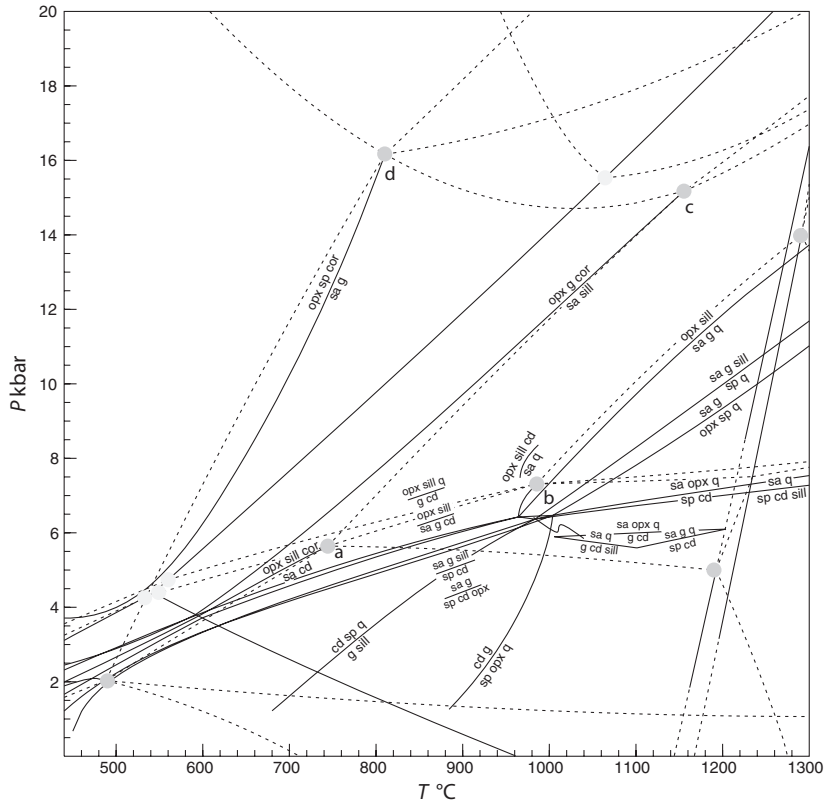


Fig. 5. P - T projection for sapphirine equilibria in the $\text{FeO}-\text{MgO}-\text{Al}_2\text{O}_3-\text{SiO}_2$ system (full curves) and the $\text{MgO}-\text{Al}_2\text{O}_3-\text{SiO}_2$ subsystem (dashed curves). a, b, c, d are invariant points in MAS from which FMAS univariants emerge. Close to MAS invariant point b is the triangle of FMAS invariant points deduced by Hensen (1972) – although his experiments contained trace H_2O and were at somewhat higher pressures (see text). For a–x relationships used, see Table S2.

coincident with reactions not involving cordierite (or [cd], i.e. cd-out) MAS univariant lines. These extend up P - T from invariant points, a and b, in Fig. 4.

Extension of the phase equilibria from MAS into the FeO-bearing system, FMAS, is shown in Fig. 5. Out of each MAS univariant point comes a FMAS univariant line, depending on which phases involved more easily incorporate FeO. Focussing on point b, the [sp] FMAS univariant extends down temperature until garnet is stabilized, and the resulting FMAS invariant point is the lower temperature one of the familiar triangle of FMAS invariant points (as shown in the adjacent inset on Fig. 5). Extending into FMASH, the [cd] FMAS univariant reactions go up to higher P - T from this triangle of FMAS invariant points to become the FMASH univariants. As discussed in Kelsey *et al.* (2004) and Baldwin *et al.* (2007), the classic experimental results of Hensen (1972) are in (at least) FMASH, not FMAS, and so occur at rather higher P - T than those shown in Fig. 5, corresponding to the small amount of water in his experiments.

Sulphur

As outlined above, the scope for calculating phase equilibria involving aqueous solutions, CHOS fluids and also sulphides and sulphate is now considerably increased (see above; also Evans & Powell, 2007; Evans

et al., 2010). Calculated equilibria among magnetite, hematite, pyrite, pyrrhotite, anhydrite and siderite, in the presence of calcite, are shown in Fig. 6. These are simple end-members, apart from pyrrhotite, for which the non-stoichiometry is modelled as described in Evans *et al.* (2010), and outlined above. Focussing on phase equilibria at 5 kbar, Fig. 7 shows a back-projection of the phase relationships onto the pyrrhotite one-phase field for assemblages with calcite + graphite.

The fields on Fig. 6 are labelled with tetrahedral compatibility diagrams. Simpler triangular compatibility diagrams can be drawn for graphite-, and for pyrite-saturated, conditions. Whereas compatibility diagrams of various sorts are commonly best adapted for representing mineral stabilities for geological processes (e.g. Powell *et al.*, 2005), conventionally such relationships for the minerals involved here are represented on intensive variable diagrams, involving for example log activities. An equivalent diagram, calculated at 5 kbar and 500 °C, in terms of chemical potentials, is shown in Fig. 8. The top surface of the μ - μ - μ box is for graphite presence. Note that the μ - μ - μ invariant points (a–d in Fig. 8) correspond to tie tetrahedra in the compatibility diagrams in Fig. 6. The calculations were performed on these divariant equilibria using the calcmu script in THERMOCALC, with μ_C calculated from $\mu_{\text{CO}_2} - 2\mu_{\text{O}}$, and μ_S calculated from $\mu_{\text{SO}_2} - 2\mu_{\text{O}}$. Only the higher μ_C relationships are shown (for simplicity): from the compatibility diagram

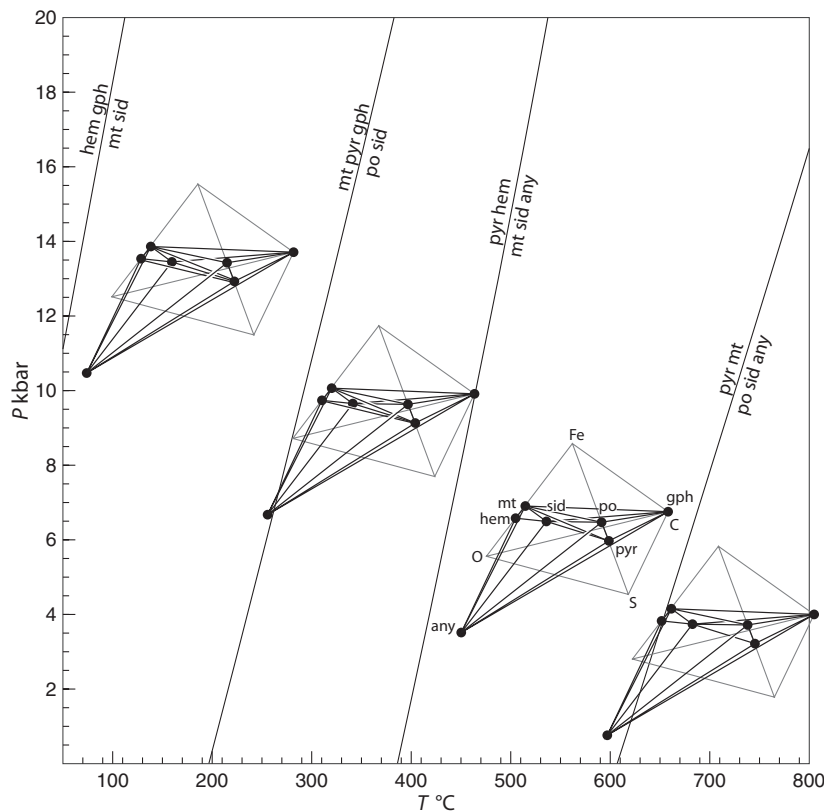


Fig. 6. P - T projection for CaO-FeO-C-O-S with excess calcite (cc) to show calculated equilibria among the phases hem (hematite), mt (magnetite), gph (graphite), sid (siderite), po (pyrrhotite), pyr (pyrite), any (anhydrite). Compatibility tetrahedra are shown – see text for discussion.

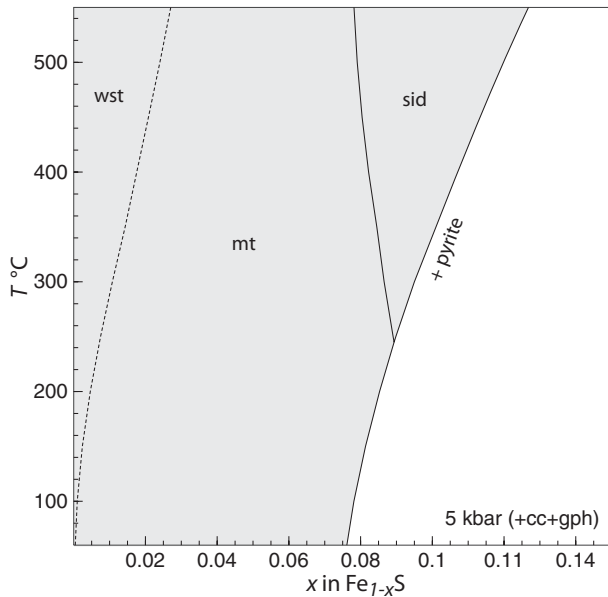


Fig. 7. T - y (po) diagram at 5 kbar, with excess calcite and graphite, showing the calculated composition of pyrrhotite coexisting with wustite (wst), magnetite (mt), siderite (sid) and pyrite.

it can be seen that at lower μ_C (moving away from the C apex), successive invariant points in the μ - μ - μ box will involve pyr + mt + sid + any (at $\mu_C = -45.0$),

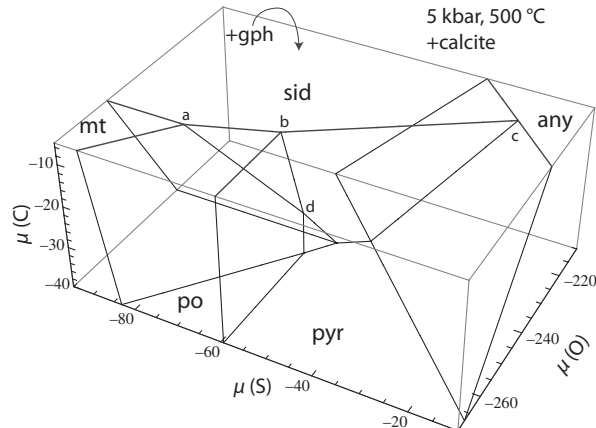


Fig. 8. $\mu(C) - \mu(S) - \mu(O)$ box at 5 kbar, 500 °C showing the fields for mt (magnetite), sid (siderite), any (anhydrite), pyr (pyrite) and po (pyrrhotite). The top surface is graphite-saturated. Invariant points a–d correspond with the compatibility tie-tetrahedra in Fig. 6.

mt + hem + sid + any (at $\mu_C = -52.0$) and pyr + po + mt + any (at $\mu_C = -60.3$)

If the mineral assemblages are considered to be in equilibrium with a CHOS fluid, the composition can be calculated with THERMOCALC. So for example, considering the tie tetrahedron pyr + po + mt + sid with a fluid involving the end-members, H_2O - CO_2 - CH_4 - H_2 - CO - H_2S - S_2 at 5 kbar and 500 °C, the proportions of these end-members are:

$$\begin{aligned}
 \text{H}_2\text{O} &= 0.549, \\
 \text{CO}_2 &= 0.450, \\
 \text{CH}_4 &= 3.1210^{-7}, \\
 \text{H}_2 &= 1.3910^{-5}, \\
 \text{H}_2\text{S} &= 6.2310^{-4}, \\
 \text{S}_2 &= 2.2310^{-9}.
 \end{aligned}$$

Phase equilibria at deep mantle pressures

A new departure in this data set is the inclusion of phases which become stable in the deeper parts of the Earth's mantle. The thermodynamic data now allow calculation of P - T grids in chosen chemical systems, and pseudosections for bulk compositions applicable to model mantle materials. This is an expanding field of endeavour, both experimentally and in modelling, and we present some examples of the types of phase diagram which may be calculated with this data set using THERMOCALC.

The first example is a P - T projection in the $\text{MgO}-\text{SiO}_2$ system (Fig. 9) involving the phases olivine, wadsleyite (wad), ringwoodite (ring), high-pressure cpx (hcpy), akimotoite (aki), perovskite (pv), periclase (per) and stishovite (stv). The diagram pertains to pressures

above the breakdown of orthopyroxene. The inferences that can be made from the MS system about mantle mineralogy are somewhat limited, and so we calculate a P - T diagram showing the MAS reactions emerging from the MS invariant points on introduction of alumina into the system (Fig. 10). Three stable invariant points ensue, labelled A, B and C in the figure, and these are the starting points for FMAS univariant reactions in the Fe-bearing system (arrow-ended curves in Fig. 10). These enable construction of the rather more petrologically interesting pseudosection for fixed bulk composition allowing portrayal of the different FMAS assemblages on the P - T diagram.

Figure 11 shows the pseudosection calculated for the Kilbourne Hole peridotite bulk composition (Takahashi, 1986; Walter, 1998), simplified into the FMAS system. It is immediately clear that the nature of the 660 km transition (~ 230 kbar) is likely to be more complex than that commonly interpreted from experimental data in smaller subsystems, changing through several assemblages involving incoming of perovskite and periclase. The range and variety of assemblages developed in P - T space shows how difficult it will be to perform and interpret experimental charges in chemically complex systems. Addition of calcium will further complicate the pattern of mineral assemblages, and such a calculation will be presented elsewhere. A word of caution is in order here, as there are a couple of major sources of uncertainty in the experiments used to

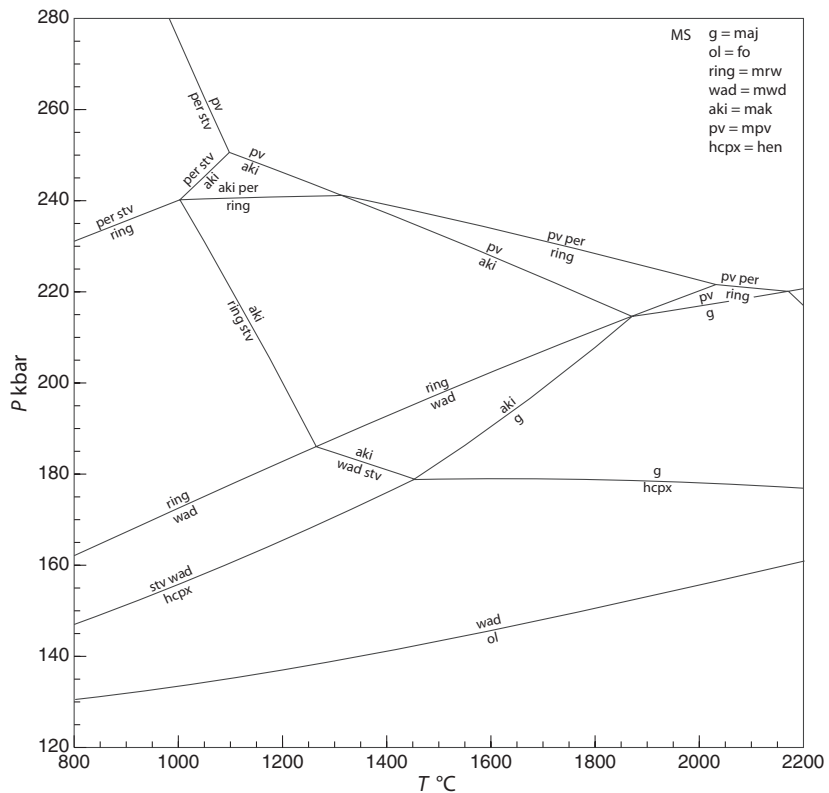


Fig. 9. P - T projection for deep mantle phases in $\text{MgO}-\text{SiO}_2$. Phases: pv, perovskite; aki, akimotoite (ilmenite); per, periclase; ring, ringwoodite; wad, wadsleyite; g, majorite garnet; stv, stishovite; hcpy, high-pressure clinoenstatite; ol, olivine. Legend provides the end-member names as used in THERMOCALC.

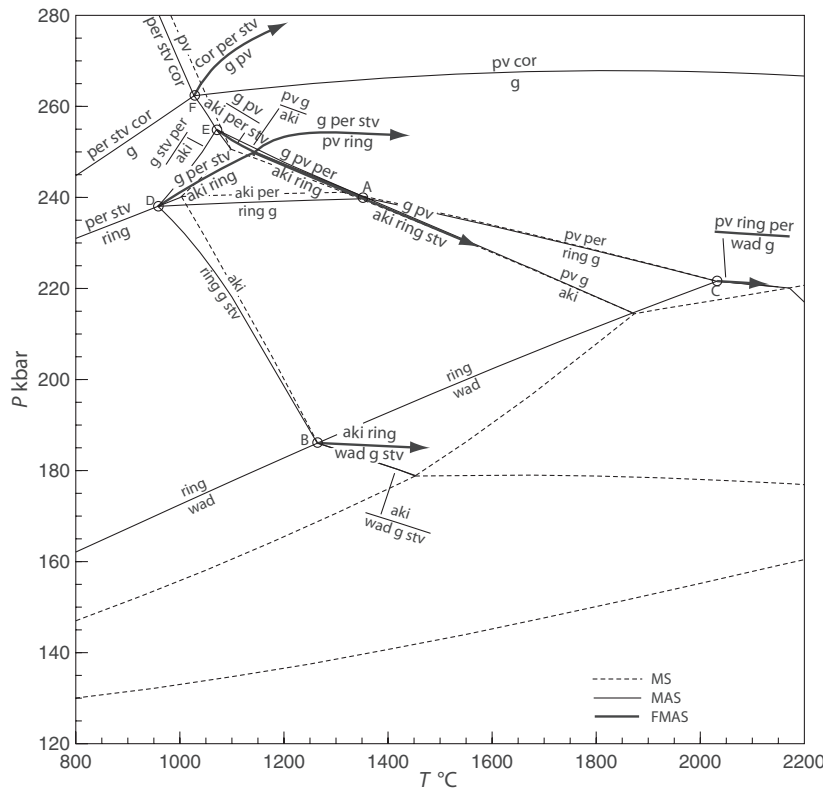


Fig. 10. P - T projection for deep mantle phase in $\text{MgO}-\text{Al}_2\text{O}_3-\text{SiO}_2$. Full thin curves are univariant equilibria in MAS and thin dashed curves are the MS equilibria. There are six MAS invariant points (A, B, C, D, E, F) with emergent $\text{FeO}-\text{MgO}-\text{Al}_2\text{O}_3-\text{SiO}_2$ univariants shown by heavy lines and arrowed ends, as well as one full FMAS invariant point close to 250 kbar and 1200 °C. cor, corundum; other phase names as in Fig. 9. For a - x relationships used, see Table S2.

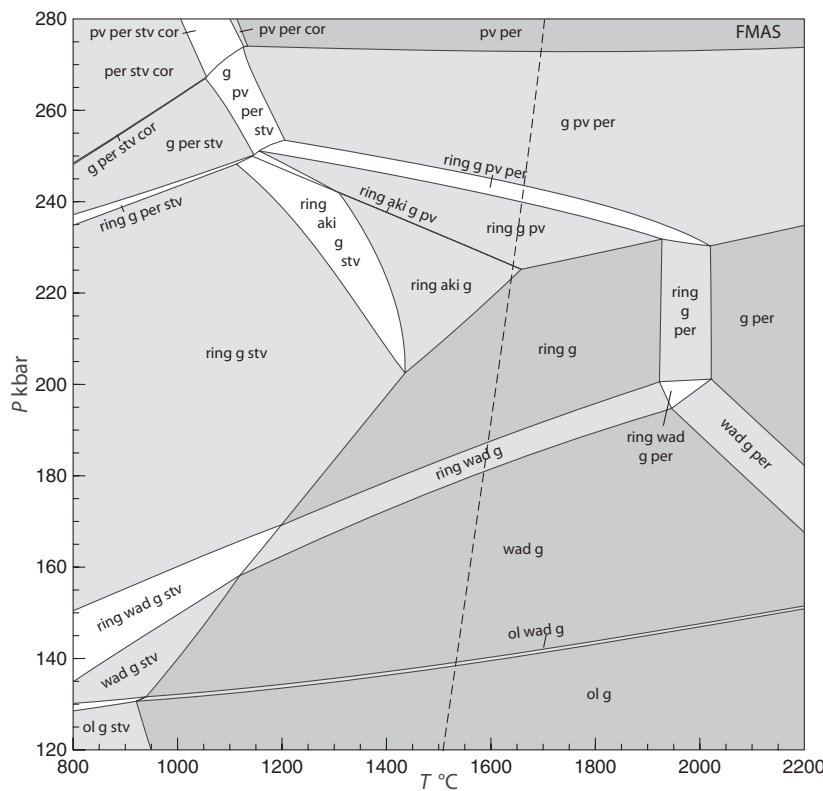


Fig. 11. P - T pseudosection for $\text{FeO}-\text{MgO}-\text{Al}_2\text{O}_3-\text{SiO}_2$ with a bulk composition corresponding to the Kilbourne Hole peridotite KLB-1 (Walter, 1998). The bulk composition sees short sections of some of the univariant curves in Fig. 10, but only below about 1400 °C and 240 kbar and so typical mantle geotherms are likely to pass to somewhat higher temperatures and may not intersect them. The dashed line represents one estimated geotherm smoothed from Stixrude & Lithgow-Bertelloni (2007). The lowest pressure part of this diagram is metastable with respect to inclusion of high-pressure cpx which was not considered for this diagram. cor, corundum; other phase names as in Fig. 9. For a - x relationships used, see Table S2.

derive these data. First, pressures and temperatures for the same experimental boundaries are often inconsistent among different investigators, and second, the pressure scale to be used in the experiments has not yet been satisfactorily resolved. Thus, the calculated equilibria may require adjustment in future as these experimental problems are resolved.

DISCUSSION

The internally consistent thermodynamic data set described here is a major improvement on previous ones because all the calorimetric and experimental data published in the 13 years since HP98 are now considered and incorporated if appropriate, and this increases the reliability of the data and expands the scope (via the incorporation of the new end-members that has become possible). The increase in reliability of the data set, in relation to the end-members already present in HP98, stems from the better implicit cross-checking between equilibria that involve the same end-members (the ‘internal consistency’) as new data become available. In detail, if before there was an equilibrium with high ‘hat’ (see HP98, table 7, or Table S1 here) – a measure of how constraining that equilibrium is – then addition of data involving that end-member will reduce the hat for the equilibria involved. Also additional data may simply suggest that equilibria taken to be correct in the past should now be considered untrustworthy and not used in data set generation. Methodological improvements also contribute to reliability. The expansion of scope is self-evident in the addition of a large number of new end-members, but also arises as a consequence of the methodological improvements that now allow calculations at high P - T , and in S-bearing systems, for example.

The ongoing development of the internally consistent thermodynamic data set is largely dependent on the calorimetric and phase equilibria experimental community, without whose best efforts our work will tend to founder. Although we think this data set is a substantial step forward in the quest for this aspect of quantification of petrological processes, much needs to be done. Obvious things are needed, for example the proper characterization of the phases in experimental charges and measurement of unit cell volumes to high pressures and temperatures, particularly those made at high temperatures at elevated pressures. As may be readily seen from Appendix 1, there remain many end-members for which no measured thermal expansion, compressibility or heat capacity values as yet exist. For some, for example, those fictive end-members which do not exist stably in nature or are not readily synthesized experimentally, such measurements will never be available but could in principle be calculated from molecular simulations. For many others in the table new measurements would be most welcome. Applications to well-characterized rocks from well-established

geological settings will provide critical input to the evaluation of the data set, and we welcome feedback relating to this from people using the data set. Of course such applications are equally reliant on the activity–composition relations used for the phases involved, as well as a realistic appraisal of the likely geological processes involved in rock formation.

In generation of the data set, the enthalpies of formation of the end-members are solved for in the weighted least squares approach. As a part of this, the uncertainty on these enthalpies are calculated, as well as the correlations between them (e.g. Powell & Holland, 1993a,b). These uncertainties can be considered as reflecting ‘known unknowns’ about the end-member properties. If in fact data used in the generation of the data set are incorrect, because the data were not sufficiently dense to identify this, then this amounts to ‘unknown unknowns’ about the end-member properties (the results are incorrect, and we have no way of knowing about it). The former source of uncertainty can be accounted for in error propagation calculations, but the latter cannot be handled in this way and introduce a bias in the results if, later, such problems are recognized. It is for this reason that validation of the data set via more experimental studies, and/or appropriate applications is important.

In using the data set, the uncertainties inherent in the data set can be propagated through calculations using THERMOCALC, as is done routinely in average P - T calculations, but also can be done for P - T projection and pseudosection calculations (via the calcsdnle script). So, for example considering Fig. 5, the uncertainty on the positions of the invariant points that form the highlighted triangle at around 6 kbar and 1000 °C, from the data set uncertainties, at 2 σ level, in {kbar, °C}, are $\{6.4 \pm 0.8, 964 \pm 142\}$, $\{6.4 \pm 1.0, 983 \pm 88\}$ and $\{6.5 \pm 0.6, 1004 \pm 40\}$, with increasing temperature. If the uncertainties on the interaction parameters of the phases (Table S2) are also included, as they can be as outlined in Powell & Holland (2008), the uncertainties will be yet larger. These uncertainties are for the invariant points individually, and a way of looking at the correlations between the positions of the points as a consequence of the uncertainties is not yet implemented. It is conceivable that the uncertainties simply translate the triangle of points, rather than cause them to be involved in an inversion of topology. Work is in progress to address this aspect of uncertainties in calculated phase diagrams. Uncertainties, but with the same problem of not being able to ascertain correlations, can be done for pseudosection calculations. So, in Fig. 11, looking at the point on the divariant field, ring + g + pv + per, where the modes of pv and per are zero, the calculated uncertainty just with data set uncertainties is $\{231.8 \pm 8.0, 1928 \pm 326\}$. In the case of propagated uncertainties for calculations at these conditions, the agreement of a pressure scale for experimental studies, as well as the reaching of a

consensus on the position of end-member equilibria in $P-T$, should dramatically reduce the size of the uncertainties.

ACKNOWLEDGEMENTS

We thank K. Evans for her enthusiasm and direct involvement with generating the sulphur part of the data set story. R. White, J. Diener and E. Green are also thanked for suggestions and discussions on data set-related matters. We thank J. Ferry, J. Ganguly, M. Gottshalk and an anonymous reviewer for their helpful reviews, and J. Connolly for comments on TEOS. We thank M. Brown yet again for his editorial handling of our work. R. Powell thanks the support of ARC DP0451770 and DP0987731.

REFERENCES

- Ackerman, D., Seifert, F. & Schreyer, W., 1975. Instability of sapphirine at high pressures. *Contributions to Mineralogy and Petrology*, **50**, 79–92.
- Adams, L.H. & Williamson, E.D., 1923. On the compressibility of minerals and rocks at high pressures. *Journal of the Franklin Institute*, **195**, 475–529.
- Akaogi, M., Ito, E. & Navrotsky, A., 1989. Olivine-modified spinel–spinel transitions in the system Mg_2SiO_4 – Fe_2SiO_4 : Calorimetric measurements, thermochemical calculation, and geophysical application. *Journal of Geophysical Research*, **94**, 15671–15686.
- Akaogi, M., Kamii, N., Kishi, A. & Kojitani, H., 2004. Calorimetric study on high-pressure transitions in $KAlSi_3O_8$. *Physics and Chemistry of Minerals*, **31**, 85–91.
- Akimoto, S., 1987. High-pressure research in geophysics: past, present and future. In: *High-Pressure Research in Mineral Physics* (eds Manghnani, M.H. & Syono, Y.), pp. 1–13. Terra Scientific Publishing Company, (TERRAPUB), Tokyo/American Geophysical Union, Washington, D.C..
- Akimoto, S., Fujisawa, H. & Katsura T., 1965. The olivine–spinel transition in Fe_2SiO_4 – Ni_2SiO_4 . *Journal of Geophysical Research*, **70**, 1969–1977.
- Akimoto, S., Komada, E. & Kushiro, I., 1967. Effect of pressure on the melting of olivine and spinel polymorphs of Fe_2SiO_4 . *Journal of Geophysical Research*, **68**, 679–686.
- Alcock, C.B. & Richardson, F.D., 1951. Thermodynamics of ferrous sulphide. *Nature*, **168**, 661–662.
- Aldebert, P. & Traverse, J.P., 1984. α - Al_2O_3 : a high-temperature thermal expansion standard. *High Temperature-High Pressure*, **16**, 127–135.
- Alexandrov, I.V., Goncharov, A.F., Zisman, A.N. & Stishov, S.M., 1987. Diamond at high pressures: Raman Scattering of light, equation of state, and high pressure scale. *Soviet Physics JETP*, **66**, 384–390.
- Allan, D.R. & Angel, R.J., 1997. A high-pressure structural study of microcline ($KAlSi_3O_8$) to 7 GPa. *European Journal of Mineralogy*, **9**, 263–275.
- Allen, J.M. & Fawcett, J.J., 1982. Zoisite-anorthite-calcite stability relations in H_2O – CO_2 fluids at 5000 bars: an experimental and SEM study. *Journal of Petrology*, **23**, 215–239.
- Anderson, G.M., Castet, S., Schott, J. & Mesmer, R.E., 1991. The density model for estimation of thermodynamic parameters of reactions at high temperatures and pressures. *Geochimica et Cosmochimica Acta*, **55**, 1769–1779.
- Anderson, O.L., 1997. Volume dependence of thermal pressure in solids. *Journal of Physics and Chemistry of Solids*, **58**, 335–343.
- Anderson, O.L. & Isaak, D.G., 1995. Elastic constants of mantle minerals at high temperature. In: *A Handbook of Physical Constants*. AGU Reference Shelf, **2**, 64–97.
- Anderson, P.A.M. & Kleppa, O.J., 1969. The thermochemistry of the kyanite–sillimanite equilibrium. *American Journal of Science*, **267**, 285–290.
- Anderson, P.A.M., Newton, R.C. & Kleppa, O.J., 1977. The enthalpy change of the andalusite–sillimanite reaction and the Al_2SiO_5 diagram. *American Journal of Science*, **277**, 585–593.
- Andrault, D., Angel, R.J., Mosenfelder, J.L. & Le Bihan, T., 2003. Equation of state of stishovite to lower mantle pressures. *American Mineralogist*, **88**, 301–307.
- Angel, R.J., 2004. Equations of state of plagioclase feldspars. *Contributions to Mineralogy and Petrology*, **146**, 506–512.
- Angel, R.J., Chopelas, A. & Ross, N.L., 1992. Stability of high-density clinoenstatite at upper-mantle pressures. *Nature*, **358**, 322–325.
- Angel, R.J., Kunz, M., Miletich, R., Woodland, A.B., Koch, M. & Knoche, R.L., 1999a. Effect of isovalent Si, Ti substitution on the bulk moduli of $Ca(Ti_{1-x}Si_x)SiO_5$ titanites. *American Mineralogist*, **84**, 282–287.
- Angel, R.J., Kunz, M., Miletich, R., Woodland, A.B., Koch, M. & Xirouchakis, D., 1999b. High-pressure phase transition in $CaTiOSiO_4$ titanite. *Phase Transitions*, **68**, 533–543.
- Angel, R.J., McMullan, R.K. & Prewitt, C.T., 1991. Substructure and superstructure of mullite by neutron diffraction. *American Mineralogist*, **76**, 332–342.
- Anovitz, L.M. & Essene, E.J., 1987. Phase equilibria in the system $CaCO_3$ – $MgCO_3$ – $FeCO_3$. *Journal of Petrology*, **28**, 389–414.
- Anovitz, L.M., Treiman, A.H., Essene, E.J. et al., 1985. The heat-capacity of ilmenite and phase equilibria in the system Fe–Ti–O. *Geochimica et Cosmochimica Acta*, **49**, 2027–2040.
- Aranovich, L.Y. & Newton, R.C., 1996. H_2O activity in concentrated NaCl solutions at high pressures and temperatures measured by the brucite-periclase equilibrium. *Contributions to Mineralogy and Petrology*, **125**, 200–212.
- Aranovich, L.Y. & Newton, R.C., 1998. Reversed determination of the reaction phlogopite + quartz = enstatite + potassium feldspar + H_2O in the ranges 750–875°C and 2–12 kbar at low H_2O activity with concentrated KCl solutions. *American Mineralogist*, **83**, 193–204.
- Aranovich, L.Y. & Newton, R.C., 1999. Experimental determination of CO_2 – H_2O activity-composition relations at 600–1000 °C and 6–14 kbar by reversed decarbonation and dehydration reactions. *American Mineralogist*, **84**, 1319–1332.
- Arima, M. & Onuma, K., 1977. The solubility of alumina in enstatite and the phase equilibria in the join $MgSiO_3$ – $MgAl_2SiO_6$ at 10–25 kbar. *Contributions to Mineralogy and Petrology*, **61**, 219–230.
- Artoli, G., Geiger, C.A. & Dapiaggi, M., 2003. The crystal chemistry of julgoldite– Fe^{3+} from Bombay, India, studied using synchrotron X-ray powder diffraction and ^{57}Fe Mössbauer spectroscopy. *American Mineralogist*, **88**, 1084–1090.
- Ashida, T., Kume, S. & Ito, E., 1987. Thermodynamic aspects of phase boundary among α -, β -, and γ - Mg_2SiO_4 . In: *High-Pressure Research in Mineral Physics* (eds Manghnani, M.H. & Syono, Y.), pp. 269–274. Terra Scientific Publishing Company, Tokyo/American Geophysical Union, Washington, DC.
- Atlas, L., 1952. The polymorphism of $MgSiO_3$, and solid-state equilibria in the system $MgSiO_3$ – $CaMgSi_2O_6$. *Journal of Geology*, **60**, 125–147.
- Baker, E.H., 1962. The calcium oxide–carbon dioxide system in the pressure range 1–300 atmospheres. *Journal of the Chemical Society*, **87**, 464–470.
- Baker, J. & Newton, R.C., 1994. Standard thermodynamic properties of meionite, $Ca_4Al_6Si_6O_{24}CO_3$, from experimental phase equilibria. *American Mineralogist*, **79**, 478–484.

- Baker, J. & Holland, T.J.B., 1996. Experimental reversals of chlorite compositions in divariant $MgO-Al_2O_3-SiO_2-H_2O$ assemblages: implications for order-disorder in chlorites. *American Mineralogist*, **81**, 676–684.
- Baker, J., 1995. Thermal expansion of scapolite. *American Mineralogist*, **79**, 878–884.
- Baldwin, J.A., Powell, R., Williams, M.L. & Goncalves, P., 2007. Formation of eclogite, and reaction during exhumation to mid-crustal levels, Snowbird tectonic zone, western Canadian Shield. *Journal of Metamorphic Geology*, **25**, 953–974.
- Balzar, D. & Ledbetter, H., 1993. Crystal structure and compressibility of 3:2 mullite. *American Mineralogist*, **78**, 1192–1196.
- Barnes, H.L. & Ernst, W.G., 1963. Ideality and ionization in hydrothermal fluids. The system $MgO-H_2O-NaOH$. *American Journal of Science*, **261**, 129–150.
- Behrens, H., 1995. Determination of water solubilities in high-viscosity melts: an experimental study on $NaAlSi_3O_8$ melts. *European Journal of Mineralogy*, **7**, 905–920.
- Berman, R.G., Aranovich, L.Y., Genkin, M. & Mader, U.K., 1995. Phase equilibrium constraints on the stability of biotite: Part 1. Mg-Al biotite in the system $K_2O-MgO-Al_2O_3-SiO_2-H_2O-CO_2$. *Current Research (Geological Survey of Canada)*, **995-E**, 253–261.
- Bertoldi, C., Dachs, E. & Theye, T., 2006. Calorimetric data for naturally occurring magnesiocarpholite and ferrocarrpholite. *American Mineralogist*, **91**, 441–445.
- Bertoldi, C., Dachs, E. & Theye, T., 2007. Heat-pulse calorimetry measurements on natural chlorite-group minerals. *American Mineralogist*, **92**, 553–559.
- Birch, F., 1966. Compressibility; elastic constants. In: *Handbook of Physical Constants* (ed. Clark, S.P.). *Geological Society of America Memoir*, **97**, 97–173.
- Bird, D.K. & Helgeson, H.C., 1980. Chemical interaction of aqueous solutions with epidote-feldspar mineral assemblages in geologic systems. 1. Thermodynamic analysis of phase relations in the system $CaO-FeO-Fe_2O_3-Al_2O_3-SiO_2-H_2O-CO_2$. *American Journal of Science*, **280**, 907–941.
- Bird, G.W. & Fawcett, J.J., 1973. Stability relations of Mg-chlorite-muscovite and quartz between 5 and 10 kbar water pressure. *Journal of Petrology*, **14**, 415–428.
- Boettcher, A.L. & Wyllie, P.J., 1968. Jadeite stability measured in the presence of silicate liquids in the system $NaAlSiO_4-SiO_2-H_2O$. *Geochimica et Cosmochimica Acta*, **32**, 999–1012.
- Boettcher, A.L., 1970. The system $CaO-Al_2O_3-SiO_2-H_2O$ at high temperatures and pressures. *Journal of Petrology*, **11**, 337–339.
- Boffa-Ballaran, T. & Angel, R.J., 2003. Equation of state and high-pressure phase transitions in lawsonite. *European Journal of Mineralogy*, **15**, 241–246.
- Bohlen, S.R. & Boettcher, A.L., 1982. The quartz-coesite transformation: a precise determination and the effects of other components. *Journal of Geophysical Research*, **87**, 7073–7078.
- Bohlen, S.R. & Liotta, J.J., 1986. A barometer for garnet amphibolites and garnet granulites. *Journal of Petrology*, **27**, 1025–1034.
- Bohlen, S.R., Boettcher, A.L., Wall, V.J. & Clemens, J.D., 1983a. Stability of phlogopite-quartz and sanidine-quartz: a model for melting in the lower crust. *Contributions to Mineralogy and Petrology*, **83**, 270–277.
- Bohlen, S.R., Wall, V.J. & Boettcher, A.L., 1983b. Experimental investigation and application of garnet granulite equilibria. *Contributions to Mineralogy and Petrology*, **83**, 52–61.
- Bohlen, S.R., Wall, V.J. & Boettcher, A.L., 1983c. Experimental investigations and geological applications of equilibria in the system $FeO-TiO_2-Al_2O_3-SiO_2-H_2O$. *American Mineralogist*, **68**, 1049–1058.
- Bohlen, S.R., Dollase, W.A. & Wall, V.J., 1986. Calibration and applications of spinel equilibria in the system $FeO-Al_2O_3-SiO_2$. *Journal of Petrology*, **27**, 1143–1156.
- Bohlen, S.R., Essene, E.J. & Boettcher, A.L., 1980. Reinvestigation and application of olivine-quartz-orthopyroxene barometry. *Earth and Planetary Science Letters*, **47**, 1–10.
- Bohlen, S.R., Montana, A. & Kerrick, D.M., 1991. Precise determination of the equilibria kyanite = sillimanite and kyanite = andalusite and a revised triple point for Al_2SiO_5 polymorphs. *American Mineralogist*, **76**, 677–680.
- Bose, K. & Ganguly, J., 1995. Quartz-coesite transition revisited: reversed experimental determination at 500–1200 °C and retrieved thermochemical properties. *American Mineralogist*, **80**, 231–238.
- Bose, K. & Navrotsky, A., 1998. Thermochemistry and phase equilibria of hydrous phases in the system $MgO-SiO_2-H_2O$ Implications for volatile transport to the mantle. *Journal of Geophysical Research*, **103**, 9713–9719.
- Bosenick, A., Ceiger, C.A. & Cemic, L., 1996. Heat capacity measurements of synthetic pyrope-grossular garnets between 320 and 1000K by differential scanning calorimetry. *Geochimica et Cosmochimica Acta*, **60**, 3215–3227.
- Bowen, N.L., 1912. The binary system: $Na_2Al_2Si_2O_8$ (nephelite, carnegieite)- $CaAl_2Si_2O_6$ (anorthite). *American Journal of Science*, **33**, 551–573.
- Bowen, N.L. & Anderson, O., 1914. The binary system $MgO-SiO_2$. *American Journal of Science*, **37**, 487–500.
- Bowen, N.L. & Greig, J.W., 1925. The crystalline modifications of $NaAlSiO_4$. *American Journal of Science*, **10**, 204–215.
- Bowen, N.L. & Schairer, J.F., 1935. The system $MgO-Fe-SiO_2$. *American Journal of Science*, **29**, 151–217.
- Bowman, A.F., 1975. An Investigation of Al_2SiO_5 Phase Equilibrium Utilizing the Scanning Electron Microscope. MS thesis, University of Oregon, Eugene, Oregon, 80 pp.
- Boyd F.R. & England, J.L., 1959. Pyrope. *Carnegie Institution of Washington Yearbook*, **58**, 83–87.
- Boyd, F.R. & England, J.L., 1963. Effect of pressure on the melting of diopside, $CaMgSi_2O_6$ and albite, $NaAlSi_3O_8$, in the range up to 50 kilobars. *Journal of Geophysical Research*, **68**, 311–323.
- Boyd, F.R. & England, J.L., 1965. The rhombic enstatite-clinoenstatite inversion. *Carnegie Institution of Washington Year Book*, **64**, 117–120.
- Boyd, F.R., 1959. Hydrothermal investigations of amphiboles. In: *Researches in Geochemistry*, 1 (ed. Abelson, P.H.), pp. 377–396. Wiley, New York.
- Brey, G., Brice, W.R., Ellis, D.J., Green, D.H., Harris, K.L. & Ryabchikov, I.D. (1983) Pyroxene-carbonate reactions in the upper mantle. *Earth and Planetary Science Letters*, **62**, 63–74.
- Brousse, C., Newton, R.C. & Kleppa, O.J., 1984. Enthalpy of formation of forsterite, enstatite, akermanite, monticellite and merwinite at 1073 K determined by alkali borate solution calorimetry. *Geochimica et Cosmochimica Acta*, **48**, 1081–1088.
- Burt, J.B., Ross, N.L., Angel, R.J. & Koch, M., 2006. Equations of state and structures of andalusite to 9.8 GPa and sillimanite to 8.5 GPa. *American Mineralogist*, **91**, 319–326.
- Burton, J.C., Taylor, L.A. & Chou, I.-M., 1982. The fO_2-T and fs_2-T stability relations of hedenbergite and of hedenbergite-johansene solid solutions. *Economic Geology*, **77**, 764–783.
- Butterman, W.C. & Foster W.R., 1967. Zircon stability and the ZrO_2-SiO_2 phase diagram. *American Mineralogist*, **52**, 880–885.
- Cameron, M., Sueno, S., Prewitt, C.T. & Papike, J.J., 1973. High-temperature crystal chemistry of acmite, diopside, hedenbergite, jadeite, spodumene, and ureyite. *American Mineralogist*, **58**, 594–618.
- Cameron, W.E., 1977. Mullite: a substituted alumina. *American Mineralogist*, **62**, 747–755.
- Carey, J.W. & Navrotsky, A., 1992. The molar enthalpy of dehydration of cordierite. *American Mineralogist*, **77**, 930–936.
- Carey, J.W., 1995. A thermodynamic formulation of hydrous cordierite. *Contributions to Mineralogy and Petrology*, **119**, 155–165.

- Carman, J.H., 1974. Synthetic sodium phlogopite and its two hydrates: stabilities, properties and mineralogic implications. *American Mineralogist*, **59**, 261–273.
- Carman, J.H., & Gilbert, M.C., 1983. Experimental studies on glaucophane stability. *American Journal of Science*, **283A**, 414–437.
- Carpenter, M.A. & Cellai, D., 1996. Microstructures and high-temperature phase transitions in kalsilite. *American Mineralogist*, **81**, 561–584.
- Carr, R.M. & Fyfe, W.S., 1960. Synthesis fields of some aluminium silicates. *Geochimica et Cosmochimica Acta*, **21**, 99–109.
- Carrington, D.P. & Harley, S.L., 1995. Partial melting and phase relations in high-grade metapelites: an experimental petrogeometric grid in KFMASH system. *Contributions to Mineralogy and Petrology*, **120**, 270–291.
- Carroll Webb, S.A. & Wood, B.J., 1986. Spinel-pyroxene-garnet relationships and their dependence on Cr/Al ratio. *Contributions to Mineralogy and Petrology*, **92**, 471–480.
- Catti, M., Ferraris, G., Hull, S. & Pavese, A., 1995. Static compression and disorder in brucite, $Mg(OH)_2$, to 11 GPa: a powder neutron diffraction study. *Physics and Chemistry of Minerals*, **22**, 200–206.
- Chai, L. & Navrotsky, A., 1993. Thermochemistry of carbonate-pyroxene equilibria. *Contributions to Mineralogy and Petrology*, **114**, 139–147.
- Chamberlin, L., Beckett, J.R. & Stolper, E., 1995. Palladium oxide equilibration and the thermodynamic properties of $MgAl_2O_4$ spinel. *American Mineralogist*, **80**, 285–296.
- Charlu, T.V., Newton, R.C. & Kleppa, O.J., 1975. Enthalpies of solution at 970K of compounds in the system $MgO-Al_2O_3-SiO_2$ by high temperature solution calorimetry. *Geochimica et Cosmochimica Acta*, **39**, 1487–1497.
- Chase, M.W.J., 1998. *NIST-JANAF Thermochemical Tables: Fourth Edition*. American Chemical Society and the American Institute of Physics for the National Institute of Standards and Technology, Gaithersburg, MD, USA.
- Chatterjee, N.D., 1970. Synthesis and upper stability of paragonite. *Contributions to Mineralogy and Petrology*, **27**, 244–257.
- Chatterjee, N.D., 1972. The upper stability limit of the assemblage paragonite + quartz and its natural occurrences. *Contributions to Mineralogy and Petrology*, **34**, 288–303.
- Chatterjee, N.D., 1974. Synthesis and upper thermal stability limit of 2M-margarite, $CaAl_2Al_2Si_2O_{10}(OH)_2$. *Schweizerische Mineralogische Petrologische Mitteilungen*, **54**, 753–767.
- Chatterjee, N.D., 1976. Margarite stability and compatibility relations in the system $CaO-Al_2O_3-SiO_2-H_2O$ as a pressure-temperature indicator. *American Mineralogist*, **61**, 699–709.
- Chatterjee, N.D. & Johannes, W., 1974. Thermal stability and standard thermodynamic properties of synthetic 2M1-muscovite, $KAl_2AlSi_3O_{10}(OH)_2$. *Contributions to Mineralogy and Petrology*, **48**, 89–114.
- Chatterjee, N.D., Johannes, W. & Leistner, H., 1984. The system $CaO-Al_2O_3-SiO_2-H_2O$: new phase equilibria data, some calculated phase relations, and their petrological applications. *Contributions to Mineralogy and Petrology*, **88**, 1–13.
- Chatterjee, N.D. & Schreyer, W., 1972. The reaction enstatite + sillimanite = sapphirine + quartz in the system $MgO-Al_2O_3-SiO_2$. *Contributions to Mineralogy and Petrology*, **36**, 49–62.
- Chen, C.-H. & Presnall, D.C., 1975. The system $Mg_2SiO_4-SiO_2$ at pressures up to 25 kilobars. *American Mineralogist*, **60**, 398–406.
- Chernosky, J.V., 1974. The upper stability of clinochlore at low pressure and the free energy of formation of Mg-cordierite. *American Mineralogist*, **59**, 496–507.
- Chernosky, J.V., 1975. Aggregate refractive indices and unit cell parameters of synthetic serpentinine in the system $MgO-Al_2O_3-SiO_2-H_2O$. *American Mineralogist*, **60**, 200–208.
- Chernosky, J.V., 1976a. Gibbs free energy of enstatite, clinochlore and hydrous Mg-cordierite evaluated from phase equilibrium data. *EOS (Transactions of the American Geophysical Union)*, **57**, 1020.
- Chernosky, J.V., 1976b. The stability of anthophyllite – a re-evaluation based on new experimental data. *American Mineralogist*, **61**, 1145–1155.
- Chernosky, J.V., 1978. The stability of clinochlore and quartz at low pressure. *American Mineralogist*, **63**, 73–82.
- Chernosky, J.V., 1982. The stability of clinohryosite. *Canadian Mineralogist*, **20**, 19–27.
- Chernosky, J.V. & Autio, L.K., 1979. The stability of anthophyllite in the presence of quartz. *American Mineralogist*, **84**, 294–300.
- Chernosky, J.V. & Berman, R.G., 1986a. Experimental reversal of the equilibrium: clinochlore + 2 magnesite = 3 forsterite + spinel + $2CO_2 + 4H_2O$. *EOS (Transactions of the American Geophysical Union)*, **67**, 1279.
- Chernosky, J.V. & Berman, R.G., 1986b. The stability of clinochlore in mixed volatile, CO_2-H_2O fluids. *EOS (Transactions of the American Geophysical Union)*, **67**, 407.
- Chernosky, J.V. & Berman, R.G., 1991. Experimental reversal of the equilibrium andalusite + calcite = anorthite + CO_2 . *American Mineralogist*, **76**, 791–802.
- Chernosky, J.V., Day, H.W. & Caruso, L.J., 1985. Equilibria in the system $MgO-SiO_2-H_2O$: experimental determination of the stability of Mg-anthophyllite. *American Mineralogist*, **70**, 223–236.
- Chinner, G.A. & Dixon, J.E., 1974. Some high pressure parageneses of the Allalin Gabbro, Valais, Switzerland. *Journal of Petrology*, **14**, 185–202.
- Cho, M., Liou, J.G. & Maruyama, S., 1986. Transition from the zeolite to prehnite-pumpellyite facies in the Karmutsen metabasites, Vancouver Island, British Columbia. *Journal of Petrology*, **27**, 467–494.
- Cho, M., Maruyama, S. & Liou, J.G., 1987. An experimental investigation of heulandite-laumontite equilibrium at 1000 and 2000 bar P_{fluid} . *Contributions to Mineralogy and Petrology*, **97**, 43–50.
- Chopin, C. & Monie, P., 1984. A unique magnesiochloritoid-bearing, high pressure assemblage from the Monte Rosa: a petrologic and $^{40}Ar-^{39}Ar$ study. *Contributions to Mineralogy and Petrology*, **87**, 388–398.
- Chopin, C. & Schreyer, W., 1983. Magnesiocarpholite and magnesiochloritoid: two index minerals of pelitic blueschists and their preliminary phase relations in the model system $MgO-Al_2O_3-SiO_2-H_2O$. *American Journal of Science*, **283A**, 72–96.
- Chopin, C. & Sobolev, N.V., 1995. Principal mineralogical indicators of UHP in crustal rocks. In: *Ultrahigh Pressure Metamorphism* (eds Coleman, R.G. & Wang, X), pp. 96–131. Cambridge University Press, Cambridge.
- Chou, I.-M., 1978. Calibration of oxygen buffers at elevated P and T using the hydrogen fugacity buffer. *American Mineralogist*, **63**, 690–703.
- Circone, S., Navrotsky, A., Kirkpatrick, R.J. & Graham, C.M., 1991. Substitution of $[^{6,4}Al]$ in phlogopite: mica characterization, unit-cell variation, ^{27}Al and ^{29}Si MAS-NMR spectroscopy, and Al-Si distribution in the tetrahedral sheet. *American Mineralogist*, **76**, 1485–1501.
- Clark, S.P., 1966. High pressure phase equilibria. In: *Handbook of Physical Constants* (ed. Clarke, S.P.). Geological Society of America Memoir, **97**, 345–370.
- Clendenen, R.L. & Drickamer, H.G., 1966. Lattice parameters of nine oxides and sulfides as a function of pressure. *Journal of Chemical Physics*, **44**, 4223–4228.
- Coggon, R. & Holland, T.J.B., 2002. Mixing properties of muscovite–celadonite–ferroceldadonite–paragonite micas and revised garnet–phengite thermobarometers. *Journal of Metamorphic Geology*, **20**, 683–696.

- Cohen, L.H. & Clement, W., 1967. High-low quartz inversion: determination to 35 kilobars. *Journal of Geophysical Research*, **72**, 4245–4251.
- Comodi, P., Gatta, G.C. & Zanazzi, P.F., 2001. High-pressure structural behaviour of heulandite. *European Journal of Mineralogy*, **13**, 497–505.
- Comodi, P., Mellini, M. & Zanazzi, P.F., 1992. Magnesiochloritoid: compressibility and high pressure structure refinement. *Physics and Chemistry of Minerals*, **18**, 483–490.
- Comodi, P., Mellini, M., Ungaretti, L. & Zanazzi, P.F., 1991. Compressibility and high pressure structure refinement of tremolite, pargasite, and glaucophane. *European Journal of Mineralogy*, **3**, 485–499.
- Comodi, P. & Zanazzi, P.F., 1995. High pressure structural study of muscovite. *Physics and Chemistry of Minerals*, **22**, 170–177.
- Comodi, P. & Zanazzi, P.F., 1997. The pressure behaviour of clinozoisite and zoisite: an X-ray diffraction study. *American Mineralogist*, **82**, 61–68.
- Comodi, P., Zanazzi, P.F., Poli, S. & Schmidt, M.W., 1997. High-pressure behavior of kyanite: compressibility and structural deformations. *American Mineralogist*, **82**, 452–459.
- Connolly, J.A.D. & Kerrick, D.M., 1985. Experimental and thermodynamic analysis of prehnite. *EOS*, **66**, 388.
- Corona, J.C. & Jenkins, D.M., 2007. An experimental investigation of the reaction: glaucophane + 2 quartz = 2 albite + talc. *European Journal of Mineralogy*, **19**, 147–158.
- Crawford, W.A. & Fyfe, W.S., 1965. Lawsonite equilibria. *American Journal of Science*, **263**, 262–270.
- Crawford, W.A. & Hoersch, A.L., 1972. Calcite-aragonite equilibrium from 50 °C to 150°C. *American Mineralogist*, **57**, 995–998.
- D'Amour, H., Schiferl, D., Denner, W., Schulz, H. & Holzapfel, W.B., 1978. High-pressure single-crystal structure determinations for ruby up to 90 kbar using an automatic diffractometer. *Journal of Applied Physics*, **49**, 4411–4416.
- Dachs, E., 1994. Annite stability revised; 1, hydrogen-sensor data for the reaction annite = sanidine + magnetite + H₂. *Contributions to Mineralogy and Petrology*, **117**, 229–240.
- Dachs, E. & Benisek, A., 1995. The stability of annite + quartz; reversed experimental data for the reaction 2 annite + 3 quartz = 2 sanidine + 3 fayalite + 2 H₂O. *Contributions to Mineralogy and Petrology*, **121**, 380–387.
- Dachs, E. & Geiger, C.A., 2008. Low-temperature heat capacity of synthetic Fe- and Mg-cordierite: thermodynamic properties and phase relations in the system FeO-Al₂O₃-SiO₂-(H₂O). *European Journal of Mineralogy*, **20**, 47–62.
- Dachs, E., Geiger, C.A., Withers, A.C. & Essene, E.J., 2009. A calorimetric investigation of spessartine: vibrational and magnetic heat capacity. *Geochimica et Cosmochimica Acta*, **73**, 3393–3409.
- Dalton, J.A. & Wood, B.J., 1993. The partitioning of Fe and Mg between olivine and carbonate and the stability of carbonate under mantle conditions. *Contributions to Mineralogy and Petrology*, **114**, 501–509.
- Danckwerth, P. & Newton, R.C., 1978. Experimental determination of the spinel peridotite to garnet peridotite reaction in the system MgO-Al₂O₃-SiO₂ in the range 900 °C–1100 °C and Al₂O₃ isopleths of enstatite in the spinel field. *Contributions to Mineralogy and Petrology*, **66**, 189–200.
- Davidson, P.M., Symmes, G.H., Cohen, B.A., Reeder, R.J. & Lindsley, D.H., 1993. Synthesis of the new compound CaFe(CO₃)₂ and experimental constraints on the (Ca,Fe)CO₃ join. *Geochimica et Cosmochimica Acta*, **58**, 5105–5109.
- Davis, B.T.C. & England, J.L., 1964. The melting of forsterite up to 50 kilobars. *Journal of Geophysical Research*, **69**, 1113–1116.
- Detrie, T.A., Ross, N.L. & Angel, R.J., 2009. Equation of state and structure of prehnite to 9.8 GPa. *European Journal of Mineralogy*, **21**, 561–570.
- Dickenson, M.P. & Hewitt, D., 1986. A garnet-chlorite geothermometer. *Geological Society of America Abstracts with Programs*, **18**, 584.
- Diener, J.A., Powell, R., White, R.W. & Holland, T.J.B., 2007. A new thermodynamic model for clino- and orthoamphiboles in Na₂O-CaO-FeO-MgO-Al₂O₃-SiO₂-H₂O-O. *Journal of Metamorphic Geology*, **25**, 631–656.
- Dollase, W., 1973. Mössbauer spectra and iron distribution in the epidote-group minerals. *Zeitschrift für Kristallographie*, **138**, 41–63.
- Dorogokupets, P.I., 1995. Equation of state for lambda transition in quartz. *Journal of Geophysical Research*, **100**, 8489–8499.
- Doroshev, A.M. & Malinovskiy, I.Y., 1974. Upper pressure limit of stability of sapphirine. *Doklady Akademii Nauk SSSR*, **219**, 136–138.
- Downs, R.T., Hazen, R.M. & Finger, L.W., 1994. The high-pressure crystal chemistry of low albite and the origin of the pressure dependency of Al-Si ordering. *American Mineralogist*, **79**, 1042–1052.
- Downs, R.T., Zha, C.-S., Duffy, T.S. & Finger, L.W., 1996. The equation of state of forsterite to 17.2 GPa and effects of pressure media. *American Mineralogist*, **81**, 51–55.
- Dubrovinsky, L.S. & Saxena, S.K., 1997. Thermal expansion of periclase (MgO) and tungsten (W) to melting temperatures. *Physics and Chemistry of Minerals*, **24**, 547–550.
- Duffy, C.J. & Greenwood, H.J., 1979. Phase equilibria in the system MgO-MgF₂-SiO₂-H₂O. *American Mineralogist*, **64**, 1156–1174.
- Dutrow, B.L. & Holdaway, M.J., 1989. Experimental determination of the upper thermal stability of Fe-staurolite + quartz at medium pressures. *Journal of Petrology*, **30**, 229–248.
- Eggert, R.G. & Kerrick, D.M., 1981. Metamorphic equilibria in the siliceous dolomite system: 6 kbar experimental data and geologic implications. *Geochimica et Cosmochimica Acta*, **45**, 1039–1049.
- Eggler, D.H., Kushiro, I. & Holloway, J.R., 1976. Free energies of decarbonation reactions at mantle pressures 1. Stability of the assemblage forsterite-enstatite-magnesite in the system MgO-SiO₂-CO₂-H₂O. *American Mineralogist*, **64**, 288–293.
- Eggleton, R.A., 1972. The crystal structure of stilpnomelane. Part II. The full cell. *Mineralogical Magazine*, **38**, 693–711.
- Engi, M., 1983. Equilibria involving Al-Cr spinel: Mg-Fe exchange with olivine. Experiments, thermodynamic analysis, and consequences for geothermometry. *American Journal of Science*, **283-A**, 29–71.
- Engi, M., 1986. Quoted in: Evans, B.W. & Guggenheim, S. 1988: Talc, pyrophyllite, and related minerals. In: Hydrous Phyllosilicates (ed. Bailey, S.W.). *Reviews in Mineralogy*, **19**, 225–294.
- Ernst, W.G., 1962. Synthesis, stability relations, and occurrence of riebeckite and riebeckite-afvedsonite solid solutions. *Journal of Geology*, **70**, 689–736.
- Essene, E.J., Boettcher, A.L. & Furst, G.A., 1972. Indirect measurements of DG for quartz + corundum = kyanite. *EOS*, **53**, 554.
- Essene, E.J., 1974. High-pressure transformations in CaSiO₃. *Contributions to Mineralogy and Petrology*, **45**, 247–250.
- Evans, B.W., 1990. Phase relations of epidote-blueschists. *Lithos*, **25**, 3–23.
- Evans, B.W., 2004. The serpentinite multisystem revisited: chrysotile is metastable. *International Geology Review*, **46**, 479–506.
- Evans, B.W. & Ghiurso, M.S., 1995. Thermodynamics and petrology of cummingtonite. *American Mineralogist*, **80**, 649–663.
- Evans, B.W., Johannes, W., Oterdoom, W.H. & Trommsdorff, V., 1976. Stability of chrysotile and antigorite in the serpentine

- multisystem. *Schweizerische Mineralogische Petrologische Mitteilungen*, **56**, 79–93.
- Evans, H.T., 1979. The thermal expansion of anhydrite to 1000°C. *Physics and Chemistry of Minerals*, **4**, 77–82.
- Evans, K.A., Powell, R. & Holland, T.J.B., 2010. Internally consistent data for sulphur-bearing phases and applications to the constructions for mafic greenschists facies rocks in $\text{Na}_2\text{O}-\text{CaO}-\text{K}_2\text{O}-\text{FeO}-\text{MgO}-\text{Al}_2\text{O}_3-\text{SiO}_2-\text{CO}_2-\text{O-S-H}_2\text{O}$. *Journal of Metamorphic Geology*, **28**, 667–687.
- Evans, K.A. & Powell, R., 2005. The thermodynamics of mixing in saline and mixed solvent solutions at elevated temperature and pressure: a framework for geological phase equilibria calculations. *Geochimica et Cosmochimica Acta*, **70**, 5488–5506.
- Fasshauer, D.W., Chatterjee, N.D. & Marler, B., 1997. Synthesis, structure, thermodynamic properties and stability relations of K-cymrite, $\text{KAlSi}_3\text{O}_8-\text{H}_2\text{O}$. *Physics and Chemistry of Minerals*, **24**, 455–462.
- Fasshauer, D.W., Wunder, B., Chatterjee, N.D. & Hohne, G.W.H., 1998. Heat capacity of wadeite-type $\text{K}_2\text{Si}_4\text{O}_9$ and the pressure-induced stable decomposition of K-feldspar. *Contributions to Mineralogy and Petrology*, **131**, 210–218.
- Fawcett, J.J. & Yoder, H.S., 1966. Phase relationships of chlorites in the system $\text{MgO}-\text{Al}_2\text{O}_3-\text{SiO}_2-\text{H}_2\text{O}$. *American Mineralogist*, **61**, 303–310.
- Fei, Y., 1999. Effects of temperature and composition on the bulk modulus of $(\text{Mg},\text{Fe})\text{O}$. *American Mineralogist*, **84**, 272–276.
- Fei, Y. & Bertka, C.M., 1999. Phase transformations in the Earth's mantle and mantle mineralogy. In: *Mantle Petrology: Field Observations and High Pressure Experimentation*, Vol. 6 (eds Fei, Y., Bertka, C.M. & Myssen, B.O.), pp. 189–207. The Geological Society, Washington, DC.
- Fei, Y. & Mao, H.K., 1993. Static compression of $\text{Mg}(\text{OH})_2$ to 78 GPa at high temperature and constraints on the equation of state of fluid H_2O . *Journal of Geophysical Research*, **98**, 11875–11884.
- Fei, Y. & van Orman, J., Li, J., et al., 2004. Experimentally determined postspinel transformation boundary in Mg_2SiO_4 using MgO as an internal pressure standard and its geophysical implications. *Journal of Geophysical Research*, **109**, B02305, doi: 10.1029/2003JB002562.
- Fei, Y., Saxena, S.K. & Navrotsky, A., 1990. Internally consistent thermodynamic data and equilibrium phase relations for compounds in the system $\text{MgO}-\text{SiO}_2$ at high pressure and high temperature. *Journal of Geophysical Research*, **95**, 6915–6928.
- Ferry, J.M., Newton, R.C. & Manning, C.E., 2002. Experimental determination of the equilibria: rutile + magnesite = geikielite + CO_2 and zircon + 2 magnesite = baddeleyite + 2CO_2 . *American Mineralogist*, **87**, 1342–1350.
- Ferry, J.M. & Spear, F.S., 1978. Experimental calibration of the partitioning of Fe and Mg between biotite and garnet. *Contributions to Mineralogy and Petrology*, **66**, 113–117.
- Finger, L.W. & Hazen, R.M., 1980. Crystal structure and isothermal compression of Fe_2O_3 , Cr_2O_3 , and V_2O_3 to 50 kbars. *Journal of Applied Physics*, **51**, 5362–5367.
- Finger, L.W., Hazen, R.M. & Hofmeister, A., 1986. High pressure crystal chemistry of spinel (MgAl_2O_4) and magnetite (Fe_3O_4): comparisons with other silicate spinels. *Physics and Chemistry of Minerals*, **13**, 215–220.
- Finger, L.W. & Ohashi, Y., 1976. The thermal expansion of diopside to 800 °C and a refinement of the crystal structure at 700 °C. *American Mineralogist*, **61**, 303–310.
- Fiquet, G. & Reynard, B., 1999. High-pressure equation of state of magnesite: new data and a reappraisal. *American Mineralogist*, **84**, 856–860.
- Fiquet, G., Richet, P. & Montagnac, D., 1999. High-temperature thermal expansion of lime, periclase, corundum and spinel. *Physics and Chemistry of Minerals*, **27**, 103–111.
- Fockenberg, T., 1995. New experimental results up to 100 GPa in the system $\text{MgO}-\text{Al}_2\text{O}_3-\text{SiO}_2-\text{H}_2\text{O}$ (MASH): preliminary stability fields of chlorite, chloritoid, staurolite, MgMgAl -pumpellyite, and pyrope. *Bochumer Geologische und Geotechnische Arbeiten*, **44**, 39–44.
- Fockenberg, T., 1998. An experimental investigation on the P-T stability of Mg-staurolite in the system $\text{MgO}-\text{Al}_2\text{O}_3-\text{SiO}_2-\text{H}_2\text{O}$. *Contributions to Mineralogy and Petrology*, **130**, 187–198.
- Fockenberg, T., 2008. Pressure-temperature stability of pyrope in the system $\text{MgO}-\text{Al}_2\text{O}_3-\text{SiO}_2-\text{H}_2\text{O}$. *European Journal of Mineralogy*, **20**, 735–744.
- Fockenberg, T., Wunder, B., Grevel, K.-D. & Burchard, M., 1996. The equilibrium diaspore-corundum at high pressures. *European Journal of Mineralogy*, **8**, 1293–1299.
- Fonarev, V.I. & Konliov, A.N., 1986. Experimental study of Fe-Mg distribution between biotite and orthopyroxene. *Contributions to Mineralogy and Petrology*, **93**, 227–235.
- Fonarev, V.I. & Korolkov, G.J., 1980. The assemblage orthopyroxene + cummingtonite + quartz. The low-temperature stability limit. *Contributions to Mineralogy and Petrology*, **73**, 413–420.
- Freund, J. & Ingalls, R., 1989. Inverted isothermal equations of state and determination of B_0 , B'_0 and B''_0 . *Journal of Physics and Chemistry of Solids*, **50**, 263–268.
- Frost, D.J., 2003. The structure and sharpness of $(\text{Mg},\text{Fe})_2\text{SiO}_4$ phase transformations in the transition zone. *Earth and Planetary Science Letters*, **216**, 313–328.
- Fukui, H., Ohtaka, O., Suzuki, T. & Funakoshi, K., 2003. Thermal expansion of $\text{Mg}(\text{OH})_2$ brucite under high pressure and pressure dependence of entropy. *Physics and Chemistry of Minerals*, **30**, 511–516.
- Ganguly, J., 1969. Chloritoid stability and related paragenesis: theory, experiments and applications. *American Journal of Science*, **267**, 910–944.
- Ganguly, J., 1972. Staurolite stability and related paragenesis: theory, experiments and applications. *Journal of Petrology*, **13**, 335–365.
- Gasparik, T. & Newton, R.C., 1984. The reversed alumina contents of orthopyroxene in equilibrium with spinel and forsterite in the system $\text{MgO}-\text{Al}_2\text{O}_3-\text{SiO}_2$. *Contributions to Mineralogy and Petrology*, **85**, 186–196.
- Gasparik, T., 1984. Experimental study of subsolidus phase relations and mixing properties of pyroxene in the system $\text{CaO}-\text{Al}_2\text{O}_3-\text{SiO}_2$. *Geochimica et Cosmochimica Acta*, **48**, 2537–2545.
- Gasparik, T., 1985. Experimental study of subsolidus phase relations and mixing properties of pyroxene and plagioclase in the system $\text{Na}_2\text{O}-\text{CaO}-\text{Al}_2\text{O}_3-\text{SiO}_2$. *Contributions to Mineralogy and Petrology*, **89**, 346–357.
- Gasparik, T., Wolf, K. & Smith, C.M., 1994. Experimental determination of phase relations in the CaSiO_3 system from 8 to 15 GPa. *American Mineralogist*, **79**, 1219–1222.
- Geiger, C.A., Newton, R.C. & Kleppa, O.J., 1987. Enthalpy of mixing of synthetic almandine-grossular and almandine-pyrope garnets from high-temperature solution calorimetry. *Geochimica et Cosmochimica Acta*, **51**, 1755–1763.
- Ghiorso, M.S. & Evans, B.W., 2002. Thermodynamics of the amphiboles: $\text{Ca}-\text{Mg}-\text{Fe}^{2+}$ quadrilateral. *American Mineralogist*, **87**, 79–98.
- Gibbons, K., Dempsey, M.J. & Henderson, C.M.B., 1981. The thermal expansion of staurolite, $\text{Fe}_4\text{Al}_{18}\text{Si}_8\text{O}_{44}(\text{OH})_4$. *Mineralogical Magazine*, **44**, 69–72.
- Gillet, P., Daniel, I., Guyot, F., Matas, J. & Chervin, J.-C., 2000. A thermodynamic model for MgSiO_3 -perovskite derived from pressure, temperature and volume dependence of the Raman mode frequencies. *Physics of the Earth and Planetary Interiors*, **117**, 361–384.
- Goldsmith, J.R., 1980a. The melting and breakdown reactions of anorthite at high pressures and temperatures. *American Mineralogist*, **65**, 272–284.

- Goldsmith, J.R., 1980b. Thermal stability of dolomite at high temperatures and pressures. *Journal of Geophysical Research*, **85**, 6949–6954.
- Goldsmith, J.R., 1981. The join $\text{CaAl}_2\text{Si}_2\text{O}_8-\text{H}_2\text{O}$ (anorthite–water) at elevated pressures and temperatures. *American Mineralogist*, **66**, 1183–1188.
- Goldsmith, J.R. & Heard, H.C., 1962. Subsolidus phase relations in the system $\text{CaCO}_3-\text{MgCO}_3$. *Journal of Geology*, **69**, 45–74.
- Goldsmith, J.R. & Jenkins, D.M., 1985. The hydrothermal melting of low and high albite. *American Mineralogist*, **70**, 924–933.
- Goldsmith, J.R. & Peterson J.W., 1990. Hydrothermal melting behaviour of KAlSi_3O_8 as microcline and sanidine. *American Mineralogist*, **75**, 1362–1369.
- Goldsmith, J.R. & Newton, R.C., 1969. P–T–X relations in the system $\text{CaCO}_3-\text{MgCO}_3$ at high temperatures and pressures. *American Journal of Science*, **267A**, 160–190.
- Goldsmith, J.R. & Newton, R.C., 1977. Scapolite-plagioclase stability relations at high pressures and temperatures in the system $\text{NaAlSi}_3\text{O}_8-\text{CaAl}_2\text{Si}_2\text{O}_8-\text{CaCO}_3-\text{CaSO}_4$. *American Mineralogist*, **62**, 1063–1081.
- Goranson, R.W., 1936. Silicate-water systems: the solubility of water in albite-melt. *Transactions of the American Geophysical Union*, **17**, 257–259.
- Gordon, T.M. & Greenwood, H.J., 1970. The reaction: dolomite + quartz + water = talc + calcite + carbon dioxide. *American Journal of Science*, **268**, 225–242.
- Green, T.H. & Helman, P.L., 1982. Fe–Mg partitioning between coexisting garnet and phengite at high pressure, and comments on a garnet-phengite geothermometer. *Lithos*, **15**, 253–266.
- Greenwood, H.J., 1967a. Mineral equilibria in the system $\text{MgO}-\text{SiO}_2-\text{H}_2\text{O}-\text{CO}_2$. In: *Researches in Geochemistry II* (ed. Abelson, P.H.), pp. 542–592. Wiley, New York.
- Greenwood, H.J., 1967b. Wollastonite: Stability in $\text{H}_2\text{O}-\text{CO}_2$ mixtures and occurrence in a contact-metamorphic aureole near Salmo, British Columbia, Canada. *American Mineralogist*, **52**, 1669–1680.
- Greig, J.W. & Barth, T.F.W., 1938. The system $\text{Na}_2\text{O}-\text{Al}_2\text{O}_3-2\text{SiO}_2$ (nephelite, carnegieite)– $\text{Na}_2\text{O}\text{Al}_2\text{O}_3-3\text{SiO}_2$ (albite). *American Journal of Science*, **35A**, 93–112.
- Grevel, K.-D., Fasshauer, D.W. & Rohling, S., 1998. P–V–T data of kyanite and Mg-staurolite for pressures up to 7.5 GPa. *Terra Abstracts* (Abstract Suppl. No. 1 to Terra Nova), **10**, 20.
- Grieve, R.A.F. & Fawcett, J.J., 1974. The stability of chloritoid below 10 kb $\text{P}_{\text{H}_2\text{O}}$. *Journal of Petrology*, **15**, 113–139.
- Gronvold, F. & Stolen, S., 1991. Thermodynamics of iron sulphides I. Heat capacity and thermodynamic properties of Fe_9S_{10} at temperatures from 5 K to 740 K. *Journal of Chemical Thermodynamics*, **23**, 261–272.
- Gronvold, F. & Stolen, S., 1992. Thermodynamics of iron sulphides II. Heat capacity and thermodynamic properties of FeS and of $\text{Fe}_{0.875}\text{S}$ at temperatures from 298.15 K to 1000 K, of $\text{Fe}_{0.98}\text{S}$ from 298.15 K to 800 K and of $\text{Fe}_{0.89}\text{S}$ from 298.15 K to about 650 K. *Journal of Chemical Thermodynamics*, **24**, 913–936.
- Grundy, H.D. & Brown, W.L., 1974. A high temperature X-ray study of low and high plagioclase feldspars. In: *The Feldspars, Proceedings of a NATO Advanced Study Institute* (eds MacKenzie, W.S. & Zussman, J.), pp. 162–173. University of Manchester Press, Manchester.
- Guggenheim, S., Chang, Y.H. & Koster Van Groos, A.F., 1987. Muscovite dehydroxylation: high-temperature studies. *American Mineralogist*, **72**, 537–550.
- Gustafson, W., 1974. The stability of andradite, hedenbergite, and related minerals in the system Ca–Fe–Si–O–H. *Journal of Petrology*, **15**, 455–496.
- Haas, H., 1972. Diaspore-corundum equilibrium determined by epitaxis of diaspore on corundum. *American Mineralogist*, **57**, 1375–1385.
- Haas, H. & Holdaway, M.J., 1973. Equilibria in the system $\text{Al}_2\text{O}_3-\text{SiO}_2-\text{H}_2\text{O}$ involving the stability limits of pyrophyllite and the thermodynamic data of pyrophyllite. *American Journal of Science*, **273**, 449–464.
- Hackler, R.T. & Wood, B.J., 1989. Experimental determination of Fe and Mg exchange between garnet and olivine and estimation of Fe–Mg mixing properties in garnet. *American Mineralogist*, **74**, 994–999.
- Harker, R.I. & Tuttle, O.F., 1955. Studies in the system $\text{CaO}-\text{MgO}-\text{CO}_2$. Part 1: the thermal dissociation of calcite, dolomite and magnesite. *American Journal of Science*, **253**, 209–224.
- Harker, R.I. & Tuttle, O.F., 1956. Experimental data on the $\text{P}_{\text{CO}_2}-\text{T}$ curve for the reaction: calcite + quartz = wollastonite + carbon dioxide. *American Journal of Science*, **254**, 239–256.
- Harker, R.I., 1959. The synthesis and stability of tilleyite, $\text{Ca}_5\text{Si}_2\text{O}_7(\text{CO}_3)_2$. *American Journal of Science*, **257**, 656–667.
- Harley, S.L., 1984. An experimental study of the partitioning of Fe and Mg between garnet and orthopyroxene. *Contributions to Mineralogy and Petrology*, **87**, 359–373.
- Harlov, D.E. & Milke, R., 2002. Stability of corundum + quartz relative to kyanite and sillimanite at high temperature and pressure. *American Mineralogist*, **78**, 424–432.
- Harlov, D.E., Milke, R. & Gottschalk, M., 2008. Metastability of sillimanite relative to corundum and quartz in the kyanite stability field: competition between stable and metastable reactions. *American Mineralogist*, **93**, 608–617.
- Harlov, D.E. & Newton, R.C., 1992. Experimental determination of the reaction 2 magnetite + 2 kyanite + 4 quartz = 2 almandine + O_2 at high pressure on the magnetite–hematite buffer. *American Mineralogist*, **77**, 558–564.
- Harlov, D.E. & Newton, R.C., 1993. Reversal of the metastable kyanite + corundum + quartz and andalusite + corundum + quartz equilibria and the enthalpy of formation of kyanite and andalusite. *American Mineralogist*, **78**, 594–600.
- Haselton, H.T., Hemingway, B.S. & Robie, R.A., 1984. Low temperature heat capacities of $\text{CaAl}_2\text{SiO}_6$ glass and pyroxene and thermal expansion of $\text{CaAl}_2\text{SiO}_6$ pyroxene. *American Mineralogist*, **69**, 481–489.
- Haselton, H.T., Robie, R.A. & Hemingway, B.S., 1987. Heat capacities of synthetic hedenbergite, ferrobustamite and $\text{CaFeSi}_2\text{O}_6$ glass. *Geochimica et Cosmochimica Acta*, **51**, 2211–2217.
- Haselton, H.T., Sharp, W.R. & Newton, R.C., 1978. CO_2 fugacity at high temperatures and pressures from experimental decarbonation reactions. *Geophysical Research Letters*, **5**, 753–756.
- Hays, J.F., 1967. Lime-alumina-silica. *Carnegie Institute of Washington Yearbook*, **65**, 234–239.
- Hazen, R.M., 1976. Effects of temperature and pressure on the crystal structure of forsterite. *American Mineralogist*, **61**, 1280–1293.
- Hazen, R.M. & Finger, L.W., 1979. Crystal structure and compressibility of zircon at high pressure. *American Mineralogist*, **64**, 196–201.
- Hazen, R.M. & Finger, L.W., 1981. Bulk moduli and high-pressure crystal structures of rutile-type compounds. *Journal of Physics and Chemistry of Solids*, **42**, 143–151.
- Hazen, R.M. & Finger, L.W., 1989. The crystal chemistry of andradite and pyrope: revised procedures for high-pressure diffraction experiments. *American Mineralogist*, **74**, 352–359.
- Hazen, R.M. & Sharp, Z.D., 1988. Compressibility of sodalite and scapolite. *American Mineralogist*, **73**, 1120–1122.
- Heinrich, W. & Althaus, E., 1980. Die obere Stabilitätsgrenze von Lawsonit plus Albit bzw. Jadeit. *Fortschritte der Mineralogie*, **58**, 49–50.
- Helgeson, H.C., Delany, J.M., Nesbitt, H.W. & Bird, D.K., 1978. Summary and critique of the thermodynamic properties of rock-forming minerals. *American Journal of Science*, **278A**, 1–229.

- Hemingway, B.S. & Robie, R.A., 1984. Heat capacity and thermodynamic functions for gehlenite and staurolite: with comments on the Schottky anomaly in the heat capacity of staurolite. *American Mineralogist*, **69**, 307–318.
- Hemingway, B.S., Bohlen, S.R., Hankins, W.B., Westrum, E.F. & Kuskov, O.L., 1998. Heat capacity and thermodynamic properties for coesite and jadeite, reexamination of the quartz-coesite equilibrium boundary. *American Mineralogist*, **83**, 409–418.
- Hemingway, B.S., Evans, H.T., Nord, G.L., Haselton, H.T., Robie, R.A. & McGee, J.J., 1986. Akermanite: phase transitions in heat capacity and thermal expansion, and revised thermodynamic data. *Canadian Mineralogist*, **24**, 425–434.
- Hemingway, B.S., Robie, R.A., Evans, H.T. & Kerrick, D.M., 1991. Heat capacities and entropies of sillimanite, fibrolite, andalusite, kyanite, and quartz and the Al_2SiO_5 diagram. *American Mineralogist*, **76**, 1597–1613.
- Hemley, J.J., Marinenko, J.W. & Luce, R.W., 1980. Equilibria in the system Al_2O_3 – SiO_2 – H_2O and some general implications for alteration/mineralisation processes. *Economic Geology*, **75**, 210–228.
- Hensen, B.J., 1972. Phase relations involving pyrope, enstatite_{ss}, and sapphirine_{ss} in the system MgO – Al_2O_3 – SiO_2 . *Carnegie Institution of Washington Yearbook*, **71**, 421–427.
- Hensen, B.J. & Essene, E.J., 1971. Stability of pyrope-quartz in the system MgO – Al_2O_3 – SiO_2 . *Contributions to Mineralogy and Petrology*, **30**, 72–83.
- Hertzberg, C.T., 1983. The reaction forsterite + cordierite = aluminous orthopyroxene + spinel in the system MgO – Al_2O_3 – SiO_2 . *Contributions to Mineralogy and Petrology*, **84**, 84–90.
- Hewitt, D.A., 1973. Stability of the assemblage muscovite-calcite-quartz. *American Mineralogist*, **58**, 785–791.
- Hewitt, D.A., 1975. Stability of the assemblage phlogopite-calcite-quartz. *American Mineralogist*, **60**, 391–397.
- Hewitt, D.A., 1978. A redetermination of the fayalite-magnetite-quartz equilibrium between 650 ° and 850 °C. *American Journal of Science*, **278**, 715–724.
- Hilairet, N., Daniel, I. & Reynard, B., 2006. P–V equations of state and the relative stabilities of serpentine varieties. *Physics and Chemistry of Minerals*, **33**, 629–637.
- Hirose K., Fei Y., Ono S., Yagi T., & Funakoshi K., 2001. In situ measurements of the phase transition boundary in $\text{-Mg}_3\text{Al}_2\text{Si}_3\text{O}_{12}$: Implications for the nature of the seismic discontinuities in the Earth's mantle. *Earth and Planetary Science Letters*, **184**, 567–573.
- Hochella, M.F., Liou, J.G., Keskinen, M.J. & Kim, H.S., 1982. Synthesis and stability relations of magnesian idocrase. *Economic Geology*, **77**, 798–808.
- Hoffmann, C., 1972. Natural and synthetic ferroglaucophane. *Contributions to Mineralogy and Petrology*, **34**, 135–149.
- Holdaway, M.J. & Lee, S.M., 1977. Fe-Mg cordierite stability in high-grade pelitic rocks based on experimental, theoretical and natural observations. *Contributions to Mineralogy and Petrology*, **63**, 175–198.
- Holdaway, M.J., 1971. Stability of andalusite and the aluminum silicate phase diagram. *American Journal of Science*, **271**, 97–131.
- Holdaway, M.J., 1972. Thermal stability of Al-Fe epidote as a function of f_{O_2} and Fe content. *Contributions to Mineralogy and Petrology*, **37**, 307–340.
- Holland, T.J.B., 1979. Experimental determination of the reaction paragonite = jadeite + kyanite + quartz + water, and internally consistent thermodynamic data for part of the system Na_2O – Al_2O_3 – SiO_2 – H_2O , with applications to eclogites and blueschists. *Contributions to Mineralogy and Petrology*, **68**, 293–301.
- Holland, T.J.B., 1980. The reaction albite = jadeite + quartz determined experimentally in the range 600–1200 °C. *American Mineralogist*, **65**, 129–134.
- Holland, T.J.B., 1988. Preliminary phase relations involving glaucophane and applications to high pressure petrology: new heat capacity and thermodynamic data. *Contributions to Mineralogy and Petrology*, **99**, 134–142.
- Holland, T.J.B., 1989. The dependence of entropy on volume for silicate and oxide minerals: a review and a predictive model. *American Mineralogist*, **74**, 5–13.
- Holland, T.J.B. & Carpenter, M.A., 1986. Aluminum/silicon disordering and melting in sillimanite at high pressures. *Nature*, **320**, 151–153.
- Holland, T.J.B. & Powell, R., 1985. An internally consistent thermodynamic dataset with uncertainties and correlations: 2. Data and results. *Journal of Metamorphic Geology*, **3**, 343–370.
- Holland, T.J.B. & Powell, R., 1996a. Thermodynamics of order-disorder in Minerals 1: symmetric formalism applied to minerals of fixed composition. *American Mineralogist*, **81**, 1413–1424.
- Holland, T.J.B. & Powell, R., 1996b. Thermodynamics of order-disorder in Minerals 2: symmetric formalism applied to solid solutions. *American Mineralogist*, **81**, 1425–1437.
- Holland, T.J.B. & Powell, R., 2003. Activity–composition relations for phases in petrological calculations: an asymmetric multicomponent formulation. *Contributions to Mineralogy and Petrology*, **145**, 492–501.
- Holland, T.J.B. & Powell, R., 1991. A compensated-Redlich-Kwong (CORK) equation for volumes and fugacities of CO_2 and H_2O in the range 1 bar to 50 kbar and 100–1600 °C. *Contributions to Mineralogy and Petrology*, **109**, 265–273.
- Holland, T.J.B. & Powell, R., 1998. An internally-consistent thermodynamic dataset for phases of petrological interest. *Journal of Metamorphic Geology*, **16**, 309–344.
- Holland, T.J.B. & Powell, R., 2001. Calculation of phase relations involving haplogranitic melts using an internally-consistent thermodynamic dataset. *Journal of Petrology*, **42**, 673–683.
- Holland, T.J.B. & Ray, N.J., 1985. Glaucophane and pyroxene breakdown reactions in the Pennine units of the eastern Alps. *Journal of Metamorphic Geology*, **3**, 417–438.
- Holland, T.J.B., Babu, E.V.S.S.K. & Waters, D.J., 1996. Phase relations of osumilite and dehydration melting in pelitic rocks: a simple thermodynamic model for the KFMASH system. *Contributions to Mineralogy and Petrology*, **124**, 383–394.
- Holland, T.J.B., Redfern, S.A.T. & Pawley, A.R., 1996. Volume behaviour of hydrous minerals at high pressure and temperature: 2. Compressibilities of lawsonite, zoisite, clinozoisite and epidote. *American Mineralogist*, **81**, 341–348.
- Holm, J.L. & Kleppa, O.J., 1966. The thermodynamic properties of the aluminum silicates. *American Mineralogist*, **51**, 1608–1622.
- Holtz, F. & Johannes, W., 1996. *Petrogenesis and Experimental Petrology of Granitoid Rocks*. Springer-Verlag, Berlin.
- Hoschek, G., 1974. Gehlenite stability in the system CaO – Al_2O_3 – SiO_2 – H_2O – CO_2 . *Contributions to Mineralogy and Petrology*, **47**, 245–254.
- Hoschek, G., 1990. Melting and subsolidus reactions in the system K_2O – CaO – MgO – Al_2O_3 – SiO_2 – H_2O : experiments and petrologic application. *Contributions to Mineralogy and Petrology*, **105**, 393–402.
- Hoschek, G., 1995. Stability relations and Al content of tremolite and talc in CMASH assemblages with kyanite + zoisite + quartz + H_2O . *European Journal of Mineralogy*, **7**, 353–362.
- Hovis, G.L., Brennan, S., Keohane, M. & Crelling, J., 1999. High-temperature X-ray investigation of sanidine-analbite crystalline solutions; thermal expansion, phase transitions, and volumes of mixing. *Canadian Mineralogist*, **37**, 701–709.
- Hovis, G.L., Crelling, J., Wattles, D. et al., 2003. Thermal expansion of nepheline-kalsilite crystalline solutions. *Mineralogical Magazine*, **67**, 535–546.
- Howald, R.A., 1992. Comments on the MgO – CaO system. *Calphad*, **16**, 25–32.

- Hsu, L.C., 1968. Selected phase relationships in the system Al–Mn–Fe–Si–O; a model for garnet equilibria. *Journal of Petrology*, **9**, 40–83.
- Huang, W.L. & Wyllie, P.J., 1975. Melting and subsolidus phase relationships for CaSiO₃ to 35 kilobars pressure. *American Mineralogist*, **60**, 213–217.
- Huang, Y.K. & Chow, C.Y., 1974. The generalized compressibility equation of Tait for dense matter. *Journal of Physics D: Applied Physics*, **7**, 2021–2023.
- Huckenholz, H.G. & Yoder, H.S., 1971. Andradite stability relations in the CaSiO₃–Fe₂O₃ join up to 30 kbar. *Neues Jahrbuch für Mineralogie Abhandlungen*, **114**, 246–280.
- Huckenholz, H.G., Hözl, E., & Lindhuber, W., 1975. Grossularite, its solidus and liquidus relations in the CaO–Al₂O₃–SiO₂–H₂O system up to 10 kbar. *Neues Jahrbuch Mineralogisches Abhandlung*, **124**, 1–46.
- Hudon, P., Jung, I. & Baker, D.R., 2002. Melting of β-quartz up to 2.0 GPa and thermodynamic optimization of the silica liquidus up to 6.0 GPa. *Physics of the Earth and Planetary Interiors*, **130**, 159–174.
- Huebner, J.S. & Eugster, H.P., 1968. Rhodochrosite decarbonation in the system MnO–SiO₂–CO₂. *Geological Society of America Special Publication*, **121**, 144–145.
- Huebner, J.S., 1969. Stability relations of rhodachrosite in the system manganese–carbon–oxygen. *American Mineralogist*, **54**, 457–481.
- Hugh-Jones, D.A. & Angel, R.J., 1994. A compressional study of MgSiO₃ orthoenstatite up to 8.5 GPa. *American Mineralogist*, **79**, 405–410.
- Hunt, J.A. & Kerrick, D.M., 1977. The stability of sphene: experimental redetermination and geological implications. *Geochimica et Cosmochimica Acta*, **41**, 279–288.
- Hynes, A. & Forest, R.C., 1988. Empirical garnet–muscovite geothermometry in low grade metapelites, Selwyn Range (Canadian Rockies). *Journal of Metamorphic Geology*, **8**, 89–124.
- Irifune, T., Ohtani, E. & Kumazawa, M., 1982. Stability field of knorringite Mg₃Cr₂Si₃O₁₂ at high pressure and its implication to the occurrence of Cr-rich pyrope in the upper mantle. *Physics of the Earth and Planetary Interiors*, **27**, 263–272.
- Irving, A.J. & Wyllie, P.J., 1975. Subsolidus and melting relationships for calcite, magnesite, and the join CaCO₃–MgCO₃ to 36 kbar. *Geochimica et Cosmochimica Acta*, **39**, 35–53.
- Irving, A.J., Huang, W.L. & Wyllie, P.J., 1977. Phase relations of portlandite, Ca(OH)₂ and brucite, Mg(OH)₂ to 33 kilobars. *American Journal of Science*, **277**, 313–321.
- Isaak, D.G., Anderson, O.L. & Oda, H., 1992. High-temperature thermal expansion and elasticity of calcium-rich garnets. *Physics and Chemistry of Minerals*, **19**, 106–120.
- Ito, E. & Takahashi, E., 1989. Post spinel transformations in the system Mg₂SiO₄–Fe₂SiO₄ and some geophysical implications. *Journal of Geophysical Research*, **94**, 10637–10646.
- Ito, E. & Yamada, H., 1982. Stability relations of silicate spinels, ilmenites and perovskites. In: *High-Pressure Research in Geophysics*, (eds S. Akimoto and M.H. Manghnani), pp. 405–419. D Reldel, Dordrecht.
- Ito, H., Kawada, K. & Akimoto, S., 1974. Thermal expansion of stishovite. *Physics of the Earth and Planetary Interiors*, **8**, 277–281.
- Ivaldi, G., Catti, M. & Ferraris, G., 1988. Crystal structure at 25 and 700 ° of magnesioclorthitoid from a high pressure assemblage (Monte Rosa). *American Mineralogist*, **73**, 358–364.
- Jackson, J.M., Palko, J.W., Andrault, D. *et al.*, 2003. Thermal expansion of natural orthoenstatite to 1473K. *European Journal of Mineralogy*, **15**, 469–473.
- Jackson, I. & Niesler, H., 1982. The elasticity of periclase to 3 GPa and some geophysical implications. In: *High-Pressure Research in Geophysics* (eds Akimoto, S. & Manghnani M. H.), pp. 93–113. Center for Academic Publications, Tokyo.
- Jackson, I., 1976. Melting of the silica isotopes SiO₂, BeF₂ and GeO₂ at elevated pressures. *Physics of the Earth and Planetary Interiors*, **13**, 218–231.
- Jacobs, M.H.G. & de Jong, B.H.W.S., 2005. An investigation into thermodynamic consistency of data for the olivine, wadsleyite and ringwoodite form of (Mg,Fe)₂SiO₄. *Geochimica et Cosmochimica Acta*, **69**, 4361–4375.
- Jacobs, M.H.G. & Oonk, H.A.J., 2000. A new equation of state based on Grover, Getting and Kennedy's empirical relation between volume and bulk modulus. The high-pressure thermodynamics of MgO. *Physical Chemistry Chemical Physics*, **2**, 2641–2646.
- Jacobs, M.H.G. & Oonk, H.A.J., 2001. The Gibbs energy formulation of the α , β and γ forms of Mg₂SiO₄ using Grover, Getting and Kennedy's empirical relation between volume and bulk modulus. *Physics and Chemistry of Minerals*, **28**, 572–585.
- Jacobs, G.K. & Kerrick, D.M., 1981. Devolatilisation equilibria in H₂O–CO₂ and H₂O–CO₂–NaCl fluids: an experimental and thermodynamic evaluation at elevated pressures and temperatures. *American Mineralogist*, **66**, 1135–1153.
- James, R.S., Turnock, A.C. & Fawcett, J.J., 1976. The stability and phase relations of iron chlorite below 8.5 kb P_{H₂O}. *Contributions to Mineralogy and Petrology*, **56**, 1–25.
- Jamieson, H.E. & Roeder, P.L., 1984. The distribution of Mg and Fe²⁺ between olivine and spinel at 1300 °C. *American Mineralogist*, **69**, 283–291.
- Jeanloz, R. & Rudy, A., 1987. Static compression of MnO manganosite to 60 GPa. *Journal of Geophysical Research*, **92**, 11433–11436.
- Jenkins, D.M. & Bozhilov, K.N., 2003. Stability and thermodynamic properties of ferroactinolite: a re-investigation. *American Journal of Science*, **303**, 723–752.
- Jenkins, D.M. & Chernosky, J.V., 1986. Phase equilibria and crystallographic properties of Mg-chlorite. *American Mineralogist*, **71**, 924–936.
- Jenkins, D.M. & Corona, J.C., 2006. The molar volume and thermal expansion of glaucophane. *Physics and Chemistry of Minerals*, **33**, 356–362.
- Jenkins, D.M., 1981. Experimental phase relations of hydrous peridotites modelled in the system H₂O–CaO–MgO–SiO₂. *Contributions to Mineralogy and Petrology*, **77**, 166–176.
- Jenkins, D.M., 1983. Stability and composition relations of calcic amphiboles in ultramafic rocks. *Contributions to Mineralogy and Petrology*, **83**, 375–384.
- Jenkins, D.M., 1984. Upper pressure stability of synthetic margarite + quartz. *Contributions to Mineralogy and Petrology*, **88**, 332–339.
- Jenkins, D.M., 1994. Experimental reversals of the aluminum content of tremolitic amphiboles in the system H₂O–CaO–MgO–Al₂O₃–SiO₂. *American Journal of Science*, **294**, 593–620.
- Jenkins, D.M., Holland, T.J.B. & Clare, A.K., 1991. Experimental determination of the pressure–temperature stability field and thermochemical properties of synthetic tremolite. *American Mineralogist*, **76**, 458–469.
- Jenkins, D.M., Newton, R.C. & Goldsmith, J.G., 1983. Fe-free clinozoisite stability relative to zoisite. *Nature*, **304**, 622–623.
- Jenkins, D.M., Newton, R.C. & Goldsmith, J.R., 1985. Relative stability of Fe-free zoisite and clinozoisite. *Journal of Geology*, **93**, 663–672.
- Johannes, W., 1968. Experimental investigation of the reaction forsterite + H₂O = serpentine + brucite. *Contributions to Mineralogy and Petrology*, **19**, 309–315.
- Johannes, W., 1969. An experimental investigation of the system MgO–SiO₂–H₂O–CO₂. *American Journal of Science*, **267**, 1083–1104.
- Johannes, W., 1980. Melting and subsolidus reactions in the system K₂O–CaO–Al₂O₃–SiO₂–H₂O. *Contributions to Mineralogy and Petrology*, **74**, 29–34.
- Johannes, W., 1984. Beginning of melting in the granite system Qz–Or–Ab–An–H₂O. *Contributions to Mineralogy and Petrology*, **86**, 264–273.

- Johannes, W. & Holtz, F., 1996. Petrogenesis and Experimental Petrology of Granitic Rocks. Springer-Verlag, Berlin.
- Johannes, W. & Metz, P., 1968. Experimentelle Bestimmung von Gleichgewichtsbeziehungen im System $MgO-CO_2-H_2O$. *Neues Jahrbuch für Mineralogie Monatshefte*, **112**, 15–26.
- Johannes, W. & Puhan, D., 1971. The calcite-aragonite transition re-investigated. *Contributions to Mineralogy and Petrology*, **31**, 28–38.
- Kahl, W.-A., Maresch, W.V. & Welch, M.D., 2003. Enthalpy of formation of pargasite by high-temperature solution calorimetry and heat capacity of pargasite and fluoropargasite by differential scanning calorimetry. *European Journal of Mineralogy*, **15**, 617–628.
- Kajiyoshi, K., 1986. *High-Temperature Equation of State for Mantle Minerals and their Anharmonic Properties*. MS Thesis, Okayama University, Okayama, Japan.
- Kandelin, J. & Weidner, D.J., 1988. Elastic properties of hedenbergite. *Journal of Geophysical Research*, **93**, 1063–1072.
- Kanzaki, M., 1987. Ultra-high pressure phase relations in the system $Mg_4Si_4O_{12}-Mg_3Al_2Si_3O_{12}$. *Physics of the Earth and Planetary Interiors*, **49**, 168–175.
- Kanzaki, M., 1990. Melting of silica up to 7 GPa. *Journal of the American Ceramic Society*, **73**, 3706–3707.
- Kanzaki, M., 1991. Stability of hydrous magnesium silicates in the mantle transition zone. *Physics of the Earth and Planetary Interiors*, **66**, 307–312.
- Kase, H.-R. & Metz, P., 1980. Experimental investigation of the metamorphism of siliceous dolomites. *Contributions to Mineralogy and Petrology*, **73**, 151–159.
- Katsura, T. & Ito, E., 1989. The system $Mg_2SiO_4-Fe_2SiO_4$ at high pressures and temperatures: precise determination of stabilities of olivine, modified spinel and spinel. *Journal of Geophysical Research*, **94**, 15663–15670.
- Kawasaki, T. & Matsui, Y., 1983. Thermodynamic analysis of equilibria involving olivine, orthopyroxene and garnet. *Geochimica et Cosmochimica Acta*, **47**, 1661–1680.
- Kelsey, D.E., White, R.W., Holland, T.J.B. & Powell, R., 2004. Calculated phase equilibria in $K_2O-FeO-MgO-Al_2O_3-SiO_2-H_2O$ for sapphirine-quartz-bearing mineral assemblages. *Journal of Metamorphic Geology*, **22**, 559–578.
- Kennedy, C.S. & Kennedy, G.C., 1976. The equilibrium boundary between graphite and diamond. *Journal of Geophysical Research*, **81**, 2467–2470.
- Kennedy, G.C., Wasserburg, G.J., Heard, H.C. & Newton, R.C., 1962. The upper three-phase region in the system SiO_2-H_2O . *American Journal of Science*, **260**, 501–521.
- Kerrick, D.M. & Heninger, S.G., 1984. The andalusite-sillimanite equilibrium revisited. *Geological Society of America Abstracts with Programs*, **16**, 558.
- Kerrick, D.M., 1968. Experiments on the upper stability limits of pyrophyllite at 1.8 kbar and 3.9 kbar water pressure. *American Journal of Science*, **266**, 204–214.
- Keskinen, M. & Liou, J.G., 1979. Synthesis and stability relations of Mn-Al piemontite, $Ca_2MnAl_2Si_3O_{12}(OH)$. *American Mineralogist*, **64**, 317–328.
- King, E.G., Barany, R., Weller, W.W. & Pankratz, L.B., 1967. Thermodynamic properties of forsterite and serpentine. *U.S. Bureau of Mines Report*, **6962**, 4320–4321.
- King, H.E. & Prewitt, C.T., 1982. High-pressure and high-temperature polymorphism of iron sulfide (FeS). *Acta Crystallographica Section B-Structural Science*, **38**, 1877–1887.
- Kiseleva, I.A. & Ogorodova, L.P., 1987. Calorimetric data on the thermodynamics of epidote, clinzoisite, and zoisite. *Geochemistry International*, **24**, 91–98.
- Kiseleva, I.A., Topor, N.D. & Andreyenko, E.D., 1974. Thermodynamic parameters of minerals of the epidote group. *Geochemistry International*, **11**, 389–398.
- Kitahara, S., Takenouchi, S. & Kennedy, G.C., 1966. Phase relations in the system $MgO-SiO_2-H_2O$ at high temperatures and pressures. *American Journal of Science*, **264**, 223–233.
- Klein, C., 1974. Greenalite, stilpnomelane, minnesotaite, crocidolite, and carbonates in a very low-grade metamorphic PreCambrian iron-formation. *Canadian Mineralogist*, **12**, 475–498.
- Klein, C., 1978. Regional metamorphism of Proterozoic iron-formation, Labrador Trough, Canada. *American Mineralogist*, **63**, 898–912.
- Klemme, S. & Ahrens, M., 2005. Low-temperature heat capacity of magnesiowilliamsite ($MgFe_2O_4$). *Physics and Chemistry of Minerals*, **32**, 374–378.
- Klemme, S. & Van Miltenburg, J.C., 2003. Thermodynamic properties of hercynite ($FeAl_2O_4$) based on adiabatic calorimetry at low temperatures. *American Mineralogist*, **88**, 68–72.
- Klemme, S., 2004. The influence of Cr on the garnet–spinel transition in the Earth's mantle: experiments in the system $MgO-Cr_2O_3-SiO_2$ and thermodynamic modelling. *Lithos*, **77**, 639–646.
- Klemme, S., O'Neill, H.StC., Schnelle, W. & Gmelin, E., 2000. The heat capacity of $MgCr_2O_4$, $FeCr_2O_4$, and Cr_2O_3 at low temperatures and derived thermodynamic properties. *American Mineralogist*, **85**, 1686–1693.
- Kleppa, J. & Newton, R.C., 1975. The role of solution calorimetry in the study of mineral equilibria. *Fortschritte der Mineralogie*, **52**, 3–20.
- Klug, F.J., Prochazka, S. & Doremus, R.H., 1987. Alumina–silica phase diagram in the Mullite Region. *Journal of the American Ceramic Society*, **70**, 750–759.
- Koch-Müller, M., Hofmeister, A.M., Fei, Y. & Liu, Z., 2002. High-pressure IR-spectra and the thermodynamic properties of chloritoid. *American Mineralogist*, **87**, 609–622.
- Koch-Müller, M. & Wirth, R., 2001. An experimental study of the effect of iron on magnesioclinozoisite–talc–clinochlore–kyanite stability. *Contributions to Mineralogy and Petrology*, **141**, 546–559.
- Koziol, A.M. & Newton, R.C., 1995. Experimental determination of the reactions magnesite + quartz = enstatite + CO_2 and magnesite = periclase + CO_2 , and enthalpies of formation of enstatite and magnesite. *American Mineralogist*, **80**, 1252–1260.
- Koziol, A.M. & Newton, R.C., 1998. Experimental determination of the reaction: magnesite + enstatite = forsterite + CO_2 in the ranges 6–25 kbar and 700–1100 °C. *American Mineralogist*, **83**, 213–219.
- Koziol, A.M. & Newton, R.C., 1988. Redetermination of the anorthite breakdown reaction and improvement of the plagioclase–garnet– Al_2SiO_5 –quartz geobarometer. *American Mineralogist*, **73**, 216–223.
- Koziol, A.M., 2004. Experimental determination of siderite stability and application to Martian Meteorite ALH84001. *American Mineralogist*, **89**, 294–300.
- Krupka, K.M., Robie, R.A. & Hemingway, B.S., 1979. High temperature heat capacities of corundum, periclase, anorthite, $CaAl_2Si_2O_8$ glass, muscovite, pyrophyllite, $KAlSi_3O_8$ glass, grossular, and $NaAlSi_3O_8$ glass. *American Mineralogist*, **64**, 86–101.
- Krupka, K.M., Robie, R.A., Hemingway, B.S., Kerrick, D.M. & Ito, J., 1985a. Low-temperature heat capacities and derived thermodynamic properties of anthophyllite, diopside, enstatite, bronzite and wollastonite. *American Mineralogist*, **70**, 249–260.
- Krupka, K.M., Robie, R.A., Hemingway, B.S. & Kerrick, D.M., 1985b. High-temperature heat capacities and derived thermodynamic properties of anthophyllite, diopside, dolomite, enstatite, bronzite, talc, tremolite and wollastonite. *American Mineralogist*, **70**, 261–271.
- Kubo, A. & Akaogi, M., 2000. Post-garnet transitions in the system $Mg_4Si_4O_{12}-Mg_3Al_2Si_3O_{12}$ up to 28 GPa: phase relations of garnet, ilmenite and perovskite. *Physics of the Earth and Planetary Interiors*, **121**, 85–102.
- Kung, J., Boasheng, L., Uchida, T. & Wang, Y., 2005. In-situ elasticity measurement for the unquenchable high-pressure

- clinopyroxene phase: implication for the upper mantle. *Geophysical Research Letters*, **32**, L01307.
- Lager, G.A. & Meagher, E.P., 1978. High-temperature study of six olivines. *American Mineralogist*, **63**, 365–377.
- Laird, J., 1982. Amphiboles in metamorphosed basaltic rocks. In: *Amphiboles. MSA Reviews in Mineralogy*, **9B**, 113–158.
- Laird, J., 1989. Chlorites: metamorphic petrology. In: Hydrous Phyllosilicates (exclusive of micas). *MSA Reviews in Mineralogy*, **19**, 405–453.
- Lambert, I.B., Robertson, J.K. & Wyllie, P.J., 1969. Melting reactions in the system $KAlSi_3O_8-SiO_2-H_2O$. *American Journal of Science*, **267**, 609–626.
- Lange, R.A., 1997. A revised model for the density and thermal expansivity of $K_2O-Na_2O-CaO-MgO-Al_2O_3-SiO_2$ liquids from 700 to 1900 K: extension to crustal magmatic temperatures. *Contributions to Mineralogy and Petrology*, **130**, 1–11.
- Lange, R.A., De Yoreo, J. & Navrotsky, A., 1991. Scanning calorimetric measurement of heat capacity during incongruent melting of diopside. *American Mineralogist*, **76**, 904–912.
- Lattard, D. & Evans, B.W., 1992. New experiments on the stability of grunerite. *European Journal of Mineralogy*, **4**, 219–238.
- Lattard, D. & LeBreton, N., 1994. The P-T-f_{O₂} stability of endmember deerite, $Fe_{12}^{2+}Fe_{2}^{3+}Si_{12}O_{40}(OH)_{10}$. *Contributions to Mineralogy and Petrology*, **115**, 474–487.
- Lee, H.Y. & Ganguly, J., 1988. Equilibrium compositions of coexisting garnet and orthopyroxene: experimental determinations in the system $FeO-MgO-Al_2O_3-SiO_2$, and applications. *Journal of Petrology*, **29**, 93–113.
- Leger, J.M., Redon, A.M. & Chateau, C., 1990. Compressions of synthetic pyrope, spessartine and uvarovite garnets up to 25 GPa. *Physics and Chemistry of Minerals*, **17**, 161–167.
- Leger, J.M., Tomaszewski, P.E., Atouf, A. & Pereira, A.S., 1993. Pressure-induced structural phase transitions in zirconia under high pressure. *Physical Review B*, **47**, 14075–14083.
- Lindsley, D.H. & Munoz, J.L., 1969. Subsolidus relations along the join hedenbergite–ferrosilite. *American Journal of Science*, **267-A**, 295–324.
- Lindsley, D.H., 1966. Melting relations of $KAlSi_3O_8$: effect of pressures up to 40 kilobars. *American Mineralogist*, **51**, 1793–1799.
- Lindsley, D.H., 1967. P-T projection for part of the system kalsilite–silica. *Carnegie Institute of Washington Yearbook*, **65**, 244–247.
- Lindsley, D.H., 1983. Pyroxene thermometry. *American Mineralogist*, **68**, 477–493.
- Liou, J.G., 1970. Synthesis and stability relations of wairakite $CaAl_2Si_4O_{12} \cdot 2H_2O$. *Contributions to Mineralogy and Petrology*, **27**, 259–282.
- Liou, J.G., 1971a. P-T stabilities of laumontite, wairakite, lawsonite, and related minerals in the system $CaAl_2Si_2O_8-SiO_2-H_2O$. *Journal of Petrology*, **12**, 379–411.
- Liou, J.G., 1971b. Stilbite-laumontite equilibrium. *Contributions to Mineralogy and Petrology*, **31**, 171–177.
- Liou, J.G., 1971c. Analcime equilibria. *Lithos*, **4**, 389–402.
- Liou, J.G., 1973. Synthesis and stability relations of epidote, $Ca_2Al_2FeSi_3O_{12}(OH)$. *Journal of Petrology*, **14**, 381–413.
- Liou, J.G., 1974. Stability relations of andradite-quartz in the system Ca–Fe–Si–O–H. *American Mineralogist*, **59**, 1016–1025.
- Liu, J., Topor, L., Zhang, J., Navrotsky, A. & Liebermann, R.C., 1996. Calorimetric study of the coesite-stishovite transformation and calculation of the phase boundary. *Physics and Chemistry of Minerals*, **23**, 11–16.
- Luo, H. & Ruoff, A.L., 1993. X-ray diffraction study of sulfur to 32 GPa: amorphization at 25 GPa. *Physical Review B*, **48**, 569–572.
- Luo, S.-N., Mosenfelder, J.L., Asimow, P.D. & Ahrens, T.J., 2002. Direct shock wave loading of Stishovite to 235 GPa: implications for perovskite stability relative to an oxide assemblage at lower mantle conditions. *Geophysical Research Letters*, **29**, doi: 10.1029/2002GL015627.
- Luth, W.C., 1967. Studies in the system $KAlSiO_4-Mg_2SiO_4-SiO_2-H_2O$: inferred phase relations and petrologic applications. *Journal of Petrology*, **8**, 372–416.
- Luth, W.C., 1969. The systems $NaAlSi_3O_8-SiO_2$ and $KAlSi_3O_8-SiO_2$ to 20 kb and the relationship between H_2O content, P_{H_2O} and P_{total} in granitic magmas. *American Journal of Science*, **267-A**, 325–341.
- Luth, R.W., 1995. Experimental determination of the reaction dolomite + 2 coesite = diopside + 2 CO₂ to 6 GPa. *Contributions to Mineralogy and Petrology*, **122**, 152–158.
- Lykins, R.W. & Jenkins, D.M., 1992. Experimental determination of pargasite stability relations in the presence of orthopyroxene. *Contributions to Mineralogy and Petrology*, **112**, 405–413.
- Mahar, E.M., Baker, J.M., Powell, R., Holland, T.J.B. & Howell, N., 1997. The effect of Mn on mineral stability in metapelites. *Journal of Metamorphic Geology*, **15**, 223–238.
- Majzlan, J., Navrotsky, A. & Neil, J.M., 2002. Energetics of anhydrite, barite, celestine, and anglesite: a high-temperature and differential scanning calorimetry study. *Geochimica et Cosmochimica Acta*, **66**, 1839–1850.
- Malcherek, T., 2001. Spontaneous strain in synthetic titanite, $CaTiSiO_4$. *Mineralogical Magazine*, **65**, 709–715.
- Malinovsky, I. Yu. & Doroshev, A.M., 1975. Low-pressure boundary of the stability field of pyrope: experimental studies in mineralogy (in Russian). *Doklady Akademii Nauk SSSR, Novosibirsk*, **220**, 95–100.
- Manghnani, M.H., 1970. Analcite-jadeite phase boundary. *Physics of the Earth and Planetary Interiors*, **3**, 456–461.
- Manning, C.E. & Bohlen, S.R., 1991. The reaction titanite + kyanite = anorthite + rutile and titanite-rutile barometry in eclogites. *Contributions to Mineralogy and Petrology*, **109**, 1–9.
- Manon, M.R.F., Dachs, E. & Essene, E.J., 2008. Low T heat capacity measurements and new entropy data for titanite (spheine): implications for thermobarometry of high-pressure rocks. *Contributions to Mineralogy and Petrology*, **156**, 709–720.
- Mao, H., Takahashi, T., Bassett, W.A., Weaver, J.S. & Akimoto, S., 1969. Effect of pressure and temperature on the molar volumes of wustite and three $(Mg,Fe)_2SiO_4$ spinel solid solutions. *Journal of Geophysical Research*, **74**, 1061–1069.
- Maresch, W.W. & Mottana, A., 1976. The pyroxmangite–rhodonite transformation for the $MnSiO_3$ composition. *Contributions to Mineralogy and Petrology*, **55**, 69–79.
- Markgraf, S.A. & Reeder, R.J., 1985. High-temperature refinements of calcite and magnesite. *American Mineralogist*, **70**, 590–600.
- Martens, R., Rosenhauer, M. & Gehlen, V.K., 1982. Compressibilities of carbonates. In: *Researches in Geoscience* (ed. Schreyer, W.), pp. 215–222. Schweizerbart'sche Verlagsbuchhandlung, Stuttgart.
- Martinez, I., Zhang, J. & Reeder, R.J., 1996. In-situ X-ray diffraction at high pressure and high temperature of aragonite and dolomite. Evidence for dolomite breakdown to aragonite and magnesite. *American Mineralogist*, **81**, 611–624.
- Massonne, H.-J., 1989. The upper thermal stability of chlorite + quartz: an experimental study in the system $MgO-Al_2O_3-SiO_2-H_2O$. *Journal of Metamorphic Geology*, **7**, 567–582.
- Massonne, H.-J., 1995. Experimental and petrogenetic study of UHPM. In: *Ultrahigh Pressure Metamorphism* (eds Coleman, R.G. & Wang, W.), pp. 33–95. Cambridge University Press, Cambridge.
- Massonne, H.-J., 1999. Experimental aspects of UHP metamorphism in pelitic systems. *International Geology Review*, **41**, 623–638.
- Massonne, H.-J., Mirwald, P.W. & Schreyer, W., 1981. Experimentelle der Reaktionskurve Chlorit + Quarz = Talk + Disthen im System $MgO-Al_2O_3-SiO_2-H_2O$. *Fortschritte der Mineralogie*, **59**, 122–123.
- Massonne, H.-J. & Szpurka, Z., 1997. Thermodynamic properties of white micas on the basis of high-pressure experiments in

- the systems $K_2O-MgO-Al_2O_3-SiO_2-H_2O$ and $K_2O-FeO-Al_2O_3-SiO_2-H_2O$. *Lithos*, **41**, 229–250.
- Massonne, H.-J. & Schreyer, W., 1989. Stability field of the high pressure assemblage talc + phengite and two new phengite barometers. *European Journal of Mineralogy*, **1**, 391–410.
- Matsui, Y. & Nishizawa, O., 1974. Iron (II)-magnesium exchange equilibrium between olivine and calcium-free pyroxene over a temperature range 800 to 1300 °C. *Bulletin Societe Mineralogie et Cristallographie*, **97**, 122–130.
- McCormick, T.C., 1986. Crystal-chemical aspects of non-stoichiometric pyroxenes. *American Mineralogist*, **71**, 1434–1440.
- McCormick, T.C., Hazen, R.M. & Angel, R.J., 1989. Compressibility of omphacite to 60 kbar—role of vacancies. *American Mineralogist*, **74**, 1287–1292.
- McPhail, D.C., 1985. *The stability of Mg-Chlorite* MSc thesis, University of British Columbia, Vancouver, BC, 45 p.
- McPhail, D.C., Berman, R.G. & Greenwood, H.J., 1990. Experimental and theoretical constraints on aluminium substitution in magnesium chlorite, and a thermodynamic model for H_2O in magnesium cordierite. *Canadian Mineralogist*, **28**, 859–874.
- Mellini, M., Trommsdorff, V. & Compagnoni, R., 1987. Antigorite polysomatism: behaviour during progressive metamorphism. *Contributions to Mineralogy and Petrology*, **97**, 147–155.
- Metz, P. & Puhan, D., 1971. Korrektur zur arbeit ‘Experimentelle untersuchung der metamorphose von kieselg dolomitischen sedimenten 1. Die gleichgewichtsdaten der reaktion 3 dolomit + 4 quartz + H_2O = talc + 3 calcit + 3 CO_2 ’. *Contributions to Mineralogy and Petrology*, **31**, 169–170.
- Metz, P., 1976. Experimental investigation of the metamorphism of siliceous dolomites III. Equilibrium data for the reaction tremolite + 11 dolomite = 8 forsterite + 13 calcite + 9 CO_2 + H_2O . *Contributions to Mineralogy and Petrology*, **58**, 137–148.
- Miller, Ch., 1986. Alpine high-pressure metamorphism in the Eastern Alps. *Schweizerische Mineralogische und Petrologische Mitteilungen*, **66**, 139–144.
- Mirwald, P.W., Malinowski, M. & Schulz, H., 1984. Isothermal compression of low cordierite to 30 kbar (25 °C). *Physics and Chemistry of Minerals*, **11**, 140–148.
- Mirwald, P.W., 1981. Thermal expansion of anhydrous Mg-cordierite between 25 and 950 °C. *Physics and Chemistry of Minerals*, **7**, 268–270.
- Mirwald, P.W., Maresch, W.V. & Schreyer, W., 1979. Der Wassergehalt von Mg-Cordierit zwischen 500 und 800 °C sowie 0.5 und 11 kbar. *Fortschritte der Mineralogie*, **57**, 101–102.
- Miyano, T. & Klein, C., 1989. Phase equilibria in the system $K_2O-FeO-MgO-Al_2O_3-SiO_2-H_2O-CO_2$ and the stability limit of stilpnomelane in metamorphosed Precambrian iron formations. *Contributions to Mineralogy and Petrology*, **102**, 478–491.
- Moecher, D.P. & Chou, I.M., 1990. Experimental investigation of andradite and hedenbergite equilibria employing the hydrogen sensor technique, with revised estimates of for andradite and hedenbergite. *American Mineralogist*, **75**, 1327–1341.
- Morlidge, M., Pawley, A. & Droop, G., 2006. Double carbonate breakdown reactions at high pressures: an experimental study in the system $CaO-MgO-FeO-MnO-CO_2$. *Contributions to Mineralogy and Petrology*, **152**, 365–373.
- Mukhopadhyay, B. & Holdaway, M.J., 1984. Cordierite-garnet-sillimanite-quartz equilibrium I. New experimental calibration in the system $FeO-Al_2O_3-SiO_2-H_2O$ and certain P-T-X(H_2O) relations. *Contributions to Mineralogy and Petrology*, **116**, 462–472.
- Myers, J. & Eugster, H.P., 1983. The system Fe–Si–O: oxygen buffer calibration to 1500 K. *Contributions to Mineralogy and Petrology*, **82**, 75–90.
- Navrotsky, A., 1995. Thermodynamic Properties of Minerals. In: *Mineral Physics and Crystallography: A Handbook of Physical Constants* (ed. Ahrens, T.J.), pp. 18–27. American Geophysical Union, Washington, DC.
- Navrotsky, A. & Coons, W.E., 1976. Thermochemistry of some pyroxenes and related compounds. *Geochimica et Cosmochimica Acta*, **40**, 1281–1288.
- Nekvasil, H. & Carroll, W., 1996. Experimental constraints on the compositional evolution of crustal magmas. *Journal of the Royal Society of Edinburgh: Earth Sciences*, **87**, 139–146.
- Nelson, D.O. & Guggenheim, S., 1993. Inferred limits to the oxidation of Fe in chlorites: a high-temperature single-crystal X-ray study. *American Mineralogist*, **78**, 1197–1207.
- Newton, R.C. & Harlov, D.E., 1993. Standard thermodynamic properties of almandine. *Canadian Mineralogist*, **31**, 391–399.
- Newton, R.C. & Kennedy, G.C., 1963. Some equilibrium relations on the join $CaAl_2Si_2O_8-H_2O$. *Journal of Geophysical Research*, **68**, 2967–2983.
- Newton, R.C. & Smith, J.V., 1967. Investigation concerning the breakdown of albite at depth in the earth. *Journal of Geology*, **75**, 268–286.
- Newton, R.C., 1965. The thermal stability of zoisite. *Journal of Geology*, **73**, 431–441.
- Newton, R.C., 1966a. *Kyanite-sillimanite equilibrium at 750 °C*. *Science*, **151**, 1222–1225.
- Newton, R.C., 1966b. *Kyanite-andalusite equilibrium from 700–800 °C*. *Science*, **153**, 170–171.
- Newton, R.C., 1966c. Some calcite-silicate equilibrium relations. *American Journal of Science*, **264**, 204–222.
- Newton, R.C., 1972. An experimental determination of the high pressure stability limits of magnesian cordierite under wet and dry conditions. *Journal of Geology*, **80**, 398–420.
- Nitsch, K.-H., 1972. Das P-T-X CO_2 -Stabilitätsfeld von Lawsonit. *Contributions to Mineralogy and Petrology*, **34**, 116–134.
- Nitsch, K.-H., 1974. Neue Erkenntnisse zur Stabilität für Lawsonit. *Fortschritte der Mineralogie*, **51**, 34–35.
- Nitsch, K.-H., Storre, B. & Topfer, U., 1981. Experimentelle bestimmung der gleichgewichtsdaten die reaktion Margarit + Quartz = Anorthit + Andalusit/Disthen + H_2O . *Fortschritte der Mineralogie*, **59**, 139–140.
- O'Neill, H.St.C., 1987a. Free energies of formation of NiO , CoO , Ni_2SiO_4 , and CO_2SiO_4 . *American Mineralogist*, **72**, 280–291.
- O'Neill, H.St.C., 1987b. Quartz-fayalite-iron and quartz-fayalite-magnetite equilibria and the free energy of formation of fayalite (Fe_2SiO_4) and magnetite (Fe_3O_4). *American Mineralogist*, **72**, 67–75.
- O'Neill, H.St.C., 1988. Systems Fe–O and Cu–O: thermodynamic data for the equilibria Fe–“ FeO ”, $Fe-Fe_3O_4$, $Fe_3O_4-Fe_2O_3$, $Cu-Cu_2O$, and Cu_2O-CuO from EMF measurements. *American Mineralogist*, **73**, 470–486.
- O'Neill, H.St.C. & Wood, B.J., 1979. An experimental study of Fe-Mg partitioning between garnet and olivine and its calibration as a geothermometer. *Contributions to Mineralogy and Petrology*, **70**, 59–70.
- O'Neill, H.St.C., Pownceby, M.I. & Wall, V.J., 1988. Ilmenite-rutile-iron and ulvöspinel-ilmenite-iron equilibria and the thermochemistry of ilmenite ($FeTiO_3$) and ulvöspinel. *Geochimica et Cosmochimica Acta*, **52**, 2065–2072.
- O'Neill, H.St.C., 2006. Free energy of formation of zircon and hafnon. *American Mineralogist*, **91**, 1134–1141.
- Ohtani, E. & Kumazawa, M., 1981. Melting of forsterite Mg_2SiO_4 up to 15 GPa. *Physics of the Earth and Planetary Interiors*, **27**, 32–38.
- Ohtani, E., Kagawa, N., & Fujino, K., 1991. Stability of majorite ($Mg, Fe)SiO_3$ at high pressures and 1800°C. *Earth and Planetary Science Letters*, **102**, 158–166.
- Okajima, S., Suzuki, I., Seya, K. & Sumino, Y., 1978. Thermal expansion of single-crystal tephroite. *Physics and Chemistry of Minerals*, **3**, 111–115.
- Olesch, M. & Seifert, F., 1981. The restricted stability of osumilite under hydrous conditions in the system

- $K_2O-MgO-Al_2O_3-SiO_2-H_2O$. Contributions to Mineralogy and Petrology, **76**, 362–367.
- Origlieri, M.J., Downs, R.T., Thompson, R.M., Pommier, C.J.S., Denton, M.B. & Harlow, G.E., 2003. High-pressure crystal structure of kosmochlor, $NaCrSi_2O_6$, and systematics of anisotropic compression in pyroxenes. American Mineralogist, **88**, 1025–1032.
- Osborn, E.F. & Schairer, J.F., 1941. The ternary system pseudowollastonite–akermanite–gehlenite. American Journal of Science, **239**, 713–763.
- Ostrovsky, I.A., 1966. PT-diagram of the system SiO_2-H_2O . Journal of Geology, **5**, 127–134.
- Pacalo, R.E.G. & Gasparik, T., 1990. Reversals of the orthoenstatite–clinostatite transition at high pressures and high temperatures. Journal of Geophysical Research, **9**, 15853–15858.
- Palmer, D.C., Salje, E.K.H. & Schmahl, W.W., 1989. Phase transitions in leucite: X-ray diffraction studies. Physics and Chemistry of Minerals, **16**, 714–719.
- Parra, T., Vidal, O. & Theye, T., 2005. Experimental data on the Tschermark substitution in Fe-chlorite. American Mineralogist, **90**, 359–370.
- Pattison, D.R.M., Spear, F.S., Debuhr, C.L., Cheney, J.T. & Guidotti, C.V., 2002. Thermodynamic modelling of the reaction muscovite + cordierite = Al_2SiO_5 + biotite + quartz + H_2O : constraints from natural assemblages and implications for the metapelite petrogenetic grid. Journal of Metamorphic Geology, **20**, 99–118.
- Paukov, I.E., Kovalevskaya, Y.A., Rahmoun, N.S. & Geiger, C.A., 2006. A low-temperature heat capacity study of synthetic anhydrous Mg-cordierite ($Mg_2Al_4Si_5O_{18}$). American Mineralogist, **91**, 35–38.
- Pavese, A., Diella, V., Pischedda, V., Merli, M., Bocchio, R. & Mezouar, M., 2001a. Pressure-volume-temperature equation of state of andradite and grossular, by high-pressure and -temperature powder diffraction. Physics and Chemistry of Minerals, **28**, 242–248.
- Pavese, A., Levy, D. & Pischedda, V., 2001b. Elastic properties of andradite and grossular, by synchrotron X-ray diffraction at high pressure conditions. European Journal of Mineralogy, **13**, 929–937.
- Pavese, A., Levy, D., Curetti, N., Diella, V., Fumagalli, P. & Sani, A., 2003. Equation of state and compressibility of phlogopite by in-situ high-pressure X-ray powder diffraction. European Journal of Mineralogy, **15**, 455–463.
- Pawley, A.R., 1998. The reaction talc plus forsterite = enstatite plus H_2O : new experimental results and petrological implication. American Mineralogist, **83**, 51–57.
- Pawley, A.R., 2000. Stability of clinohumite in the system $MgO-SiO_2-H_2O$. Contributions to Mineralogy and Petrology, **138**, 284–291.
- Pawley, A.R., 2003. Chlorite stability in mantle peridotite: the reaction clinochlore plus enstatite = forsterite + pyrope + H_2O . Contributions to Mineralogy and Petrology, **144**, 449–456.
- Pawley, A.R., Clark, S.M. & Chinnery, N.J., 2002. Equation of state measurements of chlorite, pyrophyllite, and talc. American Mineralogist, **87**, 1172–1182.
- Pawley, A.R., Redfern, S.A.T. & Holland, T.J.B., 1996. Volume behaviour of hydrous minerals at high pressure and temperature: 1. Thermal expansion of lawsonite, zoisite, clinzoisite and diaspore. American Mineralogist, **81**, 335–340.
- Pawley, A.R., Redfern, S.A.T. & Wood, B.J., 1995. Thermal expansivities and compressibilities of hydrous phases in the system $MgO-SiO_2-H_2O$: talc, phase A and 10-Å phase. 340. Contributions to Mineralogy and Petrology, **122**, 301–307.
- Pawley, A.R. & Wood, B.J., 1995. The high pressure stability of talc and 10Å phase: potential storage sites for H_2O in subduction zones. American Mineralogist, **80**, 998–1003.
- Pawley, A.R. & Wood, B.J., 1996. The low-pressure stability of phase A, $Mg_7Si_2O_8(OH)_6$. Contributions to Mineralogy and Petrology, **124**, 90–97.
- Perchuk, L.L. & Aranovich, L.Y., 1979. Thermodynamics of minerals of variable composition: andradite–grossularite and pistacite–clinzoisite solid solutions. Physics and Chemistry of Minerals, **5**, 1–14.
- Perchuk, L.L. & Lavrent'eva, I.V., 1983. Experimental investigation of exchange equilibria in the system cordierite–garnet–biotite. In: Kinetics and Equilibrium in Mineral Reactions (ed. Saxena, S.K.), pp. 199–240. Springer Verlag, New York.
- Perkins, D. & Vielzeuf, D., 1992. Reinvestigation of fayalite + orthorhombite = garnet. Contributions to Mineralogy and Petrology, **111**, 260–263.
- Perkins, D., 1983. The stability of Mg-rich garnet in the system $CaO-MgO-Al_2O_3-SiO_2$ at 1000–1300 °C and high pressure. American Mineralogist, **68**, 355–364.
- Perkins, D., Holland, T.J.B. & Newton, R.C., 1981. The Al_2O_3 contents of enstatite in equilibrium with garnet in the system $MgO-Al_2O_3-SiO_2$ at 15–40 kbar and 900 °C–1600 °C. Contributions to Mineralogy and Petrology, **78**, 99–109.
- Perkins, D., Westrum, E.F. & Essene, E.J., 1980. The thermodynamic properties and phase relations of some minerals in the system $CaO-Al_2O_3-SiO_2-H_2O$. Geochimica et Cosmochimica Acta, **44**, 61–84.
- Peters, T., 1971. Pyroxmangite: stability in H_2O-CO_2 mixtures at a total pressure of 2000 bars. Contributions to Mineralogy and Petrology, **32**, 267–273.
- Peterson, J.W. & Newton, R.C., 1990. Experimental biotite–quartz melting in the KMASH– CO_2 system and the role of CO_2 in the petrogenesis of granites and related rocks. American Mineralogist, **75**, 1029–1042.
- Philipp, R.W. & Girsberger, S., 1990. In: Trommsdorff, V. & Connolly, J.A.D. 1990. Constraints on phase diagram topology in the system $CaO-MgO-SiO_2-CO_2-H_2O$. Contributions to Mineralogy and Petrology, **104**, 1–7.
- Pigage, L.C. & Greenwood, H.J., 1982. Internally consistent estimates of pressure and temperature: the staurolite problem. American Journal of Science, **282**, 943–969.
- Pinckney, L.R. & Burnham, C.W., 1988. High-temperature crystal structure of pyroxmangite. American Mineralogist, **73**, 809–317.
- Pitzer, K.S. & Stern, S.M., 1995. Equations of state valid continuously from zero to extreme pressures with H_2O and CO_2 as examples. International Journal of Thermophysics, **16**, 511–518.
- Podlesskii, K.K., 1996. Sapphirine-bearing equilibria in the system $MgO-Al_2O_3-SiO_2$. Terra Abstracts, **8** (Suppl. 1), 51.
- Podlesskii, K.K., Aranovich, L.Y., Gerya, T.V. & Kosyakova, N.A., 2008. Sapphirine-bearing assemblages in the system $MgO-Al_2O_3-SiO_2$: a continuing ambiguity. European Journal of Mineralogy, **20**, 721–734.
- Powell, R., Guiraud, M. & White, R.W., 2005. Truth and beauty in metamorphic mineral equilibria: conjugate variables and phase diagrams. Canadian Mineralogist, **43**, 21–33.
- Powell, R. & Holland, T.J.B., 1993a. Is least squares an appropriate methodology to be used in the extraction of thermodynamic data from experimentally-bracketed mineral equilibria? American Mineralogist, **78**, 107–112.
- Powell, R. & Holland, T.J.B., 1993b. On the formulation of simple mixing models for complex phases. American Mineralogist, **78**, 1174–1180.
- Powell, R. & Holland, T.J.B., 2008. On thermobarometry. Journal of Metamorphic Geology, **26**, 155–180.
- Pownceby, M.I., Wall, V.J. & O'Neill, H.S.C., 1987. Fe–Mn partitioning between garnet and ilmenite: experimental calibration and applications. Contributions to Mineralogy and Petrology, **97**, 116–126.
- Puhan, D. & Johannes, W., 1974. Experimentelle untersuchung der reaktion Dolomit + Kalifeldspat + H_2O = phlogopit +

- calcit + CO₂. *Contributions to Mineralogy and Petrology*, **48**, 23–31.
- Puhan, D., 1978. Experimental study of the reaction: dolomite + K-feldspar + H₂O = phlogopite + calcite + CO₂ at the total gas pressures of 4000 and 6000 bars. *Neues Jahrbuch für Mineralogie Monatshefte*, **110**, 117–127.
- Rankin, G.A. & Wright, F.E., 1915. The ternary system of CaO–Al₂O₃–SiO₂. *American Journal of Science*, **39**, 1–79.
- Rao, B. & Johannes, W., 1979. Further data on the stability of staurolite + quartz. *Neues Jahrbuch für Mineralogie Monatshefte*, **10**, 437–447.
- Rao, K.V.K. & Murthy, K.S., 1970. Thermal expansion of manganese carbonate. *Journal of Materials Science*, **5**, 82–83.
- Rasmussen, M.G., Evans, B.W. & Kuehner, S.M., 1998. Low temperature fayalite, greenalite, and minnesotaite from the overlook gold deposit, Washington: phase relations in the system FeO–SiO₂–H₂O. *The Canadian Mineralogist*, **36**, 147–162.
- Rau, H., 1976. Energetics of defect formation and interaction in pyrrhotite Fe_{1-x}S and its homogeneity range. *Journal of Physics and Chemistry of Solids*, **37**, 425–429.
- Redfern, S.A.T. & Angel, R.J., 1999. High-pressure behaviour and equation of state of calcite, CaCO₃. *Contributions to Mineralogy and Petrology*, **134**, 102–106.
- Reeder, R.J. & Markgraf, S.A., 1986. High-temperature crystal chemistry of dolomite. *American Mineralogist*, **71**, 775–804.
- Reid, R.C., Prausnitz, J.M. & Sherwood, T.K., 1977. *The Properties of Gases and Liquids*. McGraw-Hill, New York.
- Richardson, S.W., 1968. Staurolite stability in a part of the system Fe–Al–Si–O–H. *Journal of Petrology*, **9**, 467–488.
- Richardson, S.W., Bell, P.M. & Gilbert, M.C. 1968. Kyanite–sillimanite equilibrium between 700 and 1500 °C. *American Journal of Science*, **266**, 513–541.
- Richardson, S.W., Gilbert, M.C. & Bell, P.M. 1969. Experimental determination of kyanite–andalusite and andalusite–sillimanite equilibria; the aluminium silicate triple point. *American Journal of Science*, **267**, 259–272.
- Richert, P. & Bottinga, Y., 1986. Thermochemical properties of silicate glasses and liquids: A review: *Reviews of Geophysics*, **24**, 1–25.
- Richert, P. & Fiquet, G., 1991. High-temperature heat capacity and premelting of minerals in the system MgO–CaO–Al₂O₃–SiO₂. *Journal of Geophysical Research*, **96**, 445–456.
- Richert, P., Gillet, P. & Fiquet, G., 1992. Thermodynamic properties of minerals: macroscopic and microscopic approaches. *Advances in Physical Geochemistry*, **10**, 98–131.
- Richert, P., Robie, R.A. & Hemingway, B.S., 1991. Thermodynamic properties of wollastonite, pseudowollastonite and CaSiO₃ glass and liquid. *European Journal of Mineralogy*, **3**, 475–484.
- Richert, P., Robie, R.A., Rogez, J., Hemingway, B.S., Courtial, P. & Tequi, C., 1990. Thermodynamics of open networks: ordering and entropy in NaAlSiO₄, glass, liquid, and polymorphs. *Physics and Chemistry of Minerals*, **17**, 385–394.
- Richert, P., Xu, J. & Mao, H.K., 1988. Quasi-hydrostatic compression of ruby to 500kbar. *Physics and Chemistry of Minerals*, **16**, 207–211.
- Robertson, E.C., Birch, A.F. & MacDonald, G.J.F., 1957. Experimental determination of jadeite stability relations between 700 °C and 1500 °C. *American Journal of Science*, **255**, 115–137.
- Robie, R.A. & Hemingway, B.S., 1995. Thermodynamic properties of minerals and related substances at 298.15K and 1 bar (10⁵ Pascals) pressure and at higher temperatures. *United States Geological Survey Bulletin*, **2131**, 461.
- Robie, R.A., Bethke, P.E. & Beardsley, K.M., 1967. Selected X-ray crystallographic data, molar volumes, and densities of minerals and related substances. *United States Geological Survey Bulletin*, **1248**, 87.
- Rose, N.M. & Bird, D.K., 1987. Prehnite-epidote phase relations in the Nordre Aputiteq and Kruuse Fjord layered gabbros East Greenland. *Journal of Petrology*, **28**, 1193–1218.
- Rosenberg, P.E., 1967. Subsolidus relations in the system CaCO₃–MgCO₃–FeCO₃ between 350 and 550C. *American Mineralogist*, **52**, 787–797.
- Rosenqvist, T., 1954. A thermodynamic study of the iron, cobalt, and nickel sulphides. *Journal of the Iron and Steel Institute*, **176**, 37–57.
- Ross, N.L. & Crichton, W.A., 2001. Compression of synthetic hydroxylclinohumite [Mg₂Si₁₆O₁₆(OH)₂] and hydroxyl-chondrodite [Mg₅Si₂O₈(OH)₂]. *American Mineralogist*, **86**, 990–996.
- Ross, N.L. & Reeder, R.J., 1992. High-pressure structural study of dolomite and ankerite. *American Mineralogist*, **77**, 412–421.
- Russell, R.L. & Guggenheim, S., 1999. Crystal structures of near-end-member phlogopite at high temperatures and heat-treated Fe-rich phlogopite; the influence of the O, OH, F site. *Canadian Mineralogist*, **37**, 711–720.
- Rutherford, M.J., 1973. The phase relations of aluminous iron biotites in the system KAlSi₃O₈–KAlSiO₄–Al₂O₃–Fe–O–H. *Journal of Petrology*, **14**, 159–180.
- Robie, R.A., Hemingway, B.S. & Takei, H., 1982. Heat capacities and entropies of Mg₂SiO₄, Mn₂SiO₄, and Ca₂SiO₄ between 5 and 380 K. *American Mineralogist*, **67**, 470–482.
- Roots, M., 1994. Molar volumes on the cinochlore–amésite binary: some new data. *European Journal of Mineralogy*, **6**, 279–283.
- Sawamoto, H., 1987. Phase diagram of MgSiO₃ at pressures up to 24 GPa and temperatures up to 2200K: phase stability and properties of tetragonal garnet. In: *High Pressure Research in Mineral Physics, Geophysical Monograph Series*, **39** (eds Manghnani, M.H. & Syono, Y.), pp. 209–219. AGU, Washington, DC.
- Saxena, S.K., 1996. Earth mineralogical model: Gibbs free energy minimization computation in the system MgO–FeO–SiO₂. *Geochimica et Cosmochimica Acta*, **60**, 2379–2395.
- Scarfe, C.M., Luth, W.C. & Tuttle, O.F., 1966. An experimental study bearing on the absence of leucite in plutonic rocks. *American Mineralogist*, **51**, 726–735.
- Schairer, J.F. & Bowen, N.L., 1947. The system anorthite–leucite–silica. *Commission Géologique de Finlande, Bulletin*, **20**, 67–87.
- Schairer, J.F. & Bowen, N.L., 1956. The system Na₂O–Al₂O₃–SiO₂. *American Journal of Science*, **254**, 129–195.
- Schiffman, P. & Liou, J.G., 1980. Synthesis and stability relations of Mg-Al pumpellyite, Ca₄Al₅MgSi₆O₂₁(OH)₇. *Journal of Petrology*, **21**, 441–474.
- Schlenger, J.L., Gibbs, G.V., Hill, E.G., Crews, S.S. & Myers, R.H., 1977. Thermal expansion coefficients for indialite, emerald and beryl. *Physics and Chemistry of Minerals*, **1**, 243–255.
- Schmidt, M.W. & Poli, S., 1994. The stability of lawsonite and zoisite at high pressures: experiments in CASH to 92 kbar and implications for the presence of hydrous phases in subducted Lithosphere. *Earth and Planetary Science Letters*, **124**, 105–118.
- Schmidt, M.W., Poli, S., Comodi, P. & Zanazzi, P.F., 1997. High-pressure behavior of kyanite: Decomposition of kyanite into stishovite and corundum. *American Mineralogist*, **82**, 460–466.
- Schmidt, M.W., Dugnani, M. & Artioli, G., 2001. Synthesis and characterization of white micas in the join muscovite–aluminoceladonite. *American Mineralogist*, **86**, 555–565.
- Schneeberg, E.P., 1973. Sulfur fugacity measurements with the electrochemical cell AgAgI|Ag_{2+x}fS₂. *Economic Geology*, **68**, 507–517.
- Schneider, H. & Eberhard, E., 1990. Thermal expansion of mullite. *Journal of the American Ceramic Society*, **73**, 2073–2076.

- Schramke, J.A., Kerrick, D.M. & Blencoe, J.G., 1982. The experimental determination of the brucite = periclase + H_2O equilibrium with a new volumetric technique. *American Mineralogist*, **67**, 269–276.
- Schreyer, W. & Seifert, F., 1969. High pressure phases in the system $MgO-Al_2O_3-SiO_2-H_2O$. *American Journal of Science*, **267A**, 407–443.
- Schreyer, W. & Yoder, H.S., 1964. The system Mg -cordierite– H_2O and related rocks. *Neues Jahrbuch für Mineralogie Abhandlungen*, **101**, 271–342.
- Schreyer, W., 1968. A reconnaissance study of the system $MgO-Al_2O_3-SiO_2-H_2O$ at pressures between 10 and 25 kbar. *Carnegie Institute of Washington Yearbook*, **66**, 380–392.
- Segnit, E.R. & Kennedy, G.C., 1961. Reactions and melting relations in the system muscovite-quartz at high pressures. *American Journal of Science*, **259**, 280–287.
- Seidel, E. & Okrusch, M., 1977. Chloritoid-bearing metapelites associated with glaucophane rocks in western Crete, Greece. *Contributions to Mineralogy and Petrology*, **60**, 321–324.
- Seifert, F. & Schreyer, W., 1970. Low temperature stability limit of Mg-cordierite in the range 1–7 kilobars water pressure. A redetermination. *Contributions to Mineralogy and Petrology*, **27**, 225–238.
- Seifert, F., 1970. Low temperature compatibility relations of cordierite in haplopelites of the system $K_2O-MgO-Al_2O_3-SiO_2-H_2O$. *Journal of Petrology*, **11**, 73–101.
- Seifert, F., 1973. Stability of the assemblage cordierite-corundum in the system $MgO-Al_2O_3-SiO_2-H_2O$. *Contributions to Mineralogy and Petrology*, **41**, 171–178.
- Seifert, F., 1974. Stability of sapphirine: a study of the aluminous part of the system $MgO-Al_2O_3-SiO_2-H_2O$. *Journal of Geology*, **82**, 173–204.
- Seifert, F., 1976. Stability of the assemblage cordierite + K feldspar + quartz. *Contributions to Mineralogy and Petrology*, **57**, 179–185.
- Sharp, Z.D., Essene, E.J., Anovitz, L.M., et al. 1986. The heat capacity of a natural monticellite and phase equilibria in the system $CaO-MgO-SiO_2-CO_2$. *Geochimica et Cosmochimica Acta*, **50**, 1475–1484.
- Sharp, Z.D., Helffrich, G.R., Bohlen, S.R. & Essene, E.J., 1989. The stability of sodalite in the system $NaAlSiO_4-NaCl$. *Geochimica et Cosmochimica Acta*, **53**, 1943–1954.
- Shen, G.Y. & Lazor, P., 1995. Measurement of melting temperatures of some minerals under lower mantle pressures. *Journal of Geophysical Research, Solid Earth*, **100**, 17699–17713.
- Shim, S.H., Duffy, T.S. & Shen, G.Y., 2000. The stability and P–V–T equation of state of $CaSiO_3$ perovskite in the Earth's lower mantle. *Journal of Geophysical Research*, **105**, 25955–25968.
- Shim, S.N., Duffy, T.S. & Shen, G.Y., 2001. The post-spinel transformation in Mg_2SiO_4 and its relation to the 660-km seismic discontinuity. *Nature*, **411**, 571–574.
- Shirozu, H. & Momoi, H., 1972. Synthetic Mg-chlorite in relation to natural chlorite. *Mineralogical Journal*, **6**, 464–476.
- Shmulovich, K.I., 1974. Phase equilibria in the $CaO-Al_2O_3-SiO_2-CO_2$ system. *Geochemistry International*, **11**, 883–887.
- Shulters, J.C. & Bohlen, S.R., 1989. The stability of hercynite-gahnite spinels in corundum- or quartz-bearing assemblages. *Journal of Petrology*, **30**, 1017–1031.
- Skinner, B.J., 1956. Physical properties of end-members of the garnet group. *American Mineralogist*, **41**, 428–436.
- Skinner, B.J., 1966. Thermal expansion. In: *Handbook of Physical Constants* (ed. Clark, S.P.). *Geological Society of America Memoir*, **97**, 75–96.
- Skippen, G.B. & Gunter, A.E., 1996. The thermodynamic properties of H_2O in magnesium and iron cordierite. *Contributions to Mineralogy and Petrology*, **124**, 82–89.
- Skippen, G.B., 1971. Experimental data for reactions in siliceous marbles. *Journal of Geology*, **79**, 457–481.
- Skrok, V., Grevel, K.D. & Schreyer, W., 1994. Die Stabilität von $Lawsonit, CaAl_2[Si_2O_7](OH)_2 \cdot H_2O$, bei Drücken bis zu 50 kbar. *European Journal of Mineralogy*, **6**, 270.
- Slaughter, J., Kerrick, D.M. & Wall, V.J., 1975. Experimental and thermodynamic study of equilibria in the system $CaO-MgO-SiO_2-H_2O-CO_2$. *American Journal of Science*, **275**, 143–162.
- Smith, P., 2003. *The Melting Curve of Nepheline*. PhD dissertation, University of Cambridge, 256pp.
- Smyth, F.H. & Adams, L.H., 1923. The system calcium oxide–carbon dioxide. *Journal of the American Chemical Society*, **45**, 1167–1184.
- Smyth, J.R. & McCormick, T.C., 1995. Crystallographic data for minerals. In: *Mineral Physics and Crystallography: A Handbook of Physical Constants* (ed. Ahrens, T.J.), pp. 1–17. American Geophysical Union, Washington, DC.
- Smyth, J.R., 1975. High-temperature crystal chemistry of fayalite. *American Mineralogist*, **60**, 1092–1097.
- Stacey, F.D., 2005. High pressure equations of state and planetary interiors. *Reports on Progress in Physics*, **68**, 341–383.
- Staudigel, H. & Schreyer, W., 1977. The upper thermal stability of clinochlore at 10–35 kbar $P(H_2O)$. *Contributions to Mineralogy and Petrology*, **61**, 187–198.
- Stephenson, D.A., Sclar, C.B. & Smith, J.Y., 1966. Unit cell volumes of synthetic orthoenstatite and low clinoenstatite. *Mineralogical Magazine*, **35**, 838–846.
- Stixrude, L. & Lithgow-Bertelloni, C., 2005. Mineralogy and elasticity of the oceanic upper mantle: origin of the low-velocity zone. *Journal of Geophysical Research*, **110**, B03204.doi: 10.1029/2004JB002965.
- Stixrude, L. & Lithgow-Bertelloni, C., 2007. Influence of phase transformations on lateral heterogeneity and dynamics in the Earth's mantle. *Earth and Planetary Science Letters*, **263**, 45–55.
- Storre, B. & Nitsch, K.-H., 1974. Zur Stabilität von Margarit im System $CaO-Al_2O_3-SiO_2-H_2O$. *Contributions to Mineralogy and Petrology*, **43**, 1–24.
- Sueno, S., Cameron, M., Papike, J.J. & Prewitt, C.T., 1973. The high-temperature crystal chemistry of tremolite. *American Mineralogist*, **58**, 649–664.
- Sueno, S., Cameron, M. & Prewitt, C.T., 1976. Orthoferrosilite: high temperature crystal chemistry. *American Mineralogist*, **61**, 38–53.
- Sugiyama, K. & Takeuchi, Y., 1991. The crystal structure of rutile as a function of temperature up to 1600 °C. *Zeitschrift für Mineralogie*, **194**, 305–313.
- Suito, K., Namba, J., Horikawa, T., et al. 2001. Phase relations of $CaCO_3$ at high pressure and high temperature. *American Mineralogist*, **86**, 997–1002.
- Suzuki, I., 1979. Thermal expansion of $\gamma-Mg_2SiO_4$. *Journal of Physics of the Earth*, **28**, 53–61.
- Suzuki, I., 1980. Thermal expansion of modified spinel $\beta-Mg_2SiO_4$. *Journal of Physics of the Earth*, **27**, 273–280.
- Suzuki, I. & Anderson, O.L., 1983. Elasticity and thermal expansion of a natural garnet up to 1000 K. *Journal of Physics of the Earth*, **31**, 125–138.
- Suzuki, I., Okajima, S. & Seya, K., 1979. Thermal expansion of single-crystal manganosite. *Journal of Physics of the Earth*, **27**, 63–69.
- Suzuki, I., Seya, K., Takai, H. & Sumino, Y., 1981. Thermal expansion of fayalite. *Physics and Chemistry of Minerals*, **1**, 60–63.
- Symmes, G.H., 1986. *The Thermal Expansion of Natural Muscovite, Paragonite, Margarite, Pyrophyllite, Phlogopite, and Two Chlorites: The Significance of High TP Volume Studies on Calculated Phase Equilibria*, BA thesis. Amherst College, Amherst, MA, USA.
- Takahashi, T., Bassett, W.A. & Mao, H.K., 1968. Isothermal compression of the alloys of iron up to 300 kbar at room temperature: iron-nickel alloys. *Journal of Geophysical Research*, **73**, 4717–4725.

- Takahashi, T. & Liu, L.C., 1970. Compression of ferromagnesian garnets and the effect of solid solutions on the bulk modulus. *Journal of Geophysical Research*, **75**, 5757–5766.
- Taylor-Jones, K. & Powell, R., 2010. Calculated phase equilibria in $\text{FeO}-\text{MgO}-\text{Al}_2\text{O}_3-\text{SiO}_2-\text{TiO}_2-\text{O}$: the stability of sapphirine + quartz. *Journal of Metamorphic Geology*, **28**, 615–633.
- Taylor, B.E. & Liou, J.G., 1978. The low-temperature stability of andradite in C–O–H fluids. *American Mineralogist*, **63**, 378–393.
- Taylor, L.A., 1970. Low temperature phase relations in the Fe–S system. *Carnegie Institute of Washington Year Book*, **68**, 259–267.
- Tenailleau, C., Etschmann, B., Wang, H., Pring, A., Grguric, B.A. & Studer, A., 2005. Thermal expansion of troilite and pyrrhotite determined by in situ cooling (873 to 373K) neutron powder diffraction measurements. *Mineralogical Magazine*, **69**, 205–216.
- Tequi, C., Robie, R.A., Hemingway, B.S., Neuville, D.R. & Richet, P., 1991. Melting and thermodynamic properties of pyrope ($\text{Mg}_3\text{Al}_2\text{Si}_3\text{O}_{12}$). *Geochimica et Cosmochimica Acta*, **55**, 1005–1010.
- Theye, T., Chopin, C., Grevel, K.-D. & Ockenga, E., 1997. The assemblage diaspore + quartz in metamorphic rocks: a petrological, experimental and thermodynamic study. *Journal of Metamorphic Geology*, **15**, 17–28.
- Theye, T., Seidel, E. & Vidal, O., 1992. Carpholite, sudoite, and chloritoid in low-grade high-pressure metapelites from Crete and the Peloponnese, Greece. *European Journal of Mineralogy*, **4**, 487–507.
- Thieblot, L., Tequi, C. & Richet, P., 1999. High-temperature heat capacity of grossular ($\text{Ca}_3\text{Al}_2\text{Si}_3\text{O}_{12}$), enstatite (MgSiO_3), and titanite (CaTiSiO_5). *American Mineralogist*, **84**, 848–855.
- Thompson, A.B., 1970. Laumontite equilibria and the zeolite facies. *American Journal of Science*, **269**, 267–275.
- Thompson, A.B., 1971. Analcite–albite equilibria at low temperatures. *American Journal of Science*, **271**, 79–92.
- Thompson, P., 1994. The sanidine–sanidine hydrate’ reaction boundary. *Mineralogical Magazine*, **58A**, 897.
- Toulmin, III P., & Barton, Jr. P.B., 1964. Thermodynamic study of pyrite and pyrrhotite. *Geochimica et Cosmochimica Acta*, **28**, 641–671.
- Tribaudino, M. & Prencipe, M., 1999. A high temperature in situ single-crystal study of P4/n vesuvianite. *European Journal of Mineralogy*, **11**, 1037–1042.
- Tribaudino, M. & Prencipe, M., 2001. The compressional behavior of P4/N vesuvianite. *Canadian Mineralogist*, **39**, 145–151.
- Turkin, A.I., Doroshev, A.M. & Yu, I., 1983. Study of the phase composition of garnet-bearing associations of the system $\text{MgO}-\text{Al}_2\text{O}_3-\text{SiO}_2-\text{Cr}_2\text{O}_3$ system at high temperatures and pressures [in Russian]. *Silicate Systems Under High Pressure*, 5–24. Institute of Geology and Geophysics, Novosibirsk.
- Urakawa, S., Kondo, T., Igawa, N., Shimomura, O. & Ohno, H., 1994. Synchrotron radiation study on the high-pressure and high-temperature phase relations of KAlSi_3O_8 . *Physics and Chemistry of Minerals*, **21**, 387–391.
- Vaidya, S.N. & Kennedy, G.C., 1971. Compressibility of 27 halides to 45 kbar. *Journal of the Physics and Chemistry of Solids*, **32**, 951–964.
- Vaidya, S.N., Bailey, S., Pasternak, T. & Kennedy, G.C., 1973. Compressibility of fifteen minerals to 45 kilobars. *Journal of Geophysical Research*, **78**, 6893–6898.
- Vidal, O., Theye, T. & Chopin, C., 1994. Experimental study of chloritoid stability at high pressure and various fO_2 conditions. *Contributions to Mineralogy and Petrology*, **118**, 256–270.
- Vidal, O., Goffé, B. & Theye, T., 1992. Experimental study of the stability of sudoite and magnesiocarpholite and calculation of a new petrogenetic grid for the system $\text{MgO}-\text{Al}_2\text{O}_3-\text{SiO}_2-\text{H}_2\text{O}$. *Journal of Metamorphic Geology*, **10**, 603–614.
- Vidal, O., Goffé, B., Bousquet, R. & Parra, T., 1999. Calibration and testing of an empirical chloritoid-chlorite Mg–Fe exchange thermometer and thermodynamic data for daphnite. *Journal of Metamorphic Geology*, **17**, 25–39.
- Vidal, O., Parra, T. & Trotet, F., 2001. A thermodynamic model for Fe–Mg aluminous chlorite using data from phase equilibrium experiments and natural pelitic assemblages in the 100–600 °C, 1–25 kbar range. *American Journal of Science*, **6**, 557–592.
- Viswanathan, K. & Seidel, E., 1979. Crystal chemistry of Fe–Mg Carpholites. *Contributions to Mineralogy and Petrology*, **70**, 41–47.
- Voigt, R. & Will, G., 1981. Das System $\text{Fe}_2\text{O}_3-\text{H}_2\text{O}$ unter hohen Drucken. *Neues Jahrbuch für Mineralogie Monatshefte*, **2**, 89–96.
- von Seckendorff, V. & O'Neill, H. St. C., 1993. An experimental study of Fe–Mg partitioning between olivine and orthopyroxene at 1173, 1273 and 1423K and 1.6 GPa. *Contributions to Mineralogy and Petrology*, **113**, 196–207.
- Wagner, V.H., 1932. Zur Thermochemie der Metasilikate des Calciums und Magnesiums und des Diopsids. *Zeitschrift für Anorganische und allgemeine Chemie*, **208**, 1–22.
- Walker, D., Verma, P.K., Cranswick, L.M.D., Jones, R.L., Clark, S.M. & Buhre, S., 2004. Halite–sylvite thermoelasticity. *American Mineralogist*, **89**, 204–210.
- Wallis, J., Sigalas, I. & Hart, S., 1986. Determination of the thermal expansion of orthorhombic sulfur. *Journal of Applied Crystallography*, **19**, 273–274.
- Walter, L.S., 1963. Experimental studies on Bowen's decarbonation series: I: P–T univariant equilibria of the “monticellite” and “akermanite” reactions. *American Journal of Science*, **261**, 488–500.
- Walter, L.S., 1965. Experimental studies on Bowen's decarbonation series III: P–T univariant equilibrium of the reaction: spurrite + monticellite = merwinite + calcite and analysis of assemblages found at Crestmore, California. *American Journal of Science*, **263**, 64–77.
- Walter, M.J., 1998. Melting of garnet peridotite and the origin of komatiite and depleted lithosphere. *Journal of Petrology*, **39**, 29–60.
- Walter, M.J., Kubo, A., Yoshino, T., Brodholt, J., Koga, K.T. & Ohishi, Y., 2004. Phase relations and equation-of-state of aluminous Mg-silicate perovskite and implications for Earth's lower mantle. *Earth and Planetary Science Letters*, **222**, 501–516.
- Watanabe, H., 1982. Thermochemical properties of synthetic high-pressure compounds relevant to the earth's mantle. In: *High-Pressure Research in Geophysics* (eds Manghnani, M.H. & Akimoto, S.), pp. 441–464. Center for Academic Publications, Japan.
- Waters, D.J., 1986. Metamorphic history of sapphirine-bearing and related magnesian gneisses from Namaqualand, South Africa. *Journal of Petrology*, **27**, 541–565.
- Wechsler, B.A. & Prewitt, C.T., 1984. Crystal structure of ilmenite (FeTiO_3) at high temperature and at high pressure. *American Mineralogist*, **69**, 176–185.
- Werner, A. & Hochheimer, H.D., 1982. High-pressure x-ray of Cu_2O and Ag_2O . *Physical Review B*, **25**, 5929–5935.
- Westrich, H.R. & Holloway, J.R., 1981. Experimental dehydration of pargasite and calculation of its entropy and Gibbs energy. *American Journal of Science*, **281**, 922–934.
- Westrum, E.F., Essene, E.J. & Perkins, D., 1979. Thermophysical properties of the garnet grossular: $\text{CaAl}_2\text{Si}_3\text{O}_{12}$. *Journal of Chemical Thermodynamics*, **11**, 57–66.
- White, R.W., Powell, R. & Holland, T.J.B., 2001. Calculation of partial melting equilibria in the system $\text{Na}_2\text{O}-\text{CaO}-\text{K}_2\text{O}-\text{FeO}-\text{MgO}-\text{Al}_2\text{O}_3-\text{SiO}_2-\text{H}_2\text{O}$ (NCKFMASH). *Journal of Metamorphic Geology*, **19**, 139–153.
- White, W.P., 1919. Silicate specific heats. *American Journal of Science*, **47**, 1–21.
- Williams, Q., Knittle, E., Reichlin, R., Martin, S. & Jeanloz, R., 1990. Structural and electronic properties of Fe_2SiO_4 -fayalite at ultrahigh pressures: amorphization and gap closure. *Journal of Geophysical Research*, **95**, 21549–21563.

- Windom, K.E. & Boettcher, A.L., 1976. The effect of reduced activity of anorthite on the reaction grossular + quartz = anorthite + wollastonite: a model for plagioclase in the earth's lower crust and upper mantle. *American Mineralogist*, **61**, 889–896.
- Winter, J.K. & Ghose, S., 1979. Thermal expansion and high-temperature crystal chemistry of the Al_2SiO_5 polymorphs. *American Mineralogist*, **64**, 573–586.
- Winter, J.K., Okamura, F.P. & Ghose, S., 1979. A high-temperature structural study of high albite, monalbite and the albite-monalbite phase transition. *American Mineralogist*, **64**, 409–423.
- Wood, B.J., 1976. The reaction phlogopite + quartz = enstatite + sanidine + H_2O . *Progress in Experimental Petrology*, 3rd NERC Report, **6**, 17–19.
- Wood, B.J. & Banno, S., 1973. Garnet–orthopyroxene and orthopyroxene–clinopyroxene relationships in simple and complex systems. *Contributions to Mineralogy and Petrology*, **42**, 109–124.
- Wood, B.J., Hackler, R.T. & Dobson, D.P., 1994. Experimental determination of Mn–Mg mixing properties in garnet, olivine and oxide. *Contributions to Mineralogy and Petrology*, **115**, 438–448.
- Wunder, B. & Schreyer, W., 1997. Antigorite: high-pressure stability in the system $\text{MgO}-\text{SiO}_2-\text{H}_2\text{O}$ (MSH). *Lithos*, **41**, 213–227.
- Wunder, B., 1998. Equilibrium experiments in the system $\text{MgO}-\text{SiO}_2-\text{H}_2\text{O}$ (MSH): stability fields of clinohumite–OH [$\text{Mg}_9\text{Si}_4\text{O}_{16}(\text{OH})_2$], chondrodite–OH [$\text{Mg}_5\text{Si}_2\text{O}_8(\text{OH})_2$] and phase A [$\text{Mg}_7\text{Si}_2\text{O}_8(\text{OH})_6$]. *Contributions to Mineralogy and Petrology*, **132**, 111–120.
- Wunder, B., Rubie, D.C., Ross, C.R., Medenbach, O., Seifert, F. & Schreyer, W., 1993. Synthesis, stability and properties of $\text{Al}_2\text{SiO}_4(\text{OH})_2$: a fully hydrated analogue of topaz. *American Mineralogist*, **78**, 285–297.
- Xu, J., Hu, J., Ming, L., Huang, E. & Xie, H., 1994. The compression of diaspore, $\text{AlO}(\text{OH})$ at room temperature up to 27 GPa. *Geophysical Research Letters*, **21**, 161–164.
- Yagi, T., Akaogi, M., Shimomura, O., Suzuki, T. & Akimoto, S., 1987. In situ observation of the olivine–spinel phase transformation in Fe_2SiO_4 using synchrotron radiation. *Journal of Geophysical Research*, **92**, 6207–6213.
- Yagi, A., Suzuki, T. & Akaogi, M., 1994. High pressure transitions in the system $\text{KAlSi}_3\text{O}_8-\text{NaAlSi}_3\text{O}_8$. *Physics and Chemistry of Minerals*, **21**, 12–17.
- Yamamoto, K., Akimoto, S., 1977. The system $\text{MgO}-\text{SiO}_2-\text{H}_2\text{O}$ at high pressures and temperatures – stability field for hydroxyl-chondrodite, hydroxyl-clinohumite and 10 Å-phase. *American Journal of Science*, **277**, 288–312.
- Yin, H.-A. & Greenwood, H.J., 1983. Displacement of equilibria of OH-tremolite and F-tremolite solid solution. I. Determination of the equilibrium P–T curve of OH-tremolite. *EOS (Transactions of the American Geophysical Union)*, **64**, 347.
- Yoder, H.S., 1968. Akermanite and related melilite-bearing assemblages. *Carnegie Institute of Washington Yearbook*, **66**, 471–477.
- Yong, W., Dachs, E., Withers, A.C. & Essene, E.J., 2006. Heat capacity and phase equilibria of hollandite polymorph of KAlSi_3O_8 . *Physics and Chemistry of Minerals*, **33**, 167–177.
- Yong, W., Dachs, E., Withers, A.C. & Essene, E.J., 2008. Heat capacity and phase equilibria of wadeite-type $\text{K}_2\text{Si}_4\text{O}_9$. *Contributions to Mineralogy and Petrology*, **155**, 137–146.
- Zhang, L. & Hafner, S., 1992. High-pressure ^{57}Fe resonance and compressibility of $\text{Ca}(\text{Fe}, \text{Mg})\text{Si}_2\text{O}_6$ clinopyroxene. *American Mineralogist*, **77**, 462–473.
- Zhang, L., Ahsbahs, H., Kutoglu, A. & Hafner, S., 1992. Compressibility of grunerite. *American Mineralogist*, **77**, 480–483.
- Zhang, J., Liebermann, R.C., Gasparik, T., Herzberg, C.T. & Fei, Y., 1993. Melting and subsolidus relations of SiO_2 at 9–14 GPa. *Journal of Geophysical Research*, **98**, 19785–19793.
- Zhang, J., Li, B., Utsumi, W. & Liebermann, R.C., 1996. In situ X-ray observations of the coesite–stishovite transition: reversed phase boundary and kinetics. *Physics and Chemistry of Minerals*, **23**, 1–10.
- Zhang, J.Z., Martinez, I., Guyot, F., Gillet, P. & Saxena, S.K., 1997. X-ray diffraction study of magnesite at high-pressure and high-temperature. *Physics and Chemistry of Minerals*, **24**, 122–130.
- Zhang, J.Z., Martinez, I., Guyot, F. & Reeder, R.J., 1998. Effects of $\text{Mg}-\text{Fe}^{2+}$ substitution in calcite-structure carbonates: thermoelastic properties. *American Mineralogist*, **83**, 280–287.
- Zhao, Y., Von Dreele, R.B. & Shankland, T.J., 1997. Thermoelastic equation of state of jadeite $\text{NaAlSi}_2\text{O}_6$: an energy-dispersive Rietveld refinement study of low symmetry and multiple phases diffraction. *Geophysical Research Letters*, **24**, 5–8.
- Zhao, Y.X. & Spain, I.L., 1989. X-ray diffraction data for graphite to 20 GPa. *Physical Review B*, **40**, 993–997.
- Zharikov, V.A. & Shmulovich, K.I., 1969. High temperature mineral equilibria in the system $\text{CaO}-\text{SiO}_2-\text{CO}_2$. *Geochemistry International*, **6**, 853–869.
- Zhu, H., Newton, R.C. & Kleppa, O.J., 1994. Enthalpy of formation of wollastonite (CaSiO_3) and anorthite ($\text{CaAl}_2\text{Si}_2\text{O}_8$) by experimental phase equilibrium measurements and high-temperature solution calorimetry. *American Mineralogist*, **79**, 134–144.
- Ziegenbein, D. & Johannes, W., 1974. Wollastonitbildung aus Quartz und calcit bei $\text{Pf} = 2, 4$, und 6 kbar. *Fortschritte der Mineralogie*, **44**, 77–79.

SUPPORTING INFORMATION

Additional Supporting Information may be found in the online version of this article:

Table S1. Complete LSQDS output for data set generation.

Table S2. Activity-composition relationships.

Please note: Wiley-Blackwell are not responsible for the content or functionality of any supporting materials supplied by the authors. Any queries (other than missing material) should be directed to the corresponding author for the article.

Appendix 1: Sources for thermodynamic data

Group	End-member	<i>S</i>	<i>V</i>	<i>C_p</i>	<i>z</i>	<i>κ</i>
Garnet and olivine	almandine (alm)	3	4	0, 3	5	6
	andradite (andr)	1	1	1	46	46
	grossular (gr)	42	1	43, 44	45, 46	46
	knorrtingite (knor)	0	47	0	0	0
	majorite (maj)	33	26	33	33	26
	pyrope (py)	0, 1	3	34	35	36, 37
	spessartine (spss)	38	39	38	40	41
	clinohumite (chum)	0	20	0	0	21
	fayalite (fa)	1	1	13	14, 15	16
	forsterite (fo)	1	1	1	10, 11	10, 12
	larnite (larn)	1	1	1	0	0
	monticellite (mont)	0, 1	1	1	18	19
	tephroite (teph)	1	1	1	17	0
Aluminosilicates	andalusite (and)	1	1	52	53	54
	kyanite (ky)	1	1	52	53	55
	sillimanite (sill)	1	1	52	53	54
	mullite (amul)	0	7	0	8	9
	mullite (smul)	0	7	0	8	9
	chloritoid (mctd)	61	59	61	62	63
	chloritoid (fctd)	61	64	61	62	63
	chloritoid (mnctd)	0	0	0	62	63
	staurolite (mst)	0	65	0	57	58
	staurolite (fst)	0	60	0	57	58
	staurolite (mnst)	0	0	0	57	58
	topaz (tpz)	0	66	0	40	0
Other orthosilicates	akermanite (ak)	2	2	2	2	0
	gehlenite (geh)	79	60	1	40	0
	julgoldite (jgd)	0	78	0	0	0
	merwinite (merw)	1	65	1	40	0
	pumpellyite (mpm)	0	77	0	0	0
	pumpellyite (fpm)	0	0	0	0	0
	rankinite (rnk)	1	1	1	40	0
	sphene (sph)	1	1	1, 88	89	90
	spurrite (spu)	1	1	0	0	0
	tilleyite (ty)	0	80	0	0	0
	zircon (zrc)	1	1	1	40	91
Sorosilicates	clinozoisite (cz)	0	71	0	69	70
	epidote (ep)	72	73	72	69	70, 74
	epidote (fep)	0	0	0	0	0
	lawsonite (law)	67	1	0, 67	69	76
	piemontite (pmt)	0	75	0	0	0
	zoisite (zo)	0, 67	68	0, 67	69	70
	vesuvianite (vsv)	0	49	0	50	51
Cyclosilicates	cordierite (ferd)	81	86	81	83	84, 85
	cordierite (hcrd)	81	0	0	83	84, 85
	cordierite (crd)	81, 82	1	81	83	84, 85
	cordierite (mnrcd)	0	0	0	83	84, 85
	osumilite (osm1)	18	18	18	0	0
	osumilite (osm2)	18	18	18	0	0
	osumilite (fosc)	18	18	18	0	0
High-pressure silicates	akimotoite (fak)	0, 33	22	33	0, 33	33
	akimotoite (mak)	0, 33	22	33	33	26
	caSi-titanite (cstn)	0	247	0	0	247
	perovskite (apv)	0, 27	22	0	0, 32	26
	perovskite (cpv)	0	246	0	0, 32	246
	perovskite (fpv)	0	249	0	0	249
	perovskite (mpv)	0, 27	22	32	32	26
	phase A (pha)	0	87	0	87	87
	ringwoodite (mrw)	0, 27	22	23	28	26
	ringwoodite (frw)	0	26	29, 30	31	30
	wadsleyite (mwrd)	0	22	23	24	25
	wadsleyite (fwd)	0	22	0	0	26
	acmite (acm)	1	60	1	92	93
Pyroxenes and pyroxenoid	Ca-tschermark's pyroxene (cats)	94	94	94	94	0
	Ca-Eskola pyroxene (caes)	0	95	0	0	0
	clinoenstatite (cen)	0	96	97, 98	40	0
	clinoenstatite (hen)	0	102	0	0	107
	diopside (di)	1	99	1	100	101
	enstatite (en)	1	1	1	40	102
	ferrosilite (fs)	1	103	1	103	104
	hedenbergite (hed)	105	105	105	92	106
	jadeite (jd)	1	1	108	92, 109	109
	kosmochlore (kos)	0	110	0	92	111
	Mg-tschermark's pyroxene (mgts)	0	112	0	0	0
	protoenstatite (pren)	0	60	0, 1	113	102
	pseudowollastonite (pswo)	1	1	0, 114	40	0
	pyroxmangite (pxmn)	1	1	1	115	115
	rhodonite (rhod)	1	1	1	115	115
	walstromite (wal)	248	248	0, 114	0, 40	0, 116
	wollastonite (wo)	1	60	114	40	116

Appendix 1. (Continued)

Group	End-member	<i>S</i>	<i>V</i>	<i>C_p</i>	<i>z</i>	<i>κ</i>
Amphiboles	actinolite (fact)	0	120	0	0	0
	anthophyllite (anth)	1	1	0	0	0
	anthophyllite (fanth)	0	0	0	0	0
	cummingtonite (cumm)	0	126	0	0	0
	glaucomphane (gl)	123	124	123	124	119
	glaucomphane (fgl)	0	0	0	0	0
	grunerite (grun)	0	127	0	0	128
	pargasite (parg)	0	122	0	103	119
	riebeckite (rieb)	0	125	0	0	0
	tremolite (tr)	0, 1	117	118	242	119
Other chain silicates	tschermakite (ts)	0	121	0	0	0
	deerite (deer)	0	129	0	0	129
	carpholite (mcar)	130	131	130	0	0
	carpholite (fcar)	130	132	130	0	0
	sapphirine (spr4)	0	133, 134	0	0	0
Mica	sapphirine (spr5)	0	133, 134	0	0	0
	sapphirine (fspr)	0	0	0	0	0
	annite (ann)	0	60	0	0	0
	biotite (mnb1)	0	0	0	0	0
Chlorite	celadonite (cel)	0	135	0	137	138
	celadonite (fcel)	0	136	0	137	138
	eastonite (east)	0	139	0	0	0
	margarite (ma)	1	1	1	140	0
	muscovite (mu)	1	1	1	137	138
	paragonite (pa)	1	1	1, 141	137	138
	phlogopite (phl)	1	1	1	142	143
	phlogopite (naph)	0	144	0	0	0
	chlorite (afchl)	145	146, 147, 148	145	149	150
	chlorite (mnchl)	0, 145	0	0	149	150
Other sheet silicates	amesite (ames)	0	146, 147, 148	145	149	150
	clinochlore (clin)	145	146, 147, 148	145	149	150
	daphnite (daph)	145	151	145	149	150
	sudoite (sud)	152	0	0	149	150
	sudoite (fsud)	0	0	0	149	150
	antigorite (atg)	0	158	159	0	160
	chrysotile (chr)	1	1	1	0	162
	lizardite (liz)	0	162	1	0	162
	greenalite (glt)	0	161	0	0	0
	kaolinite (kao)	1	1	1	0	0
Feldspar and feldspathoid	minnesotaite (min)	0	155	0	0	0
	minnesotaite (minm)	0	0	0	0	0
	stilpnomelane (mstp)	0	0, 155	0	0	0
	stilpnomelane (fstp)	0	155	0	0	0
	prehnite (pre)	67	67	67	0	156
	prehnite (fpre)	0	157	0	0	156
	pyrophyllite (prl)	1	22	153	0	150
	talc (ta)	22	1	1	154	150
	talc (fta)	0	0	0	154	150
	talc (tap)	0	0	153	0	150
	talc (tats)	0	0	0	154	150
Silica minerals	albite (ab)	1	1	1	163	164
	albite (abh)	0, 1	0, 1	1	163	164
	analcite (anl)	1	1	0	0	177
	anorthite (an)	1	1	167	168	169
	carnegieite (cg)	1	1	1	0	0
	carnegieite (cgh)	1	178	1	0	0
	kalsilite (cls)	1	179	1	179, 180	181
	leucite (lc)	1	182	0, 1	182	181
	microcline (mic)	1	1	1	165	166
	nepheline (ne)	1	1	1	40	177
Other framework silicates	sanidine (san)	1	165	1	165	166
	coesite (coe)	0, 174	1	174	0	0
	cristobalite (crst)	0, 1	0, 1	1	0	0
	quartz (q)	1	1	1, 173	0	173
	stishovite (stv)	0, 1	1	33	175	176
Oxides	tridymite (trd)	0, 1	0, 1	0, 1	0	0
	heulandite (heu)	187	187	0	0	244
	hollandite (hol)	171	172	172	172	172
	laumontite (lmt)	0	186	0	0	0
	meionite (me)	0, 183	183	0	184	185
	K-cymrite (kcm)	0	170	0	170	170
	sodalite (sdl)	245	245	245	0, 40	0, 177
	stilbite (stb)	0	188	0	0	0
	wadeite (wa)	171	170	170	172	171
	wairakite (wrk)	0	1	0	0	0

Appendix 1. (Continued)

Group	End-member	<i>S</i>	<i>V</i>	<i>C_p</i>	α	κ
	geikielite (geik)	1	1	0, 1	0	0
	hematite (hem)	1	1	1	40	202
	hercynite (here)	209	1	0	40	0
	Ilmenite (ilm)	1	1	1	204	204
	lime (lime)	1	1	1	189	190
	magnesioferrite (mft)	210	1	1	0	0
	magnetite (mt)	1	1	1	40	208
	manganosite (mang)	1	1	1	197	198
	nickel oxide (NiO)	1	1	1	0	203
	periclaste (per)	1	1	193	194	195, 196
	picrochromite (picr)	211	1	1	0	0
	pyrophanite (pnt)	1	1	0, 1	0	0
	rutile (ru)	1	1	1	191	192
	spinel (sp)	0, 1	1	1	207	208
	tenorite (ten)	1	1	1	0	0
	ulvöspinel (usp)	1	1	1	0	0
	ferropericlase (fper)	0, 1	26	1	40	26
Hydroxides	brucite (br)	1	1	0, 1	212, 213	213, 214
	diaspore (dsp)	1	22	0, 1	215	216
	goethite (gth)	1	1	0	0	0
Carbonates	ankerite (ank)	0	227	0	0	226
	aragonite (arag)	1	1	0, 1	40, 219	219
	calcite (cc)	1	1	0, 1	217	218
	dolomite (dol)	1	22	0, 1	224, 225	225, 226
	magnesite (mag)	1	1	0, 1	217, 220, 221	220, 221
	rhodochrosite (rhc)	1	1	1	222	223
	siderite (sid)	0, 1	22	0, 1	0	177
Halides and S-bearing	anhydrite (any)	1	1	235	236	177
	halite (ht)	1	1	1	228	228
	pyrite (pyr)	1	1	229	40	230
	pyrrhotite (trot)	0	231	0, 233	231	232
	pyrrhotite (trov)	0	231	0, 233	231	232
	troilite (tro)	0	231	0, 233	231	232
	troilite (lot)	0	231	0, 233	234	232
	sylvite (syv)	1	1	1	228	228
Elements	copper (Cu)	1	1	1	40	238
	diamond (diam)	1	1	1	40	240
	graphite (gph)	1	1	1	40	239
	iron (iron)	1	1	0, 1	40	237
	nickel (Ni)	1	1	0, 1	40	177
	sulphur (S)	1	1	1	243	241
Gas species	methane (CH_4)	1	—	1	—	—
	carbon monoxide (CO)	1	—	1	—	—
	carbon dioxide (CO_2)	1	—	1	—	—
	hydrogen (H_2)	1	—	1	—	—
	hydrogen sulphide (H_2S)	1	—	1	—	—
	sulphur gas (S_2)	1	—	1	—	—
	water (H_2O)	1	—	1	—	—
	oxygen (O_2)	1	—	1	—	—

Sources for entropy (*S*), molar volume (*V*), heat capacity (*C_p*), thermal expansion (α) and incompressibility (κ) data.

- 0 Estimated or optimised in this study
 1 Robie & Hemingway, 1995
 2 Hemingway *et al.*, 1986
 3 Newton & Harlov (1993)
 4 Geiger *et al.*, 1987
 5 Skinner, 1956
 6 Takahashi & Liu, 1970
 7 Cameron, 1977
 8 Schneider & Eberhard, 1990
 9 Balzar & Ledbetter, 1993
 10 Hazen, 1976
 11 Kajiyoshi, 1986
 12 Downs *et al.*, 1996
 13 Robie *et al.*, 1982
 14 Smyth, 1975
 15 Suzuki *et al.*, 1981
 16 Williams *et al.*, 1990
 17 Okajima *et al.*, 1978
 18 Lager & Meagher, 1978
 19 Sharp *et al.*, 1986
 20 Yamamoto & Akimoto, 1977
 21 Ross & Crichton, 2001
 22 Smyth & McCormick, 1995
 23 Ashida *et al.*, 1987
 24 Suzuki, 1980
 25 Jacobs & de Jong, 2005
 26 Stixrude & Lithgow-Bertelloni, 2005
 27 Fei *et al.*, 1990
 28 Suzuki, 1979
 29 Watanabe, 1982
 30 Jacobs & Oonk, 2001
- 31 Mao *et al.*, 1969
 32 Gillet *et al.*, 2000
 33 Saxena, 1996
 34 Tequi *et al.*, 1991
 35 Suzuki & Anderson, 1983
 36 Hazen & Finger, 1989
 37 Zhang *et al.*, 1998
 38 Dachs *et al.*, 2009
 39 Hsu, 1968
 40 Skinner, 1966
 41 Leger *et al.*, 1990
 42 Westrum *et al.*, 1979
 43 Bosenick *et al.*, 1996
 44 Thieblot *et al.*, 1999
 45 Isaak *et al.*, 1992
 46 Pavese *et al.*, 2001a,b
 47 Irfune *et al.*, 1982
 48 Holland *et al.*, 1996
 49 Hochella *et al.*, 1982
 50 Tribaudino & Prencipe, 1999
 51 Tribaudino & Prencipe, 2001
 52 Hemingway *et al.*, 1991
 53 Winter & Ghose, 1979
 54 Burt *et al.*, 2006
 55 Comodi *et al.*, 1997
 56 Cameron, 1977
 57 Gibbons *et al.*, 1981
 58 Grevel *et al.*, 1998
 59 Chopin & Schreyer, 1983
 60 Robie *et al.*, 1967
 61 Koch-Müller *et al.*, 2002
- 62 Ivadi *et al.*, 1988
 63 Comodi *et al.*, 1992
 64 Rao & Johannes, 1979
 65 Schreyer & Seifert, 1969
 66 Wunder *et al.*, 1993
 67 Perkins *et al.*, 1980
 68 Chatterjee, 1976
 69 Pawley *et al.*, 1996
 70 Comodi & Zanazzi, 1997
 71 Jenkins *et al.*, 1985
 72 Kiseleva *et al.*, 1974
 73 Bird & Helgeson, 1980
 74 Holland *et al.*, 1996
 75 Keskinen & Liou, 1979
 76 Boffa-Ballaran & Angel, 2003
 77 Schiffman & Liou, 1980
 78 Artioli *et al.*, 2003
 79 Hemingway & Robie, 1984
 80 Harker, 1959
 81 Dachs & Geiger, 2008
 82 Paukov *et al.*, 2006
 83 Mirwald *et al.*, 1984
 84 Mirwald, 1981
 85 Schlenker *et al.*, 1977
 86 Mukhopadhyay & Holdaway, 1994
 87 Pawley & Wood, 1995
 88 Manon *et al.*, 2008
 89 Malcherek, 2001
 90 Angel *et al.*, 1999a,b
 91 Hazen & Finger, 1979
 92 Cameron *et al.*, 1973
- 93 Kandelin & Weidner, 1988
 94 Haselton *et al.*, 1984
 95 McCormick, 1986
 96 Stephenson *et al.*, 1966
 97 White, 1919
 98 Wagner, 1932
 99 Krupka *et al.*, 1985a
 100 Finger & Ohashi, 1976
 101 McCormick *et al.*, 1989
 102 Hugh-Jones & Angel, 1994
 103 Sueno *et al.*, 1976
 104 Kandelin & Weidner, 1988
 105 Haselton *et al.*, 1987
 106 Zhang & Hafner, 1992
 107 Kung *et al.*, 2005
 108 Hemingway *et al.*, 1998
 109 Zhao *et al.*, 1997
 110 Carroll Webb & Wood, 1986
 111 Origlieri *et al.*, 2003
 112 Gasparik & Newton, 1984
 113 Jackson *et al.*, 2003
 114 Richet *et al.*, 1991
 115 Pinckney & Burnham, 1988
 116 Vaidya *et al.*, 1973
 117 Hewitt, 1975
 118 Krupka *et al.*, 1985b
 119 Comodi *et al.*, 1991
 120 Jenkins & Bozhilov, 2003
 121 Jenkins, 1994
 122 Lykins & Jenkins, 1992
 123 Holland, 1988

- 124 Jenkins & Corona, 2006
 125 Ernst, 1962
 126 Evans & Ghiorso, 1995
 127 Ghiorso & Evans, 2002
 128 Zhang *et al.*, 1992
 129 Lattard & LeBreton, 1994
 130 Bertoldi *et al.*, 2006
 131 Chopin & Schreyer, 1983
 132 Viswanathan & Seidel, 1979
 133 Seifert, 1974
 134 Chatterjee & Schreyer, 1972
 135 Schmidt *et al.*, 2001
 136 Coggon & Holland, 2002
 137 Guggenheim *et al.*, 1987
 138 Comodi & Zanazzi, 1995
 139 Circone *et al.*, 1991
 140 Symmes, 1986
 141 Holland, 1979
 142 Russell & Guggenheim, 1999
 143 Pavese *et al.*, 2003
 144 Carman, 1974
 145 Bertoldi *et al.*, 2007
 146 Baker & Holland, 1996
 147 Jenkins & Chernosky, 1986
 148 Roots, 1994
 149 Nelson & Guggenheim, 1993
 150 Pawley *et al.*, 2002
 151 Parra *et al.*, 2005
 152 Vidal *et al.*, 1992
 153 Krupka *et al.*, 1979
 154 Pawley *et al.*, 1995
 155 Miyano & Klein, 1989
- 156 Detrie *et al.*, 2009
 157 Rose & Bird, 1987
 158 Mellini *et al.*, 1987
 159 King *et al.*, 1967
 160 Bosc & Navrotsky, 1998
 161 Rasmussen *et al.*, 1998
 162 Hilairet *et al.*, 2006
 163 Winter *et al.*, 1979
 164 Downs *et al.*, 1994
 165 Hovis *et al.*, 1999
 166 Allan & Angel, 1997
 167 Richet & Fiquet, 1991
 168 Grundy & Brown, 1974
 169 Angel, 2004
 170 Fasshauer *et al.*, 1997
 171 Yong *et al.*, 2006
 172 Akaogi *et al.*, 2004
 173 Dorogokupets, 1995
 174 Hemingway *et al.*, 1998
 175 Ito *et al.*, 1974
 176 Andrault *et al.*, 2003; Luo *et al.*, 2002
 177 Birch, 1966
 178 Richet *et al.*, 1990
 179 Carpenter & Cellai, 1996
 180 Hovis *et al.*, 2003
 181 Fasshauer *et al.*, 1998
 182 Palmer *et al.*, 1989
 183 Baker & Newton, 1994
 184 Baker, 1995
 185 Hazen & Sharp, 1988
 186 Liou, 1971a
 187 Cho *et al.*, 1987
- 188 Liou, 1971b
 189 Fiquet *et al.*, 1999
 190 Richet *et al.*, 1988
 191 Sugiyama & Takeuchi, 1991
 192 Hazen & Finger, 1981
 193 Richet & Fiquet, 1991
 194 Dubrovinsky & Saxena, 1997
 195 Fei, 1999
 196 Hazen, 1976
 197 Suzuki *et al.*, 1979
 198 Jeanloz & Rudy, 1987
 199 Richet *et al.*, 1992
 200 Aldebert & Traverse, 1984
 201 D'Amour *et al.*, 1978
 202 Finger & Hazen, 1980
 203 Clendenen & Drickamer, 1966
 204 Wechsler & Prewitt, 1984
 205 Leger *et al.*, 1993
 206 Werner & Hochheimer, 1982
 207 Fiquet *et al.*, 1999
 208 Finger *et al.*, 1986
 209 Klemme & Van Miltenburg, 2003
 210 Klemme & Ahrens, 2005
 211 Klemme *et al.*, 2000
 212 Fei & Mao, 1993
 213 Fukui *et al.*, 2003
 214 Catti *et al.*, 1995
 215 Pawley *et al.*, 1996
 216 Xu *et al.*, 1994
 217 Markgraf & Reeder, 1985
 218 Redfern & Angel, 1999
 219 Martinez *et al.*, 1996
- 220 Fiquet & Reynard, 1999
 221 Zhang *et al.*, 1997
 222 Rao & Murthy, 1970
 223 Martens *et al.*, 1982
 224 Reeder & Markgraf, 1986
 225 Martinez *et al.*, 1996
 226 Ross & Reeder, 1992
 227 Davidson *et al.*, 1993
 228 Walker *et al.*, 2004
 229 Chase, 1998
 230 Adams & Williamson, 1923
 231 Tenailleau *et al.*, 2005
 232 King & Prewitt, 1982
 233 Gronvold & Stolen, 1991, 1992
 234 Taylor, 1970
 235 Majzlán *et al.*, 2002
 236 Evans, 1979
 237 Takahashi *et al.*, 1968
 238 Vaidya & Kennedy, 1971
 239 Zhao & Spain, 1989
 240 Alexandrov *et al.*, 1987
 241 Luo & Ruoff, 1993
 242 Sueno *et al.*, 1973
 243 Wallis *et al.*, 1986
 244 Comodi *et al.*, 2001
 245 Sharp *et al.*, 1989
 246 Shim *et al.*, 2000
 247 Angel *et al.*, 1999a, b
 248 Chatterjee *et al.*, 1984
 249 Walter *et al.*, 2004.

Appendix 2: Summary table of equilibria used for fitting the data set.

- 1) $2knor = 3en + 2esk$ (Irifune *et al.*, 1982)
 2) $2knor = 3en + 2esk$ (Turkin *et al.*, 1983)
 3) $knor + fo = pier + 2en$ (Klemme, 2004)

Equilibrium: crpx crsp (Carroll Webb & Wood, 1986), involving:
 4) $2kos + sp = 2jd + pier$
 5) $lot = tro$ (fix at transition)

Equilibrium: po S_2 (Rau, 1976), involving:

- 6) $16trot = 14trot + S_2$
 7) $8trot + H_2 = 7trot + H_2S$ (Lin, 1976)

Equilibrium: po S_2 (Toulmin & Barton, 1964), involving:

- 8) $16trot = 14trot + S_2$

Equilibrium: po pyr S_2 (Toulmin & Barton, 1964), involving next two reactions:

- 9) $14trot + S_2 = 16trot$

- 10) $2trot + S_2 = 2pyr$

Equilibrium: po pyr S_2 (Schneeberg, 1973), involving next two reactions:

- 11) $16trot = 14trot + S_2$

- 12) $2pyr = 2trot + S_2$

Equilibrium: iron tro fluid2 (Rosenqvist, 1954), involving:

- 13) $iron + H_2S = tro + H_2$

Equilibrium: iron tro fluid2 (Alcock & Richardson, 1951), involving:

- 14) $iron + H_2S = tro + H_2$

- 15) $en = pren$ (Atlas, 1952; Chen & Presnall, 1975)

- 16) $diam = gph$ (Kennedy & Kennedy, 1976)

- 17) $q = trd$ (Ostrovsky, 1966)

- 18) $trd = crst$ (Ostrovsky, 1966)

- 19) $q = crst$ (Ostrovsky, 1966; Jackson, 1976)

- 20) $coe = q$ (Bose & Ganguly, 1995)

- 21) $coe = q$ (Bohnet & Boettcher, 1982; Gasparik, 1984)

- 22) $stv = coe$ (Zhang *et al.*, 1996)

- 23) $arag = cc$ (Boettcher & Wyllie, 1968)

- 24) $arag = cc$ (Crawford & Hoersch, 1972)

- 25) $arag = cc$ (Johannes & Puhan, 1971)

- 26) $arag = cc$ (Goldsmith & Newton, 1969)

- 27) $arag = cc$ (Irving & Wyllie, 1975)

- 28) $arag = cc$ (Suito *et al.*, 2001)

- 29) $arag + mag = dol$ (Morlidge *et al.*, 2006)

- 30) $arag + sid = ank$ (Morlidge *et al.*, 2006)

- 31) $cen = en$ (Boyd & England, 1965)

- 32) $hen = en$ (Pacalo & Gasparik, 1990)

- 33) $hen = cen$ (Angel *et al.*, 1992)

- 34) $mwd + stv = hen$ (Sawamoto, 1987; Kanzaki, 1987)

- 35) $maj = 2hen$ (Ohtani, 1991)

- 36) $2mwd + 2stv = maj$ (Ohtani, 1991)

- 37) $mwd = fo$ (Katsura & Ito, 1989; Fei & Bertka, 1999)

- 38) $mrw = mwd$ (Katsura & Ito, 1989; Fei *et al.*, 2004)

- 39) $2mak = mwd + stv$ (Sawamoto, 1987; Kanzaki, 1987)

- 40) $4mpv = maj$ (Katsura & Ito, 1989; Ohtani 1991)

- 41) $mpv = mak$ (Katsura & Ito, 1989; Ohtani 1991)

- 42) $mpv = mak$ (Ito & Takahashi, 1989)

- 43) $frw = fa$ (Yagi *et al.*, 1987; Akimoto *et al.*, 1965, 1967)

- 44) $fwd = fa$ (Fei & Bertka, 1999; Frost, 2003; Katsura & Ito, 1989; Akimoto, 1987)

Equilibrium: ol wd rg (Fei & Bertka, 1999; Frost, 2003; Katsura & Ito, 1989; Akimoto, 1987), involving next three reactions:

- 45) $fwd = fa$

- 46) $mwd = mrw$

- 47) $mpv + per = mrw$ (Shim *et al.*, 2001; Ito & Takahashi 1989; Fei *et al.*, 2004)

- 49) $per + cor = sp$ (Akaogi *et al.*, 1989)

Equilibrium: pv aki (Ito & Yamada, 1982), involving next two reactions:

- 50) $fpv = fak$

- 51) $mpv = mak$

Equilibrium: aki rg stv (Ito & Yamada, 1982), involving next two reactions:

- 52) $2mak = mrw + stv$

- 53) $2fak = frw + stv$

Equilibrium: rg mwu stv (Ito & Yamada, 1982), involving next two reactions:

- 54) $mrw = 2per + stv$

- 55) $frw = 2fper + stv$

Equilibrium: pv aki rg mwu (Ito & Yamada, 1982), involving next three reactions:

- 56) $fpv = fak$

- 57) $mpv = mak$

- 58) $2mpv + frw = 2fpv + mrw$

Equilibrium: pvk crn py (Hirose *et al.*, 2001; Kubo & Akaogi, 2000), involving next three reactions:

- 59) $cor = apv$

- 60) $mcor = mpv$

- 61) $py = 3mpv + cor$

- 62) $wo = pswo$ (Osborn & Schairer, 1941; Huang & Wyllie, 1975)

- 63) $wal = wo$ (Chatterjee *et al.*, 1984; Essene, 1974)

- 64) $lrn + cstn = 3wal$ (Gasparik *et al.*, 1994)

- 65) $3cpv = lrn + cstn$ (Gasparik *et al.*, 1994)

- 66) $cc = lime + CO_2$ (Smyth & Adams, 1923)

- 67) $cc = lime + CO_2$ (Baker, 1962)

- 68) $cc + q = wo + CO_2$ (Zhu, Newton & Kleppa, 1993)

- 69) $cc + q = wo + CO_2$ (Jacobs & Kerrik, 1981)

- 70) $cc + q = wo + CO_2$ (Ziegenbein & Johannes, 1974)

- 71) $cc + q = wo + CO_2$ (Greenwood, 1967a,b; Harker & Tuttle, 1956)

- 72) $cc + q = wo + CO_2$ (Aranovich & Newton, 1999)

- 73) $cc + q = wo + CO_2$ (Haselton *et al.*, 1978)

- 74) $3cc + 2wo = ty + CO_2$ (Zharikov & Shmulovich, 1969)

- 75) $ty = spu + CO_2$ (Zharikov & Shmulovich, 1969)

- 76) $spu + 4wo = 3rnk + CO_2$ (Zharikov & Shmulovich, 1969)

- 77) $spu + rnk = 4lrn + CO_2$ (Zharikov & Shmulovich, 1969)

Appendix 2. (Continued)

- 78) ta + 2en = anth (Chernosky *et al.*, 1985)
 79) br = per + H₂O (Barnes & Ernst, 1963)
 80) br = per + H₂O (Aranovich & Newton, 1996)
 81) br = per + H₂O (Schramke *et al.*, 1982; Irving *et al.*, 1977)
 82) br = per + H₂O (Irving *et al.*, 1977)
 83) br = per + H₂O (Kanzaki, 1991)
 84) 2ta = 3en + 2q + 2H₂O (Chernosky, 1976a,b; Chernosky *et al.*, 1985; Skippen, 1971)
 85) 2ta = 3en + 2q + 2H₂O (Chernosky *et al.*, 1985)
 86) 2ta = 3en + 2q + 2H₂O (Jenkins *et al.*, 1991)
 87) 2ta = 3en + 2q + 2H₂O (Aranovich & Newton, 1999)
 88) 2ta = 3en + 2coo + 2H₂O (Pawley & Wood, 1995)
 89) 2fo + 2ta = 5en + 2H₂O (Chernosky, 1976a,b; Chernosky *et al.*, 1985)
 90) 2fo + 2ta = 5en + 2H₂O (Pawley, 1998)
 91) 2anth = 7en + 2q + 2H₂O (Chernosky & Autio, 1979)
 92) 7ta = 3anth + 4q + 4H₂O (Chernosky & Autio, 1979)
 93) 2anth + 2fo = 9en + 2H₂O (Chernosky *et al.*, 1985)
 94) 9ta + 4fo = 5anth + 4H₂O (Chernosky *et al.*, 1985)
 95) br + chr = 2fo + 3H₂O (Johannes, 1968; Kitahara *et al.*, 1966)
 96) 5chr = ta + 6fo + 9H₂O (Chernosky, 1982; Kitahara *et al.*, 1966)
 97) liz = chr (Chernosky, 1975)
 98) 17liz = atg + 3br (Evans, 2004)
 99) atg = 4ta + 18fo + 27H₂O (Evans *et al.*, 1976)
 100) atg = 4ta + 18fo + 27H₂O (Wunder & Schreyer, 1997)
 101) atg = 14fo + 10cen + 31H₂O (Wunder & Schreyer, 1997)
 102) atg = 14fo + 10cen + 31H₂O (Wunder & Schreyer, 1997)
 103) atg = 14fo + 10en + 31H₂O (Bose & Navrotsky, 1998)
 104) 2br + cen = 2fo + 2H₂O (Wunder & Schreyer, 1997)
 105) atg + 14ta = 45en + 45H₂O (Pawley, 1996)
 106) phA = 3br + 2fo (Pawley & Wood, 1995)
 107) 6atg + 226fo = 62phA + 153en (Bose & Navrotsky, 1998)
 108) anth = cumm (Ghiorso & Evans, 2002)
- Equilibrium: cum enfs ol q H₂O (Fonarev & Korolkov, 1980), involving next two reactions:
- 109) 2cumm = 7en + 2q + 2H₂O
 110) 2grun = 7fs + 2q + 2H₂O
 111) chum = 4fo + per + H₂O (Duffy & Greenwood, 1979)
 112) chum = 4fo + per + H₂O (Pawley, 2000)
 113) chum = 4fo + br (Pawley, 2000)
 114) 4fo + br = chum (Wunder, 1998)
 115) 4fo + br = chum (Wunder, 1998)
 116) mag = per + CO₂ (Harker & Tuttle, 1955; Goldsmith & Heard, 1962)
 117) mag = per + CO₂ (Johannes & Metz, 1968; Philipp & Girsperger, 1990; Koziol & Newton, 1995)
- 118) mag = per + CO₂ (Irving & Wyllie, 1975)
 119) 2mag + 2q = en + 2CO₂ (Johannes, 1969)
 120) 2mag + 2q = en + 2CO₂ (Koziol & Newton, 1995)
 121) 2mag + 2coe = en + 2CO₂ (Haselton *et al.*, 1978)
 122) 2mag + en = 2fo + 2CO₂ (Haselton *et al.*, 1978; Koziol & Newton, 1998)
 123) ta + 5mag = 4fo + 5CO₂ + H₂O (Greenwood, 1967a,b)
 124) 2wo + 2mont = di + merw (Yoder, 1968)
 125) wo + mont = ak (Yoder, 1968)
 126) di + merw = 2ak (Yoder, 1968)
 127) di + 3mont = fo + 2ak (Walter, 1963; Yoder, 1968)
 128) 2di + ta = tr (Jenkins *et al.*, 1991)
 129) di + 2mag = en + dol (Brey *et al.*, 1983)
 130) spu + 2mont = 2merw + cc (Walter, 1965)
 131) 2tr = 3en + 4di + 2q + 2H₂O (Yin & Greenwood, 1983)
 132) 2tr = 3en + 4di + 2q + 2H₂O (Boyd, 1959)
 133) 2tr = 3en + 4di + 2q + 2H₂O (Jenkins *et al.*, 1991)
 134) 2tr + 2fo = 5en + 4di + 2H₂O (Jenkins, 1983)
 135) dol = cc + per + CO₂ (Goldsmith, 1980)
 136) dol = cc + per + CO₂ (Harker & Tuttle, 1955)
 137) dol + 2q = di + 2CO₂ (Slaughter *et al.*, 1975; Eggert & Kerrick, 1981; Jacobs & Kerrick, 1981)
 138) dol + 2q = di + 2CO₂ (Eggler *et al.*, 1976)
 139) dol + 2coe = di + 2CO₂ (Luth, 1995)
 140) di + 3dol = 2fo + 4cc + 2CO₂ (Kase & Metz, 1980)
 141) 2dol + ta + 4q = tr + 4CO₂ (Eggert & Kerrick, 1981)
 142) di + cc = ak + CO₂ (Walter, 1963)
 143) ak + fo + cc = 3mont + CO₂ (Walter, 1963)
 144) fo + di + 2cc = 3mont + 2CO₂ (Walter, 1963)
 145) 5dol + 4ta = 6fo + 5di + 4H₂O + 10CO₂ (Skippen, 1971)
 146) ta + 3cc + 2q = 3di + H₂O + 3CO₂ (Skippen, 1971)
 147) 5dol + 8q + H₂O = tr + 3cc + 7CO₂ (Slaughter *et al.*, 1975; Eggert & Kerrick, 1981)
 148) 5ta + 6cc + 4q = 3ta + 6CO₂ + 2H₂O (Slaughter *et al.*, 1977)
 149) 3dol + 4q + H₂O = ta + 3cc + 3CO₂ (Eggert & Kerrick, 1981; Metz & Puhan, 1971; Gordon & Greenwood, 1970)
 150) tr + 3ce + 2q = 5di + 3CO₂ + H₂O (Slaughter *et al.*, 1975)
 151) tr + 11dol = 8fo + 13cc + 9CO₂ + H₂O (Metz, 1976)
 152) 3tr + 5cc = 11di + 2fo + 5CO₂ + 3H₂O (Chernosky & Berman, 1986a,b)
 153) ky = and (Holdaway, 1971; Newton, 1966a; Richardson *et al.*, 1969; Bohlen *et al.*, 1991)
 154) ky = sill (Newton, 1966b; Richardson *et al.*, 1968; Holdaway, 1971; Bohlen *et al.*, 1991)
- 155) and = sill (Pattison, personal communications)
 156) and = sill (Holdaway, 1971; Bowman, 1975; Kerrick & Heninger, 1984)
 157) and = sill (Richardson *et al.*, 1969)
 158) ky = cor + q (Harlov & Newton, 1993; Harlov & Milke, 2002)
 159) cor + q = sill (Harlov *et al.*, 2008)
 160) cor + q = and (Harlov & Newton, 1993)
 161) cor + stv = ky (Schmidt *et al.*, 1997)
 162) 2dsp = cor + H₂O (Haas, 1972; Fockenberg *et al.*, 1996)
 163) 2dsp = cor + H₂O (Vidal *et al.*, 1994)
 164) prl + 6dsp = 4and + 4H₂O (Haas & Holdaway, 1973; Hemley *et al.*, 1980)
 165) 2dsp + 4q = prl (Theye *et al.*, 1997)
 166) 2dsp + 4coe = prl (Theye *et al.*, 1997)
 167) prl = cor + 4q + H₂O (Chatterjee *et al.*, 1984)
 168) prl = and + 3q + H₂O (Hemley *et al.*, 1980; Kerrick, 1968)
 169) prl = and + 3q + H₂O (Haas & Holdaway, 1973)
 170) kao + 2q = prl + H₂O (McPhail, 1985; Hemley *et al.*, 1980)
 171) 2kao = 2dsp + prl + 2H₂O (Hemley *et al.*, 1980)
 172) tpz = ky + H₂O (Wunder *et al.*, 1993)
 173) gr + 2ky + q = 3an (Koziol & Newton, 1988; Goldsmith, 1980)
 174) gr + 2ky + q = 3an (Gasparik, 1984; Hays, 1967)
 175) gr + q = an + 2wo (Huckenholz *et al.*, 1975; Newton, 1966c; Hays, 1967; Windom & Boettcher, 1976)
 176) gr + cor = geh + an (Boettcher, 1970; Huckenholz *et al.*, 1975)
 177) 2gr = 3wo + geh + an (Huckenholz *et al.*, 1975; Hays, 1967)
 178) gr + 2cor = 3cats (Gasparik, 1984)
 179) 2cats + 2caes = 3an (Gasparik, 1984)
 180) gr + 3ky = 3an + cor (Gasparik, 1984)
 181) gr + 3cats = 2an + 2geh (Hays, 1967)
 182) 3cats = an + geh + cor (Hays, 1967)
 183) gr + 3ky = 3an + cor (Gasparik, 1984)
 184) 3an + cc = me (Baker & Newton, 1994)
 185) 3an + cc = me (Goldsmith & Newton, 1977)
 186) gr + cc + 2ky + q = me (Baker & Newton, 1994)
 187) 4zo + q = 5an + gr + 2H₂O (Boettcher, 1970; Newton, 1966; Chatterjee *et al.*, 1984)
 188) 4zo + q = 5an + gr + 2H₂O (Newton, 1966)
 189) 6zo = 6an + 2gr + cor + 3H₂O (Boettcher, 1970; Newton, 1965; Chatterjee *et al.*, 1984)
 190) 2zo + ky + q = 4an + H₂O (Goldsmith, 1981; Jenkins *et al.*, 1983; Johannes, 1984)
 191) 2zo + sill + q = 4an + H₂O (Newton, 1966; Newton & Kennedy, 1963)
 192) ma = an + cor + H₂O (Chatterjee, 1974)
 193) ma = an + cor + H₂O (Storre & Nitsch, 1974)
 194) ma + q = an + and + H₂O (Storre & Nitsch, 1974)
 195) ma + q = an + ky + H₂O (Storre & Nitsch, 1974)
 196) 4ma + 3q = 2zo + 5ky + 3H₂O (Jenkins, 1984)
 197) ma + q = an + and + H₂O (Nitsch *et al.*, 1981)
 198) ma + q = an + ky + H₂O (Nitsch *et al.*, 1981)
 199) 4ma = 2zo + 2ky + 3cor + 3H₂O (Chatterjee *et al.*, 1984)
 200) law = an + 2H₂O (Crawford & Fyfe, 1965)
 201) 4law + 2q = 2zo + prl + 6H₂O (Nitsch, 1972)
 202) 12law = 6zo + 2ky + prl + 20H₂O (Nitsch, 1972)
 203) 5law = 2zo + ma + 2q + 8H₂O (Nitsch, 1974)
 204) 2law + dsp = zo + ky + 4H₂O (Schmidt & Poli, 1994)
 205) 4law = 2zo + ky + q + 7H₂O (Schmidt & Poli, 1994; Chatterjee *et al.*, 1984)
 206) 4law = 2zo + ky + q + 7H₂O (Newton & Kennedy, 1963)
 207) 4law = 2zo + ky + q + 7H₂O (Skrok *et al.*, 1994)
 208) pre = an + wo + H₂O (Chatterjee *et al.*, 1984)
 209) 5pre = 2zo + 2gr + 3q + 4H₂O (Connolly & Kerrick, 1985)
 210) wrk = an + 2q + 2H₂O (Liou, 1970)
 211) lmt = an + 2q + 4H₂O (Thompson, 1970)
 212) lmt = wrk + 2H₂O (Liou, 1971a,b,c)
 213) law + 2q + 2H₂O = lmt (Liou, 1971a,b,c)
 214) law + 2q = wrk (Liou, 1971a,b,c)
 215) lmt + 3q + 2H₂O = heu (Cho *et al.*, 1987)
 216) stlb = lmt + 3q + 3H₂O (Liou, 1971a,b,c)
 217) 3cc + an + cor = 2geh + 3CO₂ (Shmulovich, 1974)
 218) 2cc + an = wo + geh + 2CO₂ (Shmulovich, 1974)
 219) wo + cc + an = gr + CO₂ (Hoschek, 1974)
 220) an + cor + 3cc = 2geh + 3CO₂ (Hoschek, 1974)
 221) 2an + 3cc = geh + gr + 3CO₂ (Hoschek, 1974)
 222) an + 2cc = geh + wo + 2CO₂ (Hoschek, 1974)
 223) 2zo + CO₂ = 3an + cc + H₂O (Allen & Fawcett, 1982)
 224) cc + q + and = an + CO₂ (Chernosky & Berman, 1991)
 225) cc + q + and = an + CO₂ (Jacobs & Kerrick, 1981)
 226) cc + q + ky = an + CO₂ (Jacobs & Kerrick, 1981)
 227) per + cor = sp (Chamberlin *et al.*, 1995)
- Equilibrium: opx cor py (Gasparik & Newton, 1984), involving next two reactions:
- 228) 3en + 2cor = 2py
 229) en + mgts = py
- Equilibrium: opx cor py (Fockenberg, 2008), involving next two reactions:
- 230) 3en + 2cor = 2py
 231) en + mgts = py

Appendix 2. (Continued)

Equilibrium: py q opx sill (Perkins, 1983; Hensen & Essene, 1971), involving next two reactions:
 232) $2\text{py} + 2\text{q} = 3\text{en} + 2\text{sill}$
 233) en + mgt = py

Equilibrium: py opx q ky (Hensen, 1972), involving next two reactions:
 234) $2\text{py} + 2\text{q} = 3\text{en} + 2\text{ky}$
 235) en + mgt = py

Equilibrium: fo py sp opx (Danckwerth & Newton, 1978; Gasparik & Newton, 1984), involving next two reactions:
 236) fo + py = sp + 2en
 237) en + mgt = py
 238) en + sp = mgt + fo (Gasparik & Newton, 1984)
 239) en + mgt = py (Perkins *et al.*, 1981)
 240) hrd = crd + H_2O (Mirwald *et al.*, 1979)
 241) hrd = crd + H_2O (Schreyer & Yoder, 1964)
 242) hrd = crd + H_2O (Carey, 1995; Skippen & Gunter, 1996)
 243) hrd = crd + H_2O (Mukhopadhyay & Holdaway, 1994)

Equilibrium: opx sp fo crd (Hertzberg, 1983), involving next two reactions:
 244) $5\text{en} + 2\text{sp} = 5\text{fo} + \text{crd}$
 245) en + sp = mgt + fo

Equilibrium: opx sp fo cd H_2O (Seifert, 1974; Fawcett & Yoder, 1966), involving next three reactions:
 246) $5\text{en} + 2\text{sp} = 5\text{fo} + \text{crd}$
 247) en + sp = mgt + fo
 248) hrd = crd + H_2O

Equilibrium: opx sill q crd (Newton, personal communication), involving next three reactions:
 249) en + 2sill + q = crd
 250) 2mgt + 3q = crd
 251) 3en + 6sill = 2mgt + 2crd

Equilibrium: opx sill cd cor H_2O (Newton, 1972), involving next four reactions:
 252) $3\text{en} + 6\text{sill} = 2\text{mgt} + 2\text{crd}$
 253) en + 3sill = crd + cor
 254) hrd + cor = en + 3sill + H_2O
 255) hrd = crd + H_2O

Equilibrium: opx sa q crd (Newton, 1972; Perkins *et al.*, 1981), involving next three reactions:
 256) 2crd = spr4 + 8q
 257) 5crd = 2spr5 + 2en + 19q
 258) crd = 2mgt + 3q

Equilibrium: sa q crd sill (Newton, 1972; Perkins *et al.*, 1981), involving next two reactions:
 259) 2crd = spr4 + 8q
 260) 3crd + 4sill = 2spr5 + 17q

Equilibrium: sa q opx sill (Newton, 1972; Hensen, 1972), involving next five reactions:
 261) spr4 + 6q = 2en + 4sill
 262) 2spr5 + 14q = 3en + 10sill
 263) en + spr5 = mgt + spr4
 264) spr4 + 2q = 4mgt
 265) en + spr4 + 2sill = 6mgt

Equilibrium: py opx sa sill (Boyd & England, 1959; Arima & Onuma, 1977; Hensen, 1972), involving next three reactions:
 266) 6py = spr4 + 7en + 2sill
 267) 7py = spr5 + 9en + 2sill
 268) py = en + mgt

Equilibrium: py opx sa ky (Fockenberg, 2008), involving next four reactions:
 269) 6py = spr4 + 7en + 2ky
 270) 7py = spr5 + 9en + 2ky
 271) en + spr5 = mgt + spr4
 272) py = en + mgt

Equilibrium: py sp cor sa (Ackermann *et al.*, 1975; Doroshev & Malinovskiy, 1974), involving next two reactions:
 273) 2py + 6sp + 4cor = 3spr4
 274) py + 6sp + 8cor = 3spr5

Equilibrium: py cor sa sill (Malinovskiy & Doroshev, 1975), involving next two reactions:
 275) 4py + 14cor = 3spr4 + 6sill
 276) py + 6cor = spr5 + 2sill

Equilibrium: opx cor sa sill (Malinovskiy & Doroshev, 1975), involving next two reactions:
 277) 2en + 6cor = spr4 + 2sill
 278) 3en + 14cor = 2spr5 + 4sill

Equilibrium: sa opx cd sp H_2O (Seifert, 1974), involving next four reactions:
 279) 2crd + 16sp = 5spr4
 280) 5spr5 + 5en = 3crd + 19sp
 281) hrd = crd + H_2O
 282) en + spr5 = mgt + spr4

Equilibrium: cor opx sp sa (Podlesskii, 1996), involving next three reactions:
 283) en + 4sp + 6cor = 2spr5
 284) en + 2sp + 2cor = spr4
 285) en + 2cor = 2mgt

Equilibrium: chl cor cd sa H_2O (Seifert, 1974), involving:
 286) 16cln + 64cor = 2crd + 19spr4 + 64 H_2O

Equilibrium: chl cd opx sa H_2O (Seifert, 1974), involving next two reactions:
 287) 16cln + 6crd = 32en + 7spr4 + 64 H_2O
 288) hrd = crd + H_2O

Equilibrium: chl cor sp sa H_2O (Seifert, 1974; Ackermann *et al.*, 1975), involving next two reactions:
 289) 2cln + 8cor + 2sp = 3spr4 + 8 H_2O
 290) 2cln + 20cor + 8sp = 6spr5 + 8 H_2O

Equilibrium: chl opx fo py H_2O (Pawley, 2003), involving:
 291) clin + en = 2fo + py + 4 H_2O

Equilibrium: chl opx fo sp H_2O (Baker & Holland, 1996), involving next two reactions:
 292) clin = en + fo + sp + 4 H_2O
 293) ames = en + 2sp + 4 H_2O

Equilibrium: chl opx fo H_2O (Baker & Holland, 1996), involving next two reactions:
 294) clin = 2fo + mgt + 4 H_2O
 295) 2clin = ames + 2fo + en + 4 H_2O

Equilibrium: chl cor sp H_2O (Baker & Holland, 1996), involving:
 296) 3ames = 2cln + 2cor + 2sp + 4 H_2O

Equilibrium: chl cor sp H_2O (Ackermann *et al.*, 1975), involving next two reactions:
 297) clin + 2cor = py + 2sp + 4 H_2O
 298) 2py + 6sp + 12 H_2O = 3ames + 2cor

Equilibrium: chl opx fo sp H_2O (Jenkins, 1981; Jenkins & Chernosky, 1986; Fawcett & Yoder, 1966), involving next two reactions:
 299) clin = en + fo + sp + 4 H_2O
 300) ames = en + 2sp + 4 H_2O

Equilibrium: chl opx fo sp H_2O (Jenkins, 1981; Jenkins & Chernosky, 1986; Fawcett & Yoder, 1966), involving next two reactions:
 301) clin = en + fo + sp + 4 H_2O
 302) ames = en + 2sp + 4 H_2O
 303) 2mcar = sud + q (Vidal *et al.*, 1992)

Equilibrium: chl py fo sp H_2O (Staudigel & Schreyer, 1977), involving:
 304) 2cln = py + 3fo + sp + 8 H_2O

Equilibrium: chl py fo sp H_2O (Fockenberg, 1995), involving:
 305) 2clin = py + 3fo + sp + 8 H_2O

Equilibrium: chl q ky tlc H_2O (Massonne *et al.*, 1981), involving next two reactions:
 306) 3cln + 14q = 3ky + 5ta + 7 H_2O
 307) 2cln + 4q = ames + 2ta + 2 H_2O

Equilibrium: chl opx fo cd H_2O (Jenkins & Chernosky, 1986), involving:
 308) 2cln + 3en = 7fo + crd + 8 H_2O

Equilibrium: chl cd opx sp H_2O (Jenkins & Chernosky, 1986), involving next two reactions:
 309) 5cln + crd = 10en + 7sp + 20 H_2O
 310) hrd = crd + H_2O

Equilibrium: chl fo sp cd H_2O (Chernosky, 1974; McPhail *et al.*, 1990), involving:
 311) 5cln = 10fo + 3sp + crd + 20 H_2O

Equilibrium: chl q tlc ed H_2O (Chernosky, 1978), involving:
 312) 6cln + 29q = 8ta + 3crd + 16 H_2O

Equilibrium: chl q tlc ed H_2O (Massonne, 1989), involving:
 313) 6cln + 29q = 8ta + 3crd + 16 H_2O

Equilibrium: tlc q cd H_2O (Newton, 1972), involving next four reactions:
 314) 2ta + 6sill + q = 3crd + 2 H_2O
 315) hrd = crd + H_2O
 316) 2ta + 6sill + q + H_2O = 3herd
 317) tap = sill + 3a + H_2O

Equilibrium: tlc ky q cd H_2O (Massonne & Schreyer, 1989), involving next two reactions:
 318) 2ta + 6ky + q = 3crd + 2 H_2O
 319) herd = crd + H_2O

Equilibrium: chl ky q cd H_2O (Seifert & Schreyer, 1970), involving:
 320) 2cln + 8ky + 11q = 5crd + 8 H_2O

Equilibrium: chl and q cd H_2O (Seifert & Schreyer, 1970), involving next two reactions:
 321) 2cln + 8and + 11q = 5crd + 8 H_2O
 322) herd = crd + H_2O

Equilibrium: chl and cd cor H_2O (Seifert, 1973), involving:
 323) 2cln + 19and = 5crd + 11cor + 8 H_2O

Equilibrium: chl sill cd cor H_2O (Seifert, 1973), involving:
 324) 2cln + 19sill = 5crd + 11cor + 8 H_2O

Equilibrium: chl ky cd cor H_2O (Seifert, 1973), involving:
 325) 2cln + 19ky = 5crd + 11cor + 8 H_2O

Equilibrium: chl cor cd sp H_2O (Seifert, 1974), involving:
 326) 5cln + 20cor = 3crd + 19sp + 20 H_2O

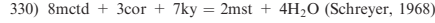
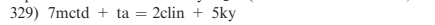
Equilibrium: chl cor cd sp H_2O (Seifert, 1974)

327) clin + 2mag = 3fo + sp + 2 CO_2 + 4 H_2O (Chernosky & Berman, 1986a,b)

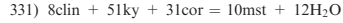
328) 3mctd = py + 2cor + 3 H_2O (Chopin & Schreyer, 1983)

Appendix 2. (Continued)

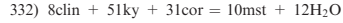
Equilibrium: mctd tlc chl ky H₂O (Koch-Müller & Wirth, 2001), involving:



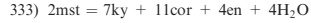
Equilibrium: chl ky cor mst H₂O (Massonne, 1995), involving:



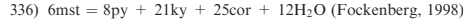
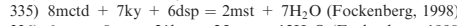
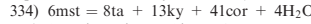
Equilibrium: chl ky cor mst H₂O (Fockenberg, 1998), involving:



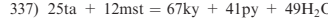
Equilibrium: mst ky cor opx H₂O (Fockenberg, 1998), involving:



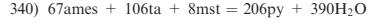
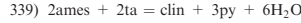
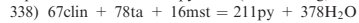
Equilibrium: mst tlc ky cor H₂O (Fockenberg, 1998), involving:



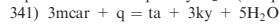
Equilibrium: tlc mst ky py H₂O (Chopin & Sobolev, 1995), involving:



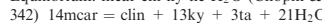
Equilibrium: tlc chl mst py H₂O (Fockenberg, 2008), involving next three reactions:



Equilibrium: mcar q tlc ky H₂O (Chopin & Schreyer, 1983), involving:



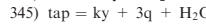
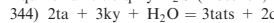
Equilibrium: mcar chl ky H₂O (Chopin & Schreyer, 1983), involving:



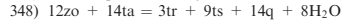
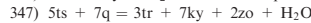
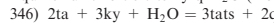
Equilibrium: mcar chl ky q H₂O (Chopin & Schreyer, 1983), involving:



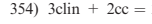
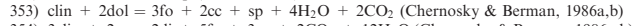
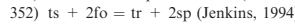
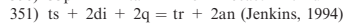
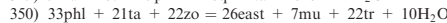
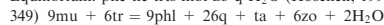
Equilibrium: tlc q ky H₂O (Hoschek, 1995), involving next two reactions:



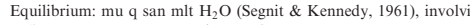
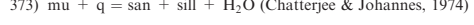
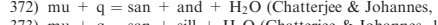
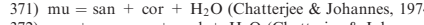
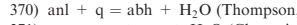
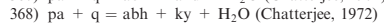
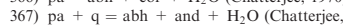
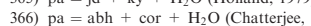
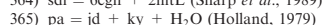
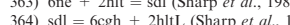
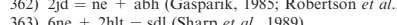
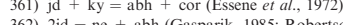
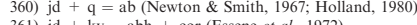
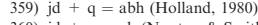
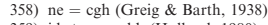
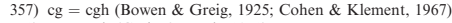
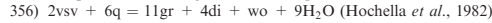
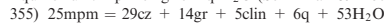
Equilibrium: zo tlc trts ky q H₂O (Hoschek, 1995), involving next three reactions:



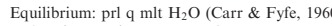
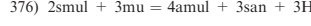
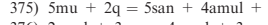
Equilibrium: phe tlc trts mbi zo q H₂O (Hoschek, 1990), involving next two reactions:



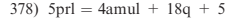
Equilibrium: mpmp cz gr chl q H₂O (Schiffman & Liou, 1980), involving:



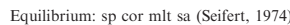
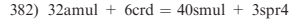
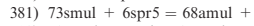
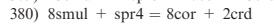
Equilibrium: mu q san mlt H₂O (Segnit & Kennedy, 1961), involving next three reactions:



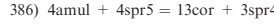
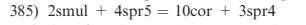
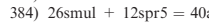
Equilibrium: prl q mlt H₂O (Carr & Fyfe, 1960), involving next two reactions:



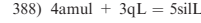
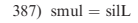
Equilibrium: crd cor mlt sa (Seifert, 1974), involving next four reactions:



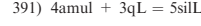
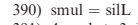
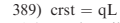
Equilibrium: sp cor mlt sa (Seifert, 1974), involving next four reactions:



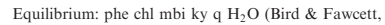
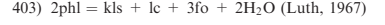
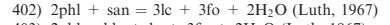
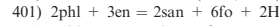
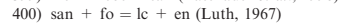
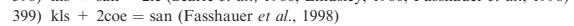
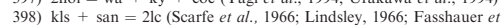
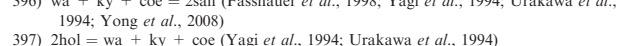
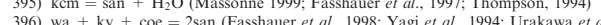
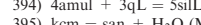
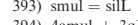
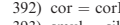
Equilibrium: mlt mqL (Klug *et al.*, 1987), involving next two reactions:



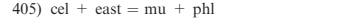
Equilibrium: mlr crst mqL (Klug *et al.*, 1987), involving next three reactions:



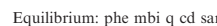
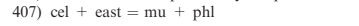
Equilibrium: mlr cor mqL (Klug *et al.*, 1987), involving next three reactions:



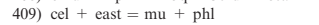
Equilibrium: phe chl mbi ky q H₂O (Bird & Fawcett, 1973), involving next two reactions:



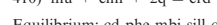
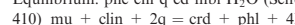
Equilibrium: phe chl mbi ky q H₂O (Massonne, unpublished), involving next two reactions:



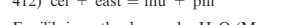
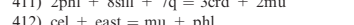
Equilibrium: phe chl mbi ky q H₂O (Seifert, 1970), involving:



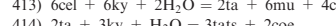
Equilibrium: ed phe mbi sill q H₂O (Seifert, 1970), involving next two reactions:



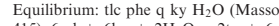
Equilibrium: tlc phe coe ky H₂O (Massonne & Schreyer, 1989), involving next two reactions:



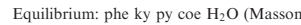
Equilibrium: tlc phe mbi ky q H₂O (Massonne & Schreyer, 1989), involving:



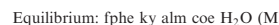
Equilibrium: phe ky py coe H₂O (Massonne & Szpurka, 1997), involving:



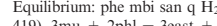
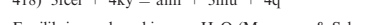
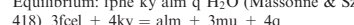
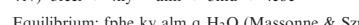
Equilibrium: fphe ky alm coe H₂O (Massonne & Szpurka, 1997), involving:



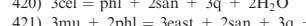
Equilibrium: fphe ky alm q H₂O (Massonne & Szpurka, 1997), involving:



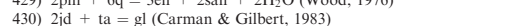
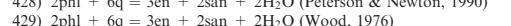
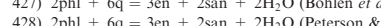
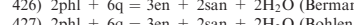
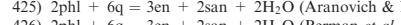
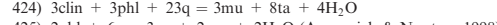
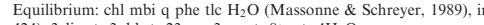
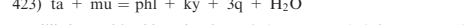
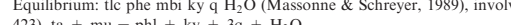
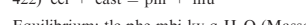
Equilibrium: ph mbi san q H₂O (Massonne & Schreyer, 1989), involving next four reactions:



Equilibrium: tlc phe mbi ky q H₂O (Massonne & Schreyer, 1989), involving:



Equilibrium: chl mbi q phe H₂O (Massonne & Schreyer, 1989), involving:



Appendix 2. (Continued)

- 447) 3fa + O₂ = 3q + 2mt (Myers & Eugster, 1983)
 448) 3fa + O₂ = 3q + 2mt (Hewitt, 1978)
 449) 3fa + O₂ = 3q + 2mt (O'Neill, 1987a)
 450) q + 2iron + O₂ = fa (O'Neill, 1987b)
 451) 3iron + 2O₂ = mt (O'Neill, 1988)
 452) 2gth = hem + H₂O (Voigt & Will, 1981)
 453) sid + hem = mt + CO₂ (Koziol, 2004)
 454) 2grun = 7fa + 2q + 2H₂O (Lattard & Evans, 1992)
 455) 2grun = 7fa + 9q + 2H₂O (Lattard & Evans, 1992)
 456) 2deer = 9fs + 6mt + 6q + 10H₂O (Lattard & Le Breton, 1994)
 457) deer + Ni = 6fs + 2mt + NiO + 5H₂O (Lattard & Le Breton, 1994)
 458) alm + 3hem = 3mt + ky + 2q (Harlov & Newton, 1992)
 459) alm + 2sill = 3hem + 5q (Bohlen *et al.*, 1986)
 460) alm + 5cor = 3herc + 3sill (Shulters & Bohlen, 1989)
 461) 2alm + 4sill + 5q = 3fcrd (Mukhopadhyay & Holdaway, 1994)
 462) 6fst + 25q = 8alm + 46ky + 12H₂O (Rao & Johannes, 1979)
 463) 6fst + 25q = 8alm + 46ky + 12H₂O (Ganguly, 1972)
 464) 6fst + 15q = 4fcrd + 10sill + 4H₂O (Richardson, 1968)
 465) 23fcfd + 7q = 2fst + 5alm + 19H₂O (Rao & Johannes, 1979)
 466) 8fcfd + 10ky = 2fst + 3q + 4H₂O (Rao & Johannes, 1979)
 467) 3fcfd = alm + 2cor + 3H₂O (Ganguly, 1969; Vidal *et al.*, 1994)
 468) 3fcfd = alm + 2cor + 3H₂O (Ganguly, 1969)
 469) 3fcfd = 4dsp + alm + H₂O (Vidal *et al.*, 1994)
 470) 6fst + 25q = 8alm + 46sill + 12H₂O (Richardson, 1968)
 471) 6fst + 25q = 8alm + 46sill + 12H₂O (Dutrow & Holdaway, 1989)
 472) 8fcfd + 10sill = 2fst + 3q + 4H₂O (Richardson, 1968)
 473) 5fcfd = fcfd + 3herc + 5H₂O (Grieve & Fawcett, 1974)
 474) 2fgl = 4abf + 3fa + q + 2H₂O (Hoffmann, 1972)
 475) rieb + 3hem = 2acm + 3mt + 4q + H₂O (Ernst, 1962)
 476) 2ann + 6sill + 9q = 3fcrd + 2san + 2H₂O (Holdaway & Lee, 1977)
 477) 2ann + 3q = 2san + 3fa + 2H₂O (Rutherford, 1973)
 478) 2ann + 3q = 2san + 3fa + 2H₂O (Dachs & Benisek, 1995)
 479) 2san + 2mt + 2H₂O = 2ann + O₂ (Dachs, 1994)
 480) gr + 2alm = 3fa + 3an (Bohlen *et al.*, 1983a,b,c)
 481) gr + 2alm = 3fa + 3an (Perkins & Vielzeuf, 1992)
 482) 2hed = 2wo + fa + q (Lindsley & Munoz, 1969)
 483) 2fact = 3fa + 5q + 4hed + 2H₂O (Jenkins & Bozhilov, 2003)
 484) 2minn = 3fa + 5q + 2H₂O (Engi, 1986)
 485) glt + 2q = minn + H₂O (Rasmussen *et al.*, 1998)
 486) 2gl + 5minn = 3grun + 6H₂O (Rasmussen *et al.*, 1998)
 487) 3sid + minm = minm + 3mag (Klein, 1974)
 488) 28fstp = 14ann + 5grun + 21alm + 79q + 156H₂O (Miyano & Klein, 1989)
 489) mstp + daph = fstp + clin (Miyano & Klein, 1989)
 490) andr = 3pswo + hem (Huckenholz & Yoder, 1971)
 491) 6andr + 3fa = 6mt + 18wo + 3q (Gustafson, 1974)
 492) 6andr + 2Ni = 4mt + 18wo + 2NiO (Gustafson, 1974)
 493) 6andr = 4mt + 18wo + O₂ (Moegher & Chou, 1990)
 494) 3andr + mt + 9q = 9hed + 2O₂ (Burton *et al.*, 1982)
 495) 2andr + q + 3fa = 4hed + 2wo + 2mt (Liou, 1974)
 496) 2andr + 4q + 2Ni = 4hed + 2wo + 2NiO (Liou, 1974)
 497) 3andr + mt + 9q = 9hed + 2O₂ (Moegher & Chou, 1990)
 498) 2andr + 4q = 4hed + 2wo + O₂ (Moegher & Chou, 1990)
 499) 3cc + hem + 3q = andr + 3CO₂ (Taylor & Liou, 1978)
 500) cz = zo (Natural pairs, unpublished)
 501) 2cz + ky + q = 4an + H₂O (Jenkins *et al.*, 1983)
- Equilibrium: epi an grd hem q H₂O (Holdaway, 1972; Liou, 1973), involving next five reactions:
 502) 2ep = andr + an + hem + q + H₂O
 503) 2ep = gr + an + hem + q + H₂O
 504) 6ep = 2andr + 6an + hem + 3H₂O
 505) 4cz + q = 5an + gr + 2H₂O
 506) 6cz + hem + 3q = andr + 9an + 3H₂O
- Equilibrium: grd q an wo (Holdaway, 1972), involving:
 507) gr + q = an + 2wo
- Equilibrium: grd trd an wo (Holdaway, 1972), involving:
 508) gr + trd = an + 2wo
- Equilibrium: epi grd (Perchuk & Aranovich, 1979), involving:
 509) 2cz + andr = 2ep + gr
 510) 12pm + 6cup = 8gr + 4spss + 12ten + 6H₂O (Keskinen & Liou, 1979)
 511) osml = crd + san + 2q (Olesch & Seifert, 1981)
 512) 4phl + 3crd + 2san + 33q = 6osm2 + 4H₂O (Olesch & Seifert, 1981)
 513) en + san + 2sill + 3q = osml (Carrington & Harley, 1995)
 514) py + osm2 = osml + 2en (Carrington & Harley, 1995)
 515) osml + fs = fosc + en (Holland *et al.*, 1996)
 516) fosc + crd = osml + ferd (Holland *et al.*, 1996)
 517) mag + ru = geik + CO₂ (Haselton *et al.*, 1978)
 518) mag + ru = geik + CO₂ (Ferry *et al.*, 2002)
 519) sph + ky = an + ru (Manning & Bohlen, 1991)
 520) ru + cc + q = sph + CO₂ (Hunt & Kerrick, 1977)
 521) ru + cc + q = sph + CO₂ (Jacobs & Kerrick, 1981)
 522) 2ilm = 2iron + 2ru + O₂ (O'Neill *et al.*, 1988)
 523) 2ilm = 2iron + 2ru + O₂ (Anovitz *et al.*, 1985)
 524) 2usp = 2ilm + 2iron + O₂ (O'Neill *et al.*, 1988)
 525) 2usp = 2ilm + 2iron + O₂ (Anovitz *et al.*, 1985)
- 526) alm + 3ru = 3ilm + sill + 2q (Bohlen *et al.*, 1983a,b,c)
 527) 2alm + gr + 6ru = 6ilm + 3an + 3q (Bohlen & Liotta, 1986)
 528) zrc = bdy + crst (Buterman & Foster, 1967)
 529) zrc + 2mag = bdy + fo + 2CO₂ (Ferry *et al.*, 2002)
 530) 2NiO = 2Ni + O₂ (O'Neill, 1987)
 531) 2mag + fa = fo + 2sid (Dalton & Wood, 1993)
 532) 2dol + fa = fo + 2ank (Dalton & Wood, 1993)
 533) dol + sid = ank + mag (Anovitz & Esse, 1987)
 534) dol + sid = ank + mag (Rosenberg, 1967)
 535) dol + sid = ank + mag (Klein, 1978)
 536) dol + sid = ank + mag (Klein, 1978)
 537) py + ann = alm + phl (Ferry & Spear, 1978)
 538) py + ann = alm + phl (Perchuk & Lavrent'eva, 1983)
 539) 3fcfd + 2py = 3crd + 2alm (Perchuk & Lavrent'eva, 1983)
 540) alm + 3cel = py + 3fecl (Green & Hellman, 1982)
 541) alm + 3cel = py + 3fecl (Hynes & Forest, 1988)
 542) alm + phl = py + ann (Hynes & Forest, 1988)
 543) phl + mu = cel + east (Hodges & spear, 1988)
 544) 2phl + mu + 2sill = 3east + 5q (Hodges & spear, 1988)
 545) 2phl + mu + 2ky = 3east + 5q (Pigage & Greenwood, 1982)
 546) 2mu + phl + py = 3east + 6a (Natural)
 547) 2mu + phl + py = 3east + 6q (Hynes & Forest)
 548) 5cel + daph = 5fecl + olin (Currie & Van Staal99)
 549) ames + cel = mu + clin (Currie & Van Staal99)
 550) 2hed + en = fs + 2di (Lindsley, 1983)
 551) 2hed + fo = fa + 2di (Perkins & Vielzeuf, 1992)
 552) fs + fo = en + fa (Matsui & Nishizawa, 1974)
 553) fs + fo = en + fa (von Seckendorff & O'Neill, 1993)
 554) 2py + 3fa = 2alm + 3fo (O'Neill & Wood, 1979)
 555) 2py + 3fa = 2alm + 3fo (Hackler & Wood, 1989)
 556) 2py + 3fs = 2alm + 3en (Lee & Ganguly, 1988)
 557) 2py + 3fs = 2alm + 3en (Kawasaki & Matsui, 1983)
 558) 2py + 3fs = 2alm + 3en (Harley, 1984)
 559) alm + 3di = hed + py (Wood, 1976)
 560) 2herc + fo = 2sp + fa (Jameson & Roeder, 1984)
 561) 2herc + fo = 2sp + fa (Engi, 1983)
 562) fa + 2mt = 2mt + fo (Jameson & Roeder, 1984)
 563) 3en + 2ann = 2phl + 3fs (Fonarev & Konilov, 1986)
 564) fact + 5di = tr + 5hed (Natural Kd)
 565) 7en + 2fanth = 2anth + 7fs (Natural Kd)
 566) 3tr + 5fl = 5gl + 3fact (Natural Kd)
 567) spr4 + 2fcfd = fspr + 2crd (Waters, 1986)
 568) spr4 + 2fs = fspr + 2en (Natural Collected)
 569) 2acm + pa + 2q = 3ab + hem + H₂O (Holland & Ray, 1985)
 570) jd + ep = acm + cz (Holland & Ray, 1985)
 571) 5alm + 3clin = 5py + 3daph (Dickenson & Hewitt, 1986; Laird, 1989)
 572) 5phl + 3daph = 5ann + 3clin (Laird, 1989)
 573) clin + fact = tr + daph (Laird, 1982)
 574) pre + ep = fpree + cz (Cho *et al.*, 1986)
 575) 5mpm + daph = 5fpmp + clin (Evans, 1990)
 576) fpmp + Sep = jgd + 5cz (Cho *et al.*, 1986)
 577) alm + 3mcfd = py + 3fcfd (Chinner & Dixon, 1974; Miller, 1986)
 578) 3fcfd + ta = 3mcfd + fta (Chinner & Dixon, 1974; Chopin & Monie, 1984; Miller, 1986)
 579) 5fcfd + clin = 5mcfd + daph (Vidal *et al.*, 1999)
 580) mcar + fcfd = fear + mcfd (Natural, Seidel & Okrusch, 1977; Theye *et al.*, 1992)
 581) 5mcar + daph = 5fecar + clin (Natural, Theye *et al.*, 1992)
 582) 5sud + 2daph = 5fsud + 2clin (Theye *et al.*, 1992)
 583) pxmn = rhod (Maresch & Mottana, 1976)
 584) rhc + q = pxmn + CO₂ (Peters, 1971)
 585) rhc = mang + CO₂ (Huebner, 1969)
 586) pxmn + rhc = teph + CO₂ (Huebner & Eugster, 1968)
 587) fo + 2mang = teph + 2per (Wood *et al.*, 1994)
 588) 2spss + 3fo = 2py + 3teph (Wood *et al.*, 1994)
 589) spss + 3ilm = alm + 3pnt (Powneby *et al.*, 1987)
 590) phl + 3mnctd = mnbi + 3mcfd (Mahar *et al.*, 1997)
 591) 4phl + 3mnst = 4mnbi + 3ms (Mahar *et al.*, 1997)
 592) 2phl + 3mnrcd = 2mnbi + 3crd (Mahar *et al.*, 1997)
 593) 5phl + 3mnch = 5mnbi + 3clin (Mahar *et al.*, 1997)
 594) phl + spss = mnbi + py (Mahar *et al.*, 1997)
 595) syv = syvL (Clark, 1966)
 596) hlt = hltL (Clark, 1966)
 597) di = diL (Clark, 1966)
 598) san = kspL (Lindsley, 1966)
 599) en = enL (Clark, 1966)
 600) pswo = woL (Yoder, 1966)
 601) cor = corL (Shen & Lazor, 1995 omitting UHP)
 602) crst = qL (Jackson, 1976)
 603) crst = qL (Jackson, 1976)
 604) q = qL (Jackson, 1976)
 605) q = qL (Hudson *et al.*, 2002)
 606) q = qL (Kanzaki, 1990)
 607) coe = qL (Kanzaki, 1990)
 608) coe = qL (Zhang *et al.*, 1993)
 609) an = anL (Clark, 1966; Goldsmith, 1980)

Appendix 2. (Continued)

Equilibrium: an H₂O anwL (Clark, 1966), involving next two reactions:

610) H₂O = H₂O
 611) an = anL
 612) l = lcL (Lindsley 1967; (approx).)
 613) per = perl (Bowen & Anderson, 1914)
 614) lime = limL (Rankin & Wright, 1915)
 615) fo = foL (Davis & England, 1964)
 616) fo = foL (subset of Ohtani & Kumazawa, 1981)
 617) fo = foL (low temperature exp's)
 618) fa = faL (Clark, 1966)
 619) sill = sill (Cameron, 1977; Holland & Carpenter, 1986)
 620) cgh = neL (Bowen, 1912)
 621) ne = neL (Smith, 2003)
 622) abh = abL (Schairer & Bowen, 1956)
 623) abh = abL (Boyd & England, 1963)
 624) abh = abL (Nekvasil & Carroll, 1996)

Equilibrium: abh H₂O abwL (Goldsmith & Jenkins, 1985), involving next two reactions:

625) H₂O L = H₂O
 626) abh = abL
 627) abh = abL (Goldsmith & Jenkins, 1985)
 628) h₂O L = H₂O (Goldsmith & Jenkins, 1985)

Equilibrium: san H₂O kspwL (Lambert *et al.*, 1969; Goldsmith & Peterson, 1990), involving next two reactions:

629) h₂O L = H₂O
 630) san = kspL

Equilibrium: trd H₂O qwL (Kennedy *et al.*, 1962), involving next two reactions:

631) h₂O L = H₂O
 632) trd = qL

Equilibrium: q H₂O qwL (Kennedy *et al.*, 1962), involving next two reactions:

633) h₂O L = H₂O
 634) q = qL
 635) h₂O L = H₂O (Johannes & Holtz, 1996)
 636) h₂O L = H₂O (Goranson, 1936)
 637) h₂O L = H₂O (Behrens, 1995)
 638) h₂O L = H₂O (Behrens, 1995)

Equilibrium: abh q abqL (Luth, 1969), involving next two reactions:

639) abh = abL
 640) q = qL

Equilibrium: abh trd abqL (Schairer & Bowen, 1956), involving next two reactions:

641) abh = abL
 642) trd = qL

Equilibrium: an anqL (Schairer & Bowen, 1947), involving:

643) an = anL

Equilibrium: trd anqL (Schairer & Bowen, 1947), involving:

644) trd = qL

Equilibrium: an trd anqL (Schairer & Bowen, 1947), involving next two reactions:

645) an = anL
 646) trd = qL

Equilibrium: ol olL (Bowen & Schairer, 1935), involving next two reactions:

647) fo = foL
 648) fa = faL

Univariant and divariant solid-solution equilibria start with the keyword 'equilibrium' and are followed by one or more equilibrium relations involving end-members in solid solutions. Solid-solution names: crpx, Cr-cpx; crsp, Cr-spinel; po, pyrrhotite; tro, troilite; ol, Fe-Mg olivine; wd, Fe-Mg wadsleyite; rg, Fe-Mg ringwoodite; pv, Fe-Mg perovskite; aki, Fe-Mg akimotoite; mwu, Fe-Mg periclase; pkv, Mg-Al perovskite; crn, Mg-Al corundum; cum, Fe-Mg cummingtonite; opx, Mg-Al opx; cd, hydrous cordierite; sa, Mg-Al sapphirine; chl, Mg-Al chlorite; tlc, Mg-Al talc; trts, Al-tremolite; phe, Mg-phengite; mbi, Al-phlogopite; mlrt, mullite; mqL, Al-Si liquid; epi, Fe-Al epidote; grd, granitite garnet; anwL, an-H₂O liquid; abwL, ab-H₂O liquid; kspwL, ksp-H₂O liquid; qwL, q-H₂O liquid; abqL, ab-q liquid; anqL, an-q liquid; olL, foL, fo-q liquid.

APPENDIX 3: OTHER DATA SET CHANGES

A list of some of the more important changes to thermodynamic data since HP98 follows. Further detailed information may be found on the website at: <http://www.esc.cam.ac.uk/people/academic-staff/tim-holland>.

- end-members but also on the mixing parameters for $\text{H}_2\text{O}-\text{CO}_2$ mixtures.

 2. The data for clinohumite has been updated to incorporate the experimental results of Pawley (2000) on the reactions $\text{chum} = 4\text{fo} + \text{per} + \text{H}_2\text{O}$ and Pawley (2000) and Wunder (1998) on $\text{chum} = 4\text{fo} + \text{br}$. Compressibility data for chum are from Ross & Crichton (2001), thermal expansion is assumed as for forsterite.
 3. Phlogopite data have been updated using the experiments of Aranovich & Newton (1998) on the reaction $2\text{phl} + 6\text{q} = 3\text{en} + 2\text{san} + 2\text{H}_2\text{O}$. There has been some controversy over the molar volume to use, as the synthetic phlogopites have a larger volume ($14.964 \text{ J}^{-1} \text{ bar}$; Robie & Hemingway, 1995; Aranovich & Newton, 1998) than natural phlogopites ($14.687 \text{ J}^{-1} \text{ bar}$; Smyth & McCormick, 1995; Pavese *et al.*, 2003). Until this is resolved we will use the synthetic volumes as they presumably reflect the synthetic material used in the experiments.
 4. The double carbonate reaction equilibrium reactions ($\text{arag} + \text{mag} = \text{dol}$ and $\text{arag} + \text{sid} = \text{ank}$) are characterized by small free energy changes and are difficult to calculate with accuracy from thermodynamic data gained from a variety of mixed carbonate-silicate equilibria. The recent experimental study of Morlidge *et al.* (2006) means that these equilibria may now be fitted and refined, such that the small differences in free energy are made consistent with the experimental pressures. In addition, the experimental data for $\text{cc} = \text{arag}$ is now known to much higher pressures and temperatures, and the experiments of Suito *et al.* (2002) may now also be fitted satisfactorily.
 5. Data for chlorite have been updated using experiments of Pawley (2003) and Fockenberg (1995). The new heat capacity and entropy data for chlorite are from Bertoldi *et al.* (2007).
 6. Compressibility data for pyrophyllite is taken from Pawley (2003). The thermal expansion has been increased somewhat higher than the measurements of Symmes (1986) to satisfy experiments.
 7. The data for phengite and aluminous biotite are updated as discussed in Coggon & Holland (2002).
 8. New experimental data on $\text{cor} + \text{q} = \text{ky}$ from Harlov & Milke (2002) and Harlov *et al.* (2008) are now incorporated in the data fitting.
 9. Heat capacity and entropy for carpholite are taken from Bertoldi *et al.* (2006).
 10. New measurements are used for heat capacity and entropy for cordierite (Paukov *et al.*, 2006; Dachs & Geiger, 2008).
 11. Ferroactinolite enthalpy is fitted to the experiments of Jenkins & Bozhilov (2003).
 12. Experimental data of Koziol (2004) on $\text{sid} + \text{hem} = \text{mt} + \text{CO}_2$ are now used to derive enthalpy data for siderite.

13. Measurements of entropy of hercynite are taken from Klemme & Van Miltenburg (2003).
14. Chloritoid–chlorite Fe–Mg natural partitioning data are taken from Vidal *et al.* (1999) and used as low temperature constraints. Heat capacity and entropy for chloritoid and carpholite end-members have been modified using data of Koch-Müller *et al.* (2002) and Bertoldi *et al.* (2006).
15. Glaucophane data have been augmented by experiments of Corona & Jenkins (2007) for $gl + q = ab + ta$; new thermal expansion data for glaucophane are taken from Jenkins & Corona (2006).
16. Thermal expansion data for staurolite are now taken from Gibbons *et al.* (1981) and compressibility from Grevel *et al.* (1998).
17. Pargasite data are now fitted to the experiments of Westrich & Holloway (1981) and Lykins & Jenkins (1992) using a higher entropy than before. The derived enthalpy agrees well with measured values of Kahl *et al.* (2003). The amphibole mixing terms are from page 264 of Diener *et al.* (2007) except that, for good agreement with temperatures and amphibole compositions in the two experimental studies above, $W_{ts,parg}$ is now set at 2 kJ rather than –40 kJ.
18. Added high pressure experiments on antigorite and phase A from Wunder & Schreyer (1997) and Bose & Navrotsky (1998).
19. Added experiments of Aranovich & Newton (1999) on $cc + q = wo + CO_2$, $mag + en = fo + CO_2$ and $ta = en + q + H_2O$, and $phl + q = san + en + H_2O$. Also, those of Koziol & Newton (1998) for $mag + en = fo + CO_2$.
20. Sphene thermodynamic data have been updated using heat capacities and entropy of Manon *et al.* (2008), thermal expansion from Malcherek (2001) and compressibility from Angel *et al.* (1999a,b).
21. Thermodynamic data for zircon and baddeleyite have been updated through the experimental data in Butterman & Foster (1967), Ferry *et al.* (2002) and are in excellent agreement with the Gibbs energies retrieved by Newton *et al.* (2010).
22. Geikelite enthalpy has been improved via the additional experiments of Ferry *et al.* (2002) on $mag + ru = geik + CO_2$.

Received 14 June 2010; revision accepted 24 November 2010.

Copyright of Journal of Metamorphic Geology is the property of Wiley-Blackwell and its content may not be copied or emailed to multiple sites or posted to a listserv without the copyright holder's express written permission. However, users may print, download, or email articles for individual use.